POLITEKNIK NEGERI BALI

Journal of Engineering Design and Technology

logic

Vol. 21 No. 1 March 2021

LOGIC

Jurnal Rancang Bangun dan Teknologi

p-ISSN. 1412-114X

e-ISSN. 2580-5649

LOGIC

Jurnal Rancang Bangun dan Teknologi

Journal of Engineering Design and Technology

Gedung P3M, lt.1 Politeknik Negeri Bali, Bukit Jimbaran
PO BOX 1064 Kuta Selatan, Badung, Bali - Indonesia
Telp. (+62)361 701981 Fax. (+62)361 701128
Email: logic@pnb.ac.id

LOGIC JOURNAL TEAM

PREFACE

Logic: Jurnal Rancang Bangun dan Teknologi (Journal of Engineering Design and Technology) is a peer-reviewed research journal aiming at promoting and publishing original high quality research in all disciplines of engineering and applied technology. All research articles submitted to Logic should be original in nature, never previously published in any journal or presented in a conference or undergoing such process across the world. All the submissions will be peer-reviewed by the panel of experts associated with particular field. Submitted papers should meet the internationally accepted criteria and manuscripts should follow the style of the journal for the purpose of both reviewing and editing.

Logic is a journal covering articles in the field of civil and mechanical engineering, design, and technology published 3 times a year in March, July, and November. Language used in this journal is English.

LOGIC. P-ISSN 1412-114X
LOGIC. E-ISSN 2580-5649
Indexing : GOOGLE SCHOLAR, DOAJ, EBSCO OPEN SCIENCE DIRECTORY, SINTA, GARUDA

Best Regard,

LOGIC Editorial Team

TABLE OF CONTENTS

University Electronic Records Management System for Northwest Samar State University, Calbayog City 1 – 7
Donald M. Patimo, Ritchie P. Maribojoc

The Effect of Fluid Velocity on the Diffusion of Trimethylene Glycol through a Reverse Osmosis Membrane in Microchannel -X 8 – 13
Sugeng Hadi Susilo, Zahratul Jannah, R.N. Akhsanu Takwim

River Transport Planning Strategy Analysis Using SWOT and AHP Methods 14 - 22
Yega Mardiansyah, Eva Azhra Latifa

Natural Lighting of Studio Apartment with East-Oriented Opening 23 – 30
Aisyah Anindya Putri, Dyah Nurwidyaningrum, Tri Wulan Sari

Comparison Between the BOQ of Conventional and BIM Method on BPJS Building in Central Jakarta 31 – 39
Mutia Hanuun Ufaira Akbar, I Ketut Sucita, Erlina Yanuarini

Settlement of Geosynthetic Encased Stone Columns Liquefaction Condition in Box Culvert 40 – 51
Maftuh Ahnan, Putera Agung Maha Agung

Planning for Maintenance and Repair of Continuous Ship Unloader Using the IRRO Method 52 – 63
Syamsul Hadi, Alfarizi Al Azis, Vinan Viyus, Etik Puspitasari, Ahmad Hanif Firdaus, Andri Setiawan

Effect of Heat Radiation on Work Load and Gamelan Crafts Productivity 64 – 69
I Ketut Gede Juli Suarbawa, M. Yusuf

Working Productivity Analysis on the Process of Drying Fish Using Solar Dryers 70 – 73
I Gede Santosa; I Gede Bawa Susana

Comparison of Inverter Types for Home Appliance Using Push-Pull Amplifier 74 – 79
Mokh Hairul Bahri, Dudi Irawan

LOGIC
Journal of Engineering Design and Technology
Vol. 21 No.1 March 2021 ; p. 1 - 7

p-ISSN : 1412-114X
e-ISSN : 2580-5649
http://ojs.pnb.ac.id/index.php/LOGIC

University Electronic Records Management System for Northwest Samar State University, Calbayog City

Engr. Ritchie P. Maribojoc [1], Donald Patimo [2]

1) Northwest Samar State University NwSSU, Main Campus Calbayog City, Philippines
2) Northwest Samar State University NwSSU, Main Campus Calbayog City, Philippines

Correponding email :
[1)] dad_ritchie@yahoo.com
[2)] donald.patimo@nwssu.edu.ph

Abstract. Effective records management program is a major element of the governance of any organization. Based from the surveys, the Northwest Samar State University was not fully aware on how to do about the implementation of this act, National Archives of the Philippines Act of 2007 (R.A 9470). The university was still relying from the university code for the records management provisions. This study was undertaken to develop and validate the acceptability of the developed University Electronic Records Management System (UeRMS) for Northwest Samar State University as perceived by the computer experts, school officials, teaching personnel and non- teaching personnel. Thus, the idea and assessment of the respondents towards the design of the system is very critical. Upon validating the developed system, they observed that it was much faster to search records compared to manual process.

Keywords : electronic records, management system, records management, database

1. INTRODUCTION

All University Electronic Management System refers to the practice of maintaining the records of the university from the time they were created up to their eventual disposal. This system is deemed necessary to facilitate easy and fast transaction of documents of the university. Organizing large volumes of physical records are difficult. Without the use of an efficient, effective, and productive document management system, it is almost certain that management of documents will be prone to human error.

Good quality management of records and information is fundamental to a well-functioning organization since it supports business activity and provides a basis for efficient and effective service delivery. It also provides the mechanism whereby both the private and public sectors can account for their decisions and actions. Records provide evidence for the public to confirm or claim their public rights and entitlements, as well as providing individuals with evidence to justify government decisions and a mechanism whereby they can have trust in private enterprise. The good records management is simply good business practice.

Furthermore, the information contained in university records needs to be managed according to a methodical approach in order to enhance the effectiveness and efficiency of the universities in carrying out their mission. Public records and archives contribute to the country's national identity by documenting the interactions of people and organizations with the government over time [1]-[3].

This study aimed to develop and validate a University Electronic Records Management System for Northwest Samar State University in Calbayog City. The researcher conducted a survey to determine the level of compliance of the university to the National Archives Act of 2007 (R.A 9470) as perceived by the officials, teaching and non-teaching personnel in terms of management of public records and administration of public archives, as well as the acceptability of the system. The researcher used appropriate statistical tools to determine the significant difference on the perception of the respondents on the level of compliance of the university to RA 9470. Thus, the researcher identified and collected the benchmark information from the respondents needed to specifically improve the design and development of the University Electronic Records Management System (UeRMS) for Northwest Samar State University, Calbayog City.

2. METHODS

This study uses the developmental method of research and the Structured Systems Analysis and Design (SSADM) in order to elicit data from the respondents. The developmental research is particularly important in the field of information technology. The most common type of developmental researches involves situations in which the product- developmental process is analyzed and described, and the final product is evaluated (Richey, 2004).

This study used random sampling to determine the size of the teaching and non-teaching personnel of the University. There were fifty percent (50%) of the teaching and non-teaching personnel and ninety percent (90%) of the school officials were tallied and tabulated as respondents.

On the other hand, purposive sampling method is considered in determining the size of the computer experts and University officials. In purposive sampling the investigator used his prudent judgment about which respondents to choose, and picks only those who best meet the purpose of the study. Purposive sampling was also used in identifying officials who deal directly with records management of the university, as well as senior officials who can assist in making records management one of the strategic priorities.

The first set of questionnaire was designed according to R.A 9470. The questionnaire asked the respondents the level of compliance of the University in relation to R.A 9470.The panel agreed that the questionnaire presented by the researcher was valid and accepted as a research instrument.

The researcher also made used of the validated research questionnaire of Ortiz [4]-[6] in his theses entitled "Research Database Management System for NwSSU". The said questionnaire was designed to validate the Assessment of the computer experts. Another set of questionnaire was also used to determine the acceptability of the developed University Electronic Records Management System as assessed by the respondents.

The data gathered through the research instruments were statistically treated and interpreted to answer problems postulated in the study. The statistical treatments used to analyze the gathered data are the following: The average weighted mean and standard deviation were used in determining the level of compliance of the University to the National Archives Act of 2007 (RA 9470) as perceived by the school officials, teaching, and non-teaching. Mean and standard deviation were also used on the evaluation of the computer experts and the school officials on the workability of the proposed University Electronic Records Management System for NwSSU. The ANOVA Single factor was used to determine the perception of the respondents on the workability and acceptability of the University Electronic Records Management System.

3. RESULTS AND DISCUSSION

As shown in Figure 1, the NwSSU was unaware of the guidelines under the National Archives Act 9470. These results could mean prioritization of the creation a of university records office. The overall rated mean result of 2.31 is clear evidence that the university needs a record management system that will cater needs concerning on the university records handling.

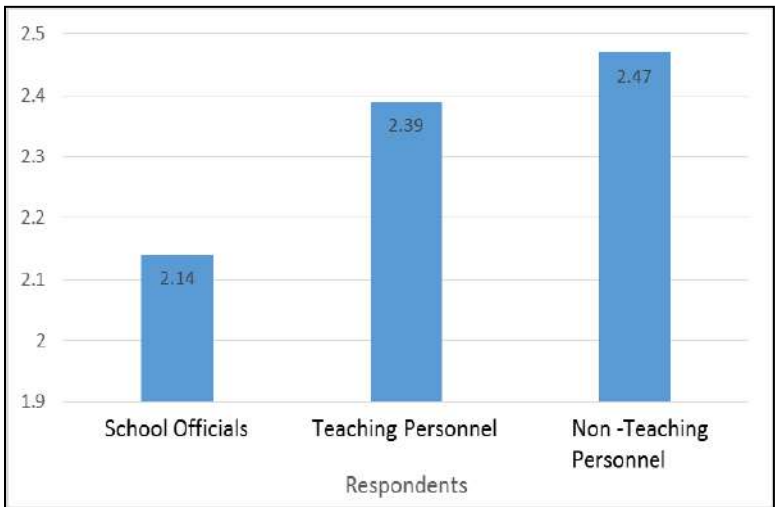

Figure 1. NwSSU Level of Compliance to R. A 9470

Most of the computer experts agree that the input design of the proposed system had been designed for user convenience and there is an efficient input and data entry as shown in the table below. The processing performance, database design and output design were also accepted and validated by the computer experts. With the recommendations coming from them that the server requirements must be followed and ensure that the software used meets the minimum requirements.

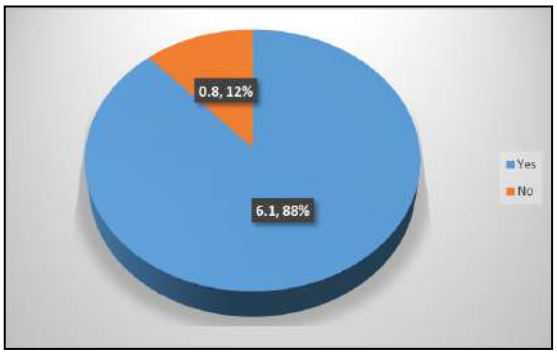

Figure 2. Validity Assessment of Computer Experts on User- Interface

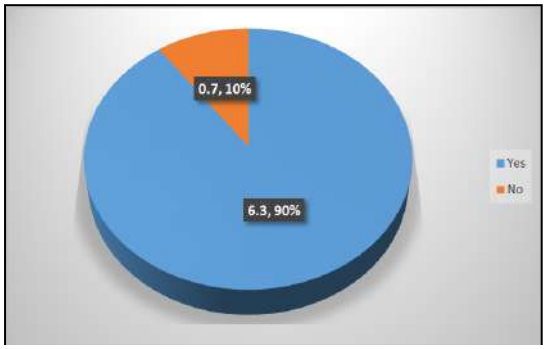

Figure 3. Validity Assessment of Computer Experts on Input Design

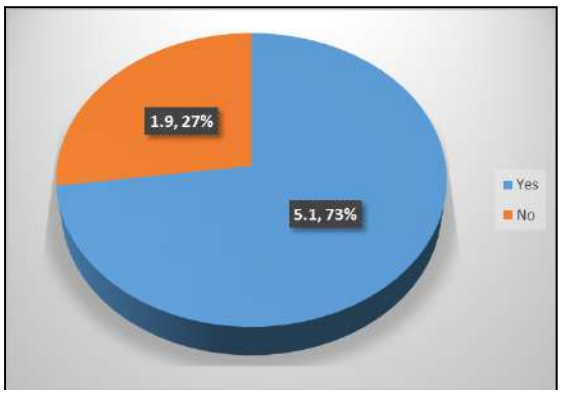

Figure 4. Validity Assessment of Computer Experts on Processing Performance

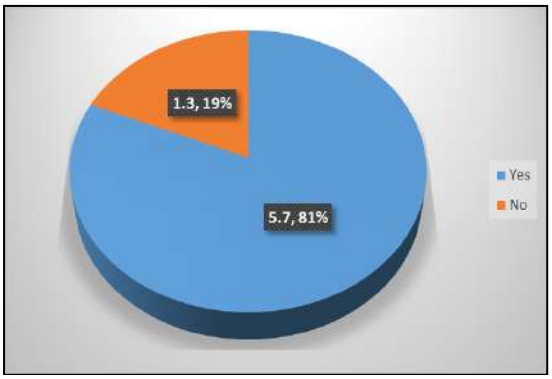

Figure 5. Validity Assessment of Computer Experts on Database Design

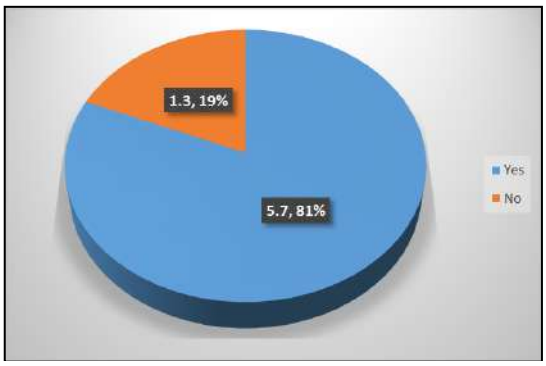

Figure 6. Validity Assessment of Computer Experts on Output Design

The researcher made used of Free Open Source Software (FOSS) for its database design as back end and development. It uses Visual Studio 2008 as the front end software. It was designed to address the need for record keeping and monitoring of a Records office in a university. It facilitates a more efficient means of creating, maintaining, and querying the databank of all the records of the university [7-10].

The design of the proposed University Electronic Records Management System for Northwest Samar State University is presented below using a functional decomposition diagram shown on figure 7. It is a fundamental analysis technique that breaks a complex problem into successive layers of more manageable and comprehensive pieces, resulting in a hierarchically structured function chart [11]-[14]. There are 6 main menus and 16 submenus that the system caters.

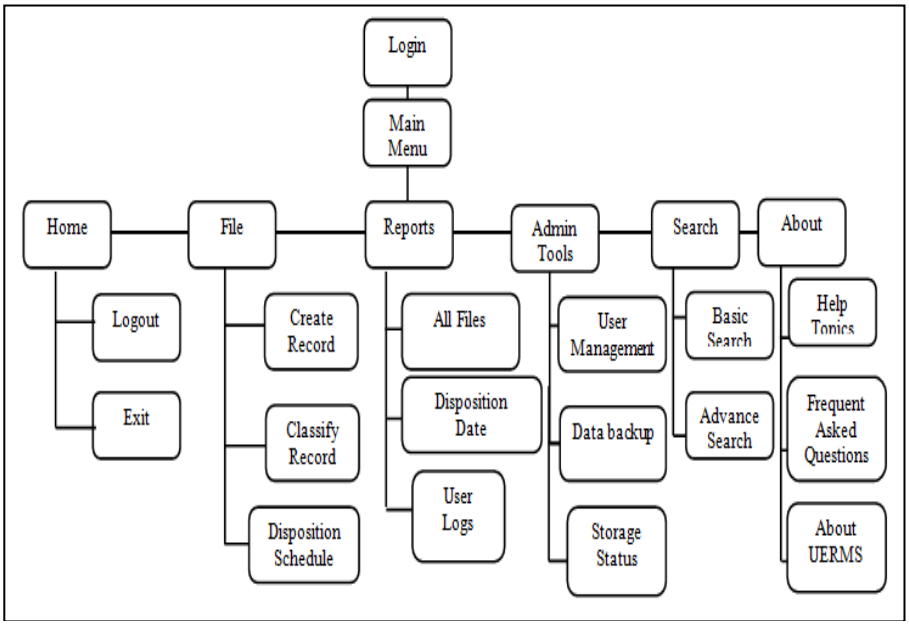

Figure 7. Design of the Proposed University Electronic Records Management System for the Northwest Samar State University

The Entity Level ERD of the proposed University Electronic Records Management System is shown below in figure 8. Thus, the proposed system contains 10 tables as presented on the figure. Five of those tables were the kinds of records that the system process. A record of each entity allows the key attribute to establish relationship. The entity identified by the key attribute assigned for the purpose identification of every record for fast search and to make easy organization of relationships for the proposed system. The figure below is an abstract way to describe the database of the proposed system.

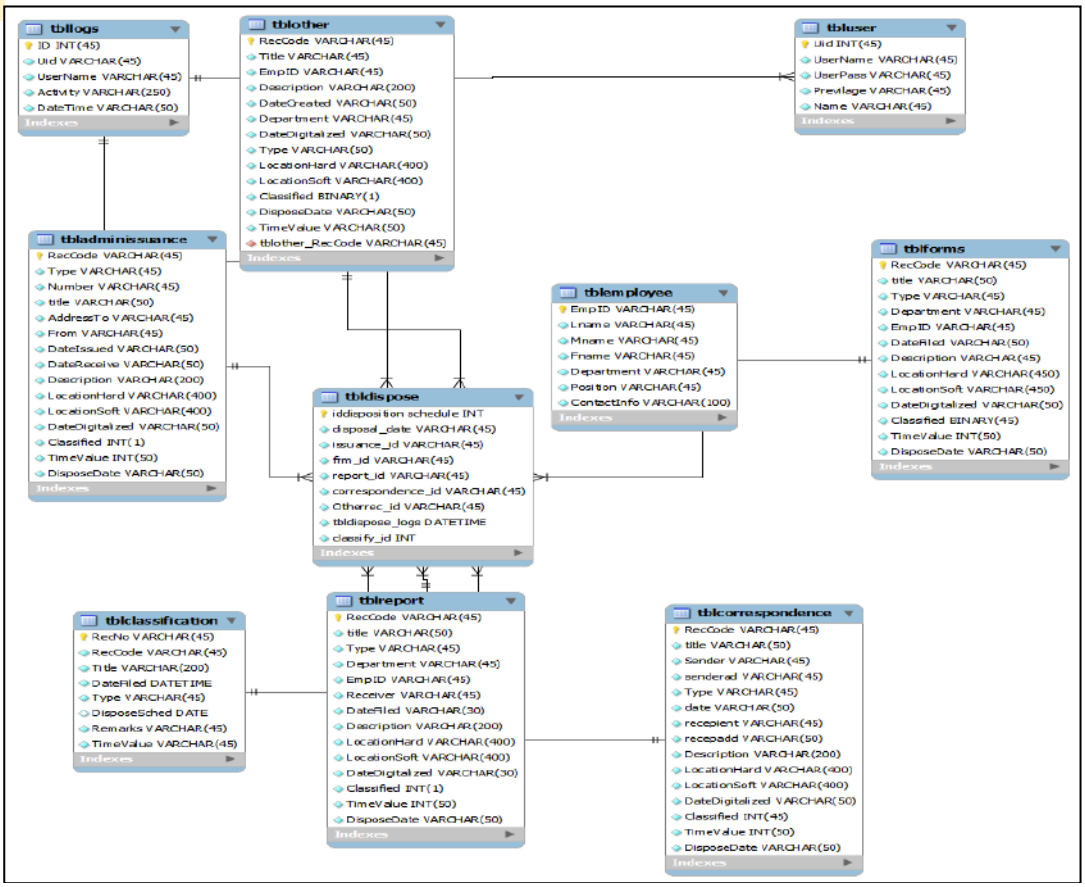

Figure 8. UERMS Entity Relationship Diagram

The succeeding figures show the user interface designs of the proposed University Electronic Records Management System for Northwest Samar State University.

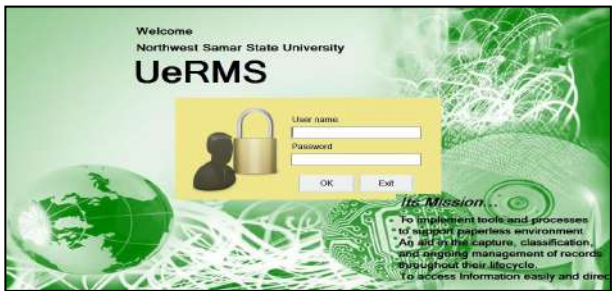

Figure 9. Log-in Screen Form

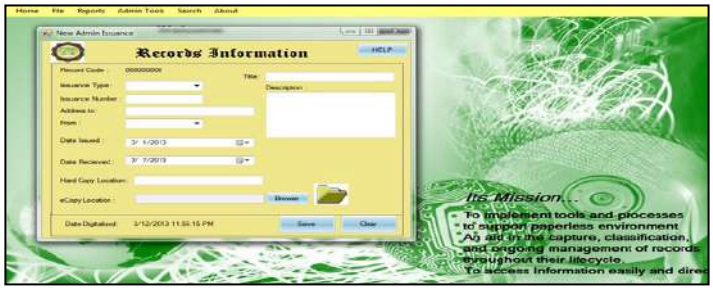

Figure 10. Record's Creation Form

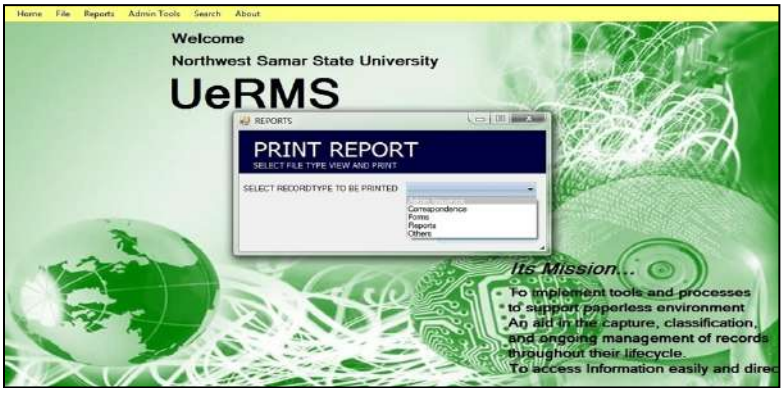

Figure 11. Print Report Form

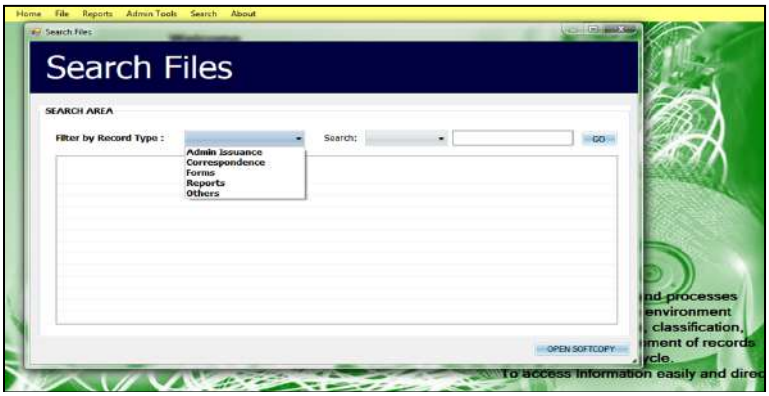

Figure 12. Search Module Form

4. CONCLUSION

Based on the findings of the study, the researchers concluded that there is a need for the whole community of the Northwest Samar State University to be acquainted with the provisions of the law on "National Archives of the Philippines Act of 2007". Furthermore, the assessment of the computer experts on the validity of the proposed system reveals that the proposed system was valid and acceptable in terms of user interface, input design, processing performance, database design, and output design. With these, improvements on the design and development of the University Electronic Records Management System were made and finalized for the effective system implementation.

5. REFERENCES

[1] M.R. Chou. 2012. Primer of Republic Act 9470. Retrieved from www.nationalarchives.gov.ph/R.A9470.pdf, April 2012.
[2] Database Management System. 2012. In Encyclopedia Britannica. Retrieved February 14, 2012 from http://www.answers.com/topic/database-management- system
[3] J. Heckman, 2008. Why Document Management: A White Paper. Retrieved 13 February, 2010, from http://www.heckmanco.com/docs/DMWhitePaper.pdf
[4] Database Management System (2009). In McGraw-Hill Encyclopedia of Science and Technology, 5th Edition, published by the McGraw- Hill Companies, Inc.
[5] De Wet, S & Du Toit, A. 2000. The challenge of implementing a records management system at the National Electricity Regulator in South Africa. Records Management Journal 10 (2) :73-86.
[6] Electronic Records Management Handbook of State of California. 2002. Sacramento, California: Calrim Publishing, Ltd.
[7] Eleoranta, E., Hameri, A. & Lati, M. 2001. "Improved Project Management through Improved Document Management". Computers in Industry, Elsevier, 45, pp. 231-243.
[8] H.L Carpon and J.A Johnson (2003). Computers: Tools for an Information Age: Philippine Edition, Pearson Education (Asia) PTE Ltd.

[9] Hajjar, D., AbouRizk, S. M. 2000. "Integrating Document Management with Project and Company Data". Journal of Computing in Civil Engineering, ASCE, 14 (1), pp. 70-77.
[10] Noname. 2019. International Records Management Trust. Retrieved from http://www.irmt.org/Project_Toolkit.pdf
[11] JISC Infonet. HEI Records Management: Guidance on Managing Research Record. Retrieved from http://www.jiscinfonet.ac.uk/partnerships/records-retention-he/managing-research-records
[12] L. Bower. 2001. ARMA 2001: an information odyssey. Records Management Bulletin 105 (December): 19–23.
[13] R. Dollado. 2002. A Computer Education Program for Teachers of Calbayog Pilot Central School: A feasibility study.
[14] R. Richey. 2004. Developmental Research: the Definition and Scope.

LOGIC
Journal of Engineering Design and Technology
Vol. 21 No.1 March 2021 ; p. 8 - 13

p-ISSN : 1412-114X
e-ISSN : 2580-5649
http://ojs.pnb.ac.id/index.php/LOGIC

THE EFFECT OF FLUID VELOCITY ON THE DIFFUSION OF TRIMETHYLENE GLYCOL THROUGH A REVERSE OSMOSIS MEMBRANE IN MICROCHANNEL -X

Sugeng Hadi Susilo[1], Zahratul Jannah[2], R.N. Akhsanu Takwim[3]

1,2,3) Department of Mechanical Engineering, State Polytechnic of Malang, Jl. Soekarno-Hatta 9 Malang-indonesia.

Correponding email [1)] : sugeng.hadi@polinema.ac.id

Abstract. The study aims to observe the diffusion process which is influenced by different velocity and fluid concentrations. Using a microfluidic system and the diffusion process through a reverse osmosis membrane. The research was carried out by flowing fluid into the microchannel. The diffusion process is known by measuring and analyzing the density of liquid waste aquades-trimethylene glycol. The results showed the amount of diffusion through the membrane was influenced by flow velocity and fluid concentration. this is because the velocity of the flow produces pressure on the wall so that it pushes the fluid to diffuse through the membrane.

Keywords : Diffusion, velocity, concentration, microchannel.

1. INTRODUCTION

The microchannel is one of the new technologies in the pharmaceutical field. In the pharmaceutical field, the microchannel is assumed to be a blood vessel of a living thing [1]–[3]. Fluid flow in the microchannel allows dynamic changes to occur at certain times and conditions. Diabetes mellitus is a disease related to blood plasma. Increased viscosity of blood plasma causes diabetes [4], [5]. The viscosity of human blood that is higher than the normal limit will have a negative effect. One negative effect is the heart's performance to pump blood heavier and can damage the walls of blood vessels [6]–[8].

The two channels on the microchannel that are insulated with a membrane represent external and internal fluids in human cells. Diffusion that occurs through a porous membrane describes the process of absorption of nutrients or drugs that enter the body through the blood [9].

The advantages of using microchannel in pharmaceutical research include, lower costs because the tool can be used repeatedly, accurate results because the channel model used is representative of metabolic and circulatory organs in the human body, and easier in terms of observation because the microchannel comes from materials transparent rather than having to do surgery on human organs, including testing for antibiotics or other drugs that enter the metabolism of living things [10], [11]. Fluid flow in the microchannel allows for differences in concentration at the meeting point of the fluid caused by the diffusion process and easier observation [12], [13].

Also, research at the micro-scale when compared with studies at the macro scale has a very different surface volume ratio, has buoyancy force, inertia force and forces on the surface such as adhesion and surface tension. Characteristics of flow in the microchannel are fluid flows considered laminar, Reynold numbers are low and there is molecular diffusion associated with diffusion between reagents [14].

The Microchannel applications include mixer, microreactor, and cytotoxity. This is related to chemical reactions at a micro-scale that is faster with a small volume and a short diffusion process to allow faster fluid mixing.

The microchannel as cytotoxicity screen, in which the core flow is enveloped by liquid fluid sheaths [15], [16]. The use of cytotoxicity as a way to send samples of cells covered with liquid fluid to the core flow area. The

form of flow cytotoxicity is adopted from the form of laminar flow and diffusion Mixing of fluids in the interphase region is entirely affected by diffusion.

The microchannel used in biotechnology for vesicle liposome generation [17]–[19]. A liposome is a nanoparticle that is in phospholipid fluid, plays a role in biotechnology and as a drug or genetic material in cells. The character of laminar flow microfluidics is caused by, among others: low temperature, shear stress and composition fluctuations in the reaction causing the product to have high mono dispersion compared to most liposome production [20]. The size of the vesicles is one of the factors that determine the amount of liposome material. The microchannel used in the field of rheology with polymeric materials [2]. The results showed that changes in the flow of liquid polymer particles in the core channel are affected by shear forces and elasticity.

The human digestive system involves several organs and works very complex. Food and medicine that enters the body will be digested into energy, nutrients and produce the remaining processes which must then be removed from the body [21], [22]. The process begins with the destruction or conversion of large molecules into small ones so that they are easily absorbed by the body. The absorption of nutrients from the gastrointestinal tract into cells is divided into several mechanisms, namely passive absorption, convective transfer, active absorption, facilitative transport, ion-pairing and pinocytosis [23], [24]. Some nutrients and drugs are absorbed in the small intestine through the surface of the large mucous villi. Gastrointestinal membranes consist of lipids and proteins so that fat-soluble drugs quickly penetrate the gastrointestinal membrane. While the cell membrane is not too much different, which consists of fat, phospholipids, cholesterol, enzymes and so on to enable the transfer of substances either actively or passively [12], [25].

Passive diffusion in the membrane consists of two mechanisms, namely through the carrier protein and channel protein. Channel proteins have holes or pores for the process of diffusion of substances from the digestive tract into body cells, but not all substances in the digestive tract can penetrate the membrane through this mechanism [16], [26], [27]. Ions that cannot penetrate through the mechanism will be assisted by ionophore, usually synthesized by microorganisms. Small, polar and uncharged molecules such as glycerol can diffuse into cells through membranes, while large, polar and uncharged molecules such as glucose and sucrose can partially enter through the membrane and some cannot. The membrane used in the experiment is a reverse osmosis membrane which generally has a membrane pore size of around 40 µm, a thickness of 120-150 µm and there is a barrier layer of layers on the surface which has a thickness of 0.2 µm. But based on experiments, the size of the membrane pore radius used in the experiment was 1.095 µm.

2. METHODS

The research work is intended to investigate the parameters of the trimethylene glycol diffusion process on Microchannel -X by experiment. This report is written with a variety of velocity a stream against its diffusion process. So that the process of trimethylene glycol diffusion process can be identified in the form of a product concentration waste.

The X-microchannel consists of the top and bottom parts, as shown in Figure 1. The red line shows the channel for Trimethylene glycol (top) flow, while the blue line shows the channel for the flow of distilled water (bottom). The pink line shows the diffusion process. The bulkhead uses a membrane with a radius of 1.0943 µm.

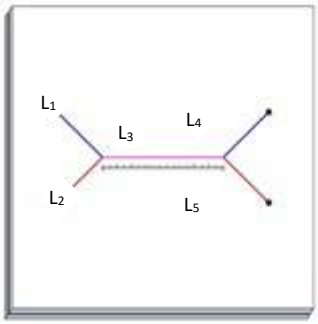

Figure 1. Microchannel type-X

The Microchannel is rectangular with a side of 200 µm, with a channel length of 1000 µm. The length of the inlet and outlet of the microchannel used in this study were L1, L2, L4, L5 = 500 um, L3 = 1000 um with the width of 200 um, and the depth of 200 um, as shown in Figure 1. The arrangement of microchannel material in size (10x10) cm with a thickness on 5 mm arranged accumulated.

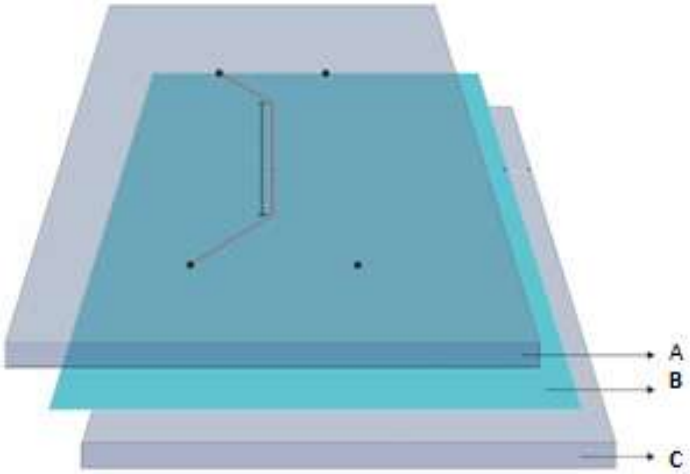

Figure 2. Microchannel Parts, A. Top Cross-section Microchannel; B. Porous Membranes; C. Lower Acrylic Section.

The two microchannel sections are joined together in the same arrangement as in Figure 2. Then the inlet section is connected to the TS-1B / W0109-1B syringe pump type and the outlet part is connected to the reservoir [28], as shown in Figure 3.

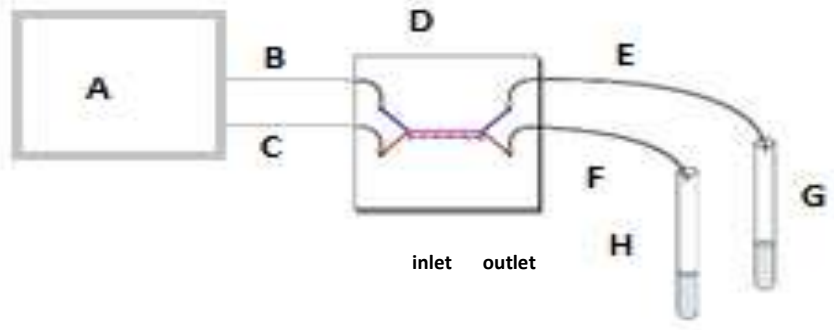

Figure 3. Experimental setup A. Sprynge pump, B. Aquades injection hose; C. Trimethylene glycol injection hose; D. Microchannel; E. Waste Aquades-Trimethylene glycol Mixed Waste Hose; F. Waste Trimethylene glycol Hose; G. waste 1; H. waste 2.

The research was performed with the velocity stream variations of 50 um/s, 100 um/s, 150 um/s and 200 um/s, and with a concentration of 0.1M; 0.25M; 0.5M; 0.75M; 1M. Syringe pumps were used to flow the fluid from the two inlets, as shown in figure 3.

3. RESULTS AND DISCUSSION

This research was conducted to determine the effect of flow velocity and concentration on the diffusion of Trimethylene glycol through a reverse osmosis membrane in a microchannel. The concentration of Trimethylene glycol which diffuses through the membrane can be determined by measuring the density of the mixture of Trimethylene glycol and distilled water outlet channels.

3.1 EFFECT OF VELOCITY ON DIFFUSION

Based on the density measurement data on the mixture of Trimethylene glycol and aquades, the magnitude of the diffusion of Trimethylene glycol through the reverse osmosis membrane is shown in Figure 4.

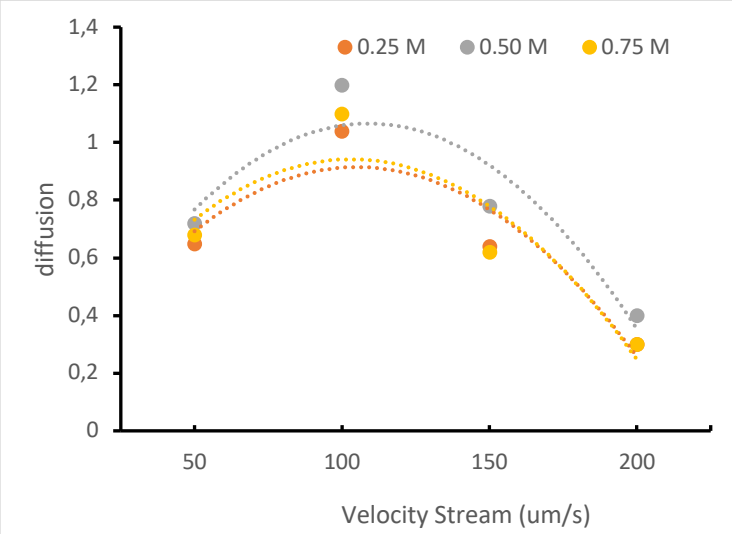

Figure 4. Relationship of Diffusion to Flow Velocity

Figure 4 presents the diffusion profile of Trimethylene glycol, showing that there are differences in the magnitude of diffusion at a different velocity. The amount of diffusion increases at a velocity of 100 um / s, then decreases with the increasing flow velocity. This happens at various concentrations. The biggest diffusion occurs at a flow rate of 100 um / s with a concentration of 0.50 M.

The amount of diffusion is strongly influenced by the pressure which is the driving force to pass through the porous membrane. The amount of pressure is affected by the flow velocity and density of the fluid. The concentration of the liquid is certainly related to density, and which easily enters the membrane between 0.1-0.50 M. At flow rates above 100um / s, diffusion seems to decrease. The faster the flow, the smaller the chance of Trimethylene glycol compounds entering the membrane. This is influenced by the Trimethylene glycol molecule in the boundary layer being driven by the flow rate toward the outlet. Resulting in a compound that diffuses decreasing.

3.2 EFFECTS OF CONCENTRATION ON DIFFUSION

Based on the measurement data of trimethylene glycol concentration (M) on diffusion through the reverse osmosis membrane is shown in figure 5.

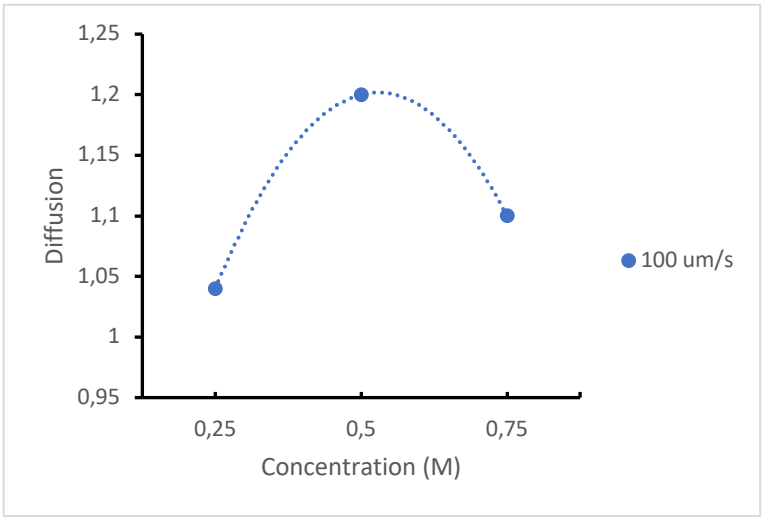

Figure 5. Relationship of concentration to diffusion at a velocity of 100 um / s.

Figure 5 shows the different magnitudes of diffusion in the microchannel channel at different concentrations. dilution of the concentration of the compound Trimethylene glycol tries to mimic the viscosity of human blood under normal conditions, anemia, and diabetics. There is a trend of a line that rises significantly and then decreases significantly with greater concentration. The difference in concentration shows that there is a relationship between the concentration and diffusion that occurs through the membrane. While the concentration is related to viscosity. When fluid flows near the membrane wall, friction occurs between the fluid and the wall

surface. This results in different flow rates. The greater the viscosity, the lower the flow velocity. The lower flow velocity causes the pressure on the membrane to decrease. Based on Figure 5 shows that at a concentration of 0.5 M a maximum diffusion is achieved at a flow velocity of 100 µm / s. Furthermore, with increasing fluid concentration, the number of diffusion decreases.

The use of aquades as a representation of cell fluids and Trimethylene glycol as cell external fluids both have different concentrations. at greater concentrations, fluid motion is slower due to the frictional force of the solution against the channel wall. The movement of fluid to diffuse will be smaller.

4. CONCLUSION

It was concluded that the amount of diffusion in the membrane is influenced by the velocity of the flow and density of the fluid. Flow velocity results in pressure on the wall thereby pushing fluid through the membrane. The concentration of Trimethylene glycol that easily enters the membrane is 0.50 M with a flow rate of 100 um/s.

5. REFERENCE

[1] A. Šalić, A. Tušek, and B. Zelić, 2012, "Application of microreactors in medicine and biomedicine," *J. Appl. Biomed.*, vol. 10, no. 3, pp. 137–153, , doi: 10.2478/v10136-012-0011-1.

[2] S. Girardo, R. Cingolani, and D. Pisignano, 2007, "Microfluidic rheology of non-newtonian liquids," *Anal. Chem.*, vol. 79, no. 15, pp. 5856–5861, doi: 10.1021/ac062405t.

[3] H. R. Kim, 2014, "Formulation of a Success Model in Pharmaceutical R&D," *SAGE Open*, vol. 4, no. 1, p. 215824401452798, doi: 10.1177/2158244014527986.

[4] N. Bag, S. Huang, and T. Wohland, 2015, "Plasma Membrane Organization of Epidermal Growth Factor Receptor in Resting and Ligand-Bound States," *Biophys. J.*, vol. 109, no. 9, pp. 1925–1936, doi: 10.1016/j.bpj.2015.09.007.

[5] C. Irace, C. Carallo, F. Scavelli, M. S. De Franceschi, T. Esposito, and A. Gnasso, 2014, "Blood viscosity in subjects with normoglycemia and prediabetes," *Diabetes Care*, vol. 37, no. 2, pp. 488–492, 2014, doi: 10.2337/dc13-1374.

[6] A. A. Siddiqui, S. A. Siddiqui, S. Ahmad, S. Siddiqui, I. Ahsan, and K. Sahu, , 2013, "Diabetes: Mechanism, pathophysiology and management-A review," *Int. J. Drug Dev. Res.*, vol. 5, no. 2, pp. 1–23.

[7] A. S. Panchbhai, 2012, "Correlation of Salivary Glucose Level with Blood Glucose Level in Diabetes Mellitus," *J. Oral Maxillofac. Res.*, vol. 3, no. 3, pp. 1–7, doi: 10.5037/jomr.2012.3303.

[8] A. Kusumi *et al.*, 2015, "Paradigm shift of the plasma membrane concept from the two-dimensional continuum fluid to the partitioned fluid: High-speed single-molecule tracking of membrane molecules," *Annu. Rev. Biophys. Biomol. Struct.*, vol. 34, no. November 2015, pp. 351–378, doi: 10.1146/annurev.biophys.34.040204.144637.

[9] K. P. Lee, T. C. Arnot, and D. Mattia, 2011, "A review of reverse osmosis membrane materials for desalination-Development to date and future potential," *J. Memb. Sci.*, vol. 370, no. 1–2, pp. 1–22, doi: 10.1016/j.memsci.2010.12.036.

[10] A. Tirella, M. Marano, F. Vozzi, and A. Ahluwalia, 2008, "A microfluidic gradient maker for toxicity testing of bupivacaine and lidocaine," *Toxicol. Vitr.*, vol. 22, no. 8, pp. 1957–1964, doi: 10.1016/j.tiv.2008.09.016.

[11] S. Prakash and S. Kumar, 2015,"Fabrication of microchannels: A review," *Proc. Inst. Mech. Eng. Part B J. Eng. Manuf.*, vol. 229, no. 8, pp. 1273–1288, doi: 10.1177/0954405414535581.

[12] R. Zwanzig, 1983, "On the relation between self-diffusion and viscosity of liquids," *J. Chem. Phys.*, vol. 79, no. 9, pp. 4507–4508, doi: 10.1063/1.446338.

[13] J. S. Collura, D. E. Harrison, C. J. Richards, T. K. Kole, and M. R. Fisch, 2002, "The effects of concentration, pressure, and temperature on the diffusion coefficient and correlation length of SDS micelles," *J. Phys. Chem. B*, vol. 105, no. 21, pp. 4846–4852, doi: 10.1021/jp004572h.

[14] Y. C. Lam, H. Y. Gan, N. T. Nguyen, and H. Lie, 2009, "Micromixer based on viscoelastic flow instability at low Reynolds number," *Biomicrofluidics*, vol. 3, no. 1, doi: 10.1063/1.3108462.

[15] Z. Wang, M. C. Kim, M. Marquez, and T. Thorsen, 2007, "High-density microfluidic arrays for cell cytotoxicity analysis," *Lab Chip*, vol. 7, no. 6, pp. 740–745, doi: 10.1039/b618734j.

[16] S. Hess and J. C. Rainwater, 1983, "Diffusion in a laminar flow: Shear rate dependence of correlation functions and of effective transport coefficients," *J. Chem. Phys.*, vol. 80, no. 3, pp. 1295–1303, doi: 10.1063/1.446808.

[17] M. Costa, J. Vasco, A. S. Pouzada, and A. J. Pontes, 2015, "Characterization of polymer behaviour in microchannels," *AIP Conf. Proc.*, vol. 1593, no. November 2015, pp. 209–212, doi: 10.1063/1.4873765.

[18] D. Carugo, E. Bottaro, J. Owen, E. Stride, and C. Nastruzzi, 2016, "Liposome production by microfluidics: Potential and limiting factors," *Sci. Rep.*, vol. 6, no. May, doi: 10.1038/srep25876.

[19] P. Pradhan, J. Guan, D. Lu, P. G. Wang, L. J. Lee, and R. J. Lee, 2008, "A facile microfluidic method for production of liposomes," *Anticancer Res.*, vol. 28, no. 2 A, pp. 943–947.

[20] R. Darros-Barbosa, M. O. Balaban, and A. A. Teixeira, 2003, "Temperature and concentration dependence of density of model liquid foods," *Int. J. Food Prop.*, vol. 6, no. 2, pp. 195–214, doi: 10.1081/JFP-120017815.

[21] P. Connes *et al.*, 2013, "Decreased hematocrit-to-viscosity ratio and increased lactate dehydrogenase level in patients with sickle cell anemia and recurrent leg ulcers," *PLoS One*, vol. 8, no. 11, pp. 6–10, doi: 10.1371/journal.pone.0079680.

[22] S. J. Jackson, H. Prior, and A. Holmes,2018, "The use of human tissue in safety assessment," *J. Pharmacol. Toxicol. Methods*, vol. 93, no. February, pp. 29–34, doi: 10.1016/j.vascn.2018.05.003.

[23] F. Skovborg, A. V. Nielsen, and J. Schlichtkrull, 1968, "Blood-viscosity and vascular flow rate blood-viscosity measured in a cone-plate viscometer and the flow rate in an isolated vascular bed," *Scand. J. Clin. Lab. Invest.*, vol. 21, no. 1, pp. 83–88, doi: 10.3109/00365516809076980.

[24] P. Stonier and H. Silva, 2014, "Pharmaceutical Medicine : History , Global Status , Evolution and Development This material is the copyright of the original publisher .," no. January 2007, 2014.

[25] N. Nguyen *et al.*, 2017, "Adult human primary cardiomyocyte-based model for the simultaneous prediction of drug-induced inotropic and pro-arrhythmia risk," *Front. Physiol.*, vol. 8, no. DEC, pp. 1–16, doi: 10.3389/fphys.2017.01073.

[26] M. Guo, H. Gelman, and M. Gruebele, 2014, "Coupled protein diffusion and folding in the cell," *PLoS One*, vol. 9, no. 12, pp. 1–17, doi: 10.1371/journal.pone.0113040.

[27] S. Yin, N. Song, and H. Yang, 2018, "Detection of Velocity and Diffusion Coefficient Change Points in Single-Particle Trajectories," *Biophys. J.*, vol. 115, no. 2, pp. 217–229, doi: 10.1016/j.bpj.2017.11.008.

[28] P. G. Miller and M. L. Shuler, 2016 "Design and demonstration of a pumpless 14 compartment microphysiological system," *Biotechnol. Bioeng.*, vol. 113, no. 10, pp. 2213–2227, doi: 10.1002/bit.25989.

LOGIC
Journal of Engineering Design and Technology
Vol. 21 No.1 March 2021; p. 14 - 22

p-ISSN : 1412-114X
e-ISSN : 2580-5649
http://ojs.pnb.ac.id/index.php/LOGIC

RIVER TRANSPORT PLANNING STRATEGY ANALYSIS USING SWOT AND AHP METHODS

Yega Mardiansyah[1], Eva Azhra Latifa✉ [2]

1) Department of Civil Engineering, Politeknik Negeri Jakarta, Jl. Prof. Dr. G.A Siwabessy, Kampus Baru UI, Depok 16424
2) Department of Civil Engineering, Politeknik Negeri Jakarta, Jl. Prof. Dr. G.A Siwabessy, Kampus Baru UI, Depok 16424

Corresponding email [1)] :
yegamardiansyah279@gmail.com
evaazhra@gmail.com ✉

Abstract. Tangerang City is the largest city in Banten Province and the third largest city in Greater Jakarta area which is split by one of the major rivers on the island of Java, namely the Cisadane River. With the increasing number of population and vehicle ownership, it is necessary to develop a public transportation network to reduce traffic volume and meet the needs of urban public transportation that is fast, easy, safe and comfortable for the citizen. The existence of the Cisadane River in Tangerang City has the potential to be developed into a public transportation route in the form of a waterway. Therefore, the right strategy is needed in the planning of river transportation. This study aims to analyze the influencing factors and strategic priorities in planning river transportation as urban public transportation using the Strength Weakness Opportunity Threat (SWOT) and Analytical Hierarchy Process (AHP) methods. In this study, a questionnaire was given to eight expert respondents related to river transportation. The respondents' answers were tested for consistency with AHP to ensure the accuracy of the answers. From the results of the SWOT analysis, it was obtained the strengths, weaknesses, opportunities and threats in river transportation planning, as well as the ST (Strength-Threat) strategy with the largest weight of 3.99 as the strategy to be used in planning river transportation. Then from the AHP analysis, the strategic priority results in planning river transportation were obtained, namely the safety criteria with a weight of 0.29 and alternative strategy for life jackets with a weight of 0.117853325 as the main priority in carrying out the chosen strategy. Respondents' answers are fairly accurate with a consistency ratio of 2.58% ≤ 10%.

Keywords : AHP; alternatives; river transportation; strategies; SWOT.

1. INTRODUCTION

Congestion is a problem that is always faced by big cities in Indonesia. With the continued growth of the population, followed by the rampant of urban development, it will increase the number of trip generators which have an impact on the accumulation of vehicles on a road in a sustainable manner. Vehicle growth that is not matched by an increase in road capacity is one of the factors causing congestion [1].

To reduce the number of motorized vehicles on roads, it is necessary to develop a public transportation network that is fast, easy, safe and comfortable for the citizen. In addition to developing transportation networks in the form of buses and trains, river transportation in the form of boats can also be developed in the Greater Jakarta area which is close to the riverside areas.

The transportation system is a unity of elements and components that support each other and work together in the procurement of transportation that has a certain range of service [2]. The transportation system in an area can be used as an indicator of regional development because in a transportation system there is a need for transportation.

One of the alternative forms of handling the current urban transportation system is to use the Transport Demand Management (TDM) concept. Transport Demand Management (TDM) is the implementation of strategies and policies that aim to maximize the efficiency of the urban transportation system by limiting the unnecessary use of private vehicles and encouraging more effective, healthy and environmentally friendly modes of transportation such as public transportation, walking, cycling and so on [3].

The Cisadane River is one of the major rivers on the island of Java, which divides Tangerang into two parts, and has the potential to be developed as a public transportation route in the form of a waterway. The government can develop the potential for river transportation not only as a means of crossing but can be developed into a means of transportation both for public and for tourism which is an alternative solution to reduce congestion and can attract tourists to support the concept of developing a riverside area as a waterfront city [4].

The purpose of this study is to analyze the right strategy in planning the Cisadane River transportation, and to determine priority strategic steps for planning river transportation as an urban public transportation in Tangerang.

This research is expected to provide benefits to the local government as an effort to solve congestion problems, meet public transportation needs for the citizen and become literature for academics in further research related to river transportation.

Ferry transportation/ river crossing transportation is transportation that functions as a bridge connecting the road network and / or railroad network separated by water to transport passengers and vehicles and their cargo. The function of river crossing as a moving bridge is the movement of traffic and transfer of passengers and vehicles and their cargo by ferry/boat [5].

River fairway are waters of rivers and lakes, river estuaries, a lane that connect two or more river estuaries which constitute a single unit of river and lake fairway which in terms of depth, width and other shipping barriers, it is considered safe to navigate. [6].

Factors that affect the transportation service system are transportation costs, the physical condition of the means of transportation, the route traveled, service crews and others. Estimated transportation demand is used as a basis for determining the means (fleet) of transportation that must be provided in the future and what mode is suitable for a particular activity to be held [7].

SWOT, which stands for strength, weakness, opportunity and threat, was created as a model for analyzing an organization that aims at profit and non-profit as a means to better understand the state of an organization comprehensively [8]

SWOT analysis, which stands for strength, weakness, opportunity, and threat, identifies several factors in a systematic way to formulate a strategy [9]. This analysis is based on logic that is useful for maximizing strength and opportunities, but can also minimize weakness and threats. The success of implementing the strategy is influenced by making the right decision.

To perform a SWOT analysis, it begins with collecting questionnaire data for phase 1, then analyzed by the following steps: Performing IFAS and EFAS calculations; Analyze and interact with the combination of strategies using the SWOT matrix by combining internal and external factors; Formulate alternatives and strategy choices with the SWOT matrix and produce SO, WO, ST, and WT strategies. Then compared the total strategy ratings and sought the largest; And you will get the results of the strategy that will be used.

In essence, the Analytical Hierarchy Process is a model in comprehensive decision making and takes into account various things that have both qualitative and quantitative characteristics. In the decision making model using the Analytical Hierarchy Process, it generally tries to cover the shortcomings of the previous models. Analytical Hierarchy Process also allows the system structure and environment into interconnected components and then unites by measuring and managing the impact arising from system error components [10].

AHP defines multi-factor and multi-criterion problems that depend into a single hierarchy. With a hierarchy, a complex problem can be arranged into each group and then arranged into a hierarchical form until the problem appears more structured and systematic [11].

AHP analysis starts from the results of the second stage questionnaire obtained, the assessment data is entered into the AHP model. The AHP model used is a comparison method for alternative solutions using the basic concept of a matrix.

To get the smoothing of answers from many respondents, the smoothing method is done by using the geometric mean method to get one particular value from all of these values [12]. Here are the geometric mean equations:

$$b_{ij} = (z_1 \times z_2 \times z_3 \ldots \times z_n)^{1/n} \quad (1)$$

n fact, absolute consistency will not be obtained. By comparing CR and RI, parameters will be obtained in determining the level of consistency in the matrix, which is called the Consistency Ratio (CR), with the following equation:

CR = CI / RI (2)

The tolerance for the consistency of a comparison matrix is 0.1. Thus, a comparison matrix will be called consistent if the CR is less than 0.1 [10]. Consistency testing is also carried out on a hierarchy with the same equations and tolerances.

The final step is to determine the alternative strategy that will be selected by determining the global weight (Wg). The alternative global weight is determined by multiplying the weight of criterion A with each alternative weight in criterion A and is carried out on each alternative for each criterion.

Wg alternative = W criteria A x W Alternative Strategy A (3)

2. METHODS

The following are the stages in this research:

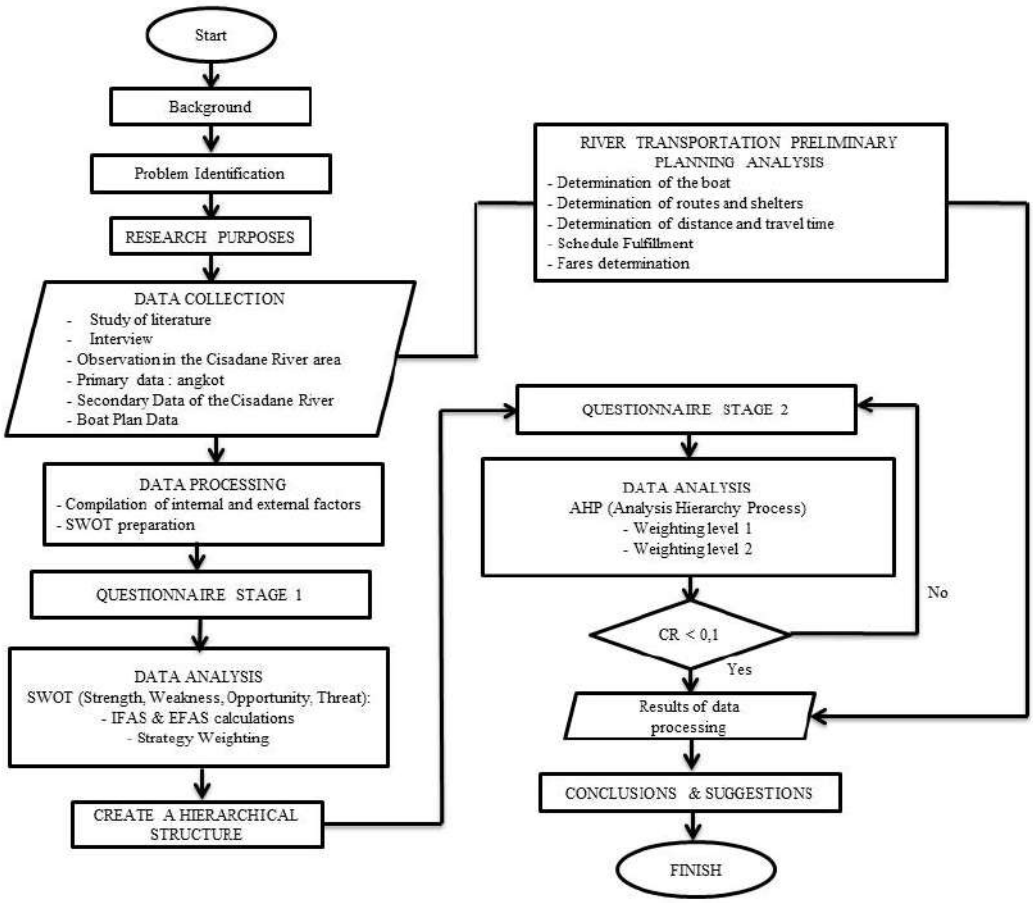

Figure 1. Flow Chart

Based on **Figure 1**, this research begins with determining the background, problem identification and objectives. Data collectionwas carried out by literature studies, interviews, field observations and data from related agencies. Then the distribution of the first stage questionnaire was carried out, the results were analyzed using the SWOT method and followed by the distribution of the second stage questionnaire, the results were analyzed using the AHP method. From the results of the analysis, it will produce a priority order for river transportation planning strategies. Besides that, an analysis of the initial planning of river transportation was also carried out, so as to obtain a mature strategy in building urban river transportation.

3. RESULTS AND DISCUSSION

3.1 SWOT Analysis

From the results of the SWOT questionnaire, the weight and rating calculations were carried out through the IFAS and EFAS matrix calculations. From the IFAS and EFAS calculations, the strategic weight values for the four factors can be seen in the following table:

Table 1. Weigthed Value of SWOT Strategy

Strategy	Weighted Value
Strength (S)	2.25
Weakness (W)	1.07
Opportunity (O)	1.62
Threat (T)	1.74

After analyzing the factors and weighting it, the next step is to interact with a combination of internal and external strategies to obtain strategic alternatives in river transportation planning. The strategic combination interactions consist of: SO (Strength-Opportunity) strategy which is a combination of strength and opportunity strategies; ST (Strength-Threat) strategy which is a combination of strength and threat strategies; the WO (Weakness-Opportunity) strategy which is a combination of weakness and opportunity strategies; and the WT (Weakness-Threat) strategy which is a combination of weakness and threat strategies. The results of the strategy combination interaction can be seen in table 2.

Table 2. Weigthed Value of Strategy Combination Interaction

Strategy	Weighted Value
Strength - Opportunity (SO)	2.25 + 1.62 = 3.87
Strenght - Threat (ST)	2.25 + 1.74 = 3.99
Weakness - Opportunity (WO)	1.07 + 1.62 = 2.69
Weakness - Threat (WT)	1.07 + 1.74 = 2.80

From the results of the interaction of the strategy combination, the final result of the ST (Strength - Threat) weight is 3.99 as the highest weight that will be used as a strategy in river transportation planning which will then be calculated priorities through AHP analysis.

The results of the combination of Strength and Threat (S-T) strategies are: implementing a payment system that is cheap, easy and practical; provide comfortable facilities and infrastructure for the passengers; choosing a stopping point in a strategic area; ensure the safety of passengers; as well as anticipating floods / rainy season. Then it is concluded into criteria: payment, facilities and infrastructure, selection of stopping points, safety and security.

3.2 AHP Analysis

From the data, the final results of the SWOT analysis are then used as criteria in the AHP analysis. Then, several proposed alternative strategies (sub-criteria) were obtained from literature studies and also the input from respondents.

From the data of AHP questionnaire to 8 selected respondents, a pairwise comparison scale matrix between criteria and between sub-criteria (alternative strategies) is made. The geometric mean answer smoothing method is used in the pairwise comparison of criteria and subcriteria (alternative strategies).

Furthermore, consistency testing is carried out on each comparison matrix, namely the criteria comparison matrix and strategy alternatives. The consistency test of the comparison matrix aims to determine the consistency of a comparison matrix. If the CR (Consistency Ratio) exceeds 10% or 0.1 then the matrix is inconsistent and needs to be corrected or re-questionnaire. In the comparison between criteria, the CR value was 0.03 or 3%, the alternative payment strategy was 0.00021 or 0.021%, the alternative strategy for selecting a stop point was 0.07 or 7%, an alternative safety strategy was 0.04 or 4%, alternative facilities and infrastructure strategy was 0.01 or 1% and alternative security strategy was 0.02 or 2%.

From the results of the hierarchical consistency test, the CRH value was 0.0258 or 2.58%, so the answers from the respondents could be considered consistent (CRH <0.1).

From the calculation of global weight priority determination, the highest weight was the safety criterion with a weight of 0.29, as well as an alternative life jacket with a value of 0.117853325, so that safety aspects and the availability of life jackets are the most important strategies in planning urban river transportation.

3.3 Planning Analysis

River transportation on the Cisadane River (Cisadane Waterway) is planned to be on the Cisadane River flow path in Tangerang City along +/- 11 km from the upstream river at the border of Kota Tangerang and Kota Tangerang Selatan downstream at the Pasar Baru Dam. There are 6 shelters planned with the initial operation of 5 boats.

Figure 2. Shelter Plan (A)

Figure 3. Shelter Plan (B)

Figure 4. Shelter Plan (C)

The boat planned is a passenger boat with a capacity of 50 seated passengers + 18 standing passengers with a maximum speed of 30 knots.

The following is the fairway planned for this river transportation:

Figure 5. Route Plan Map

Boat travel time is obtained by dividing the distance by the speed and then multiplying by 60 to get the time in minutes. Boat speed is obtained based on boat data. The following is a table of distances and travel times between stopping points / shelters:

Table 3. Distance and Travel Time

Shelters	Distance (km)	Travel Time (minutes)
Bendungan Pasar baru (A)		
	0.94592	1.135104
Pintu Air (B)		
	1.30848	1.570176
Pasar Lama (C)		
	2.13727	2.564724
Cikokol (D)		
	3.34775	4.0173
Karawaci (E)		
	3.05004	3.660048
Gading Serpong (F)		
Total	10.78946	12.94735

Taking the example of a river transportation video on the Chao Praya River in Bangkok, an analysis was carried out so that the calculated stop time was obtained from the boat starting to reduce speed then stopping to pick up and drop off passengers until just after the boat had tightened its speed again, which was 1.2 minutes which was then rounded to 1.5 minutes, so the total estimated time for one sailing travel (Bendungan PB Shelter – Gading Serpong Shelter - Bendungan PB Shelter) is 26.447 minutes.

Fulfilment of the schedule is one of the minimum service standards for deployment for ship/ boat operations [13]. Fulfilment of the schedule referred to consists of ship travel schedules, ship operating schedules, operational readiness schedules, rest schedules and docking schedules. Ship operating schedule is for 11 months or 330 days per year and ship dock schedule for 1 month or 30 days per year [14].

During peak hour, the boat heading time is planned every 10 minutes and non-peak hours for every 15 minutes. With 5 boats, 1 boat will start its journey every 50 minutes during peak hours and 75 minutes during non-peak hours, where 26.447 minutes is the time for one sailing travel and the rest is the time for resting the boat at the first shelter.

Fare determination is based on the calculation of the basic fare for ferry transportation, which is the total main cost divided by production over a period of 1 (one) year. Main cost consists of components of direct costs and indirect costs. In accordance with the ferry fare calculation formulation in the Regulation of the Minister of Transportation of the Republic of Indonesia No. 66 of 2019 [14], then the passenger fare per kilometre is obtained of Rp. 993.47 / km. By multiplying the distance with the fare per kilometre, the fare between the shelters are as follows:

3.4 Strategy Priority Analysis

Based on the results of the analysis of the five criteria, a strategic priority order is obtained starting from the provision of life jackets, boat maintenance, river discharge control, integrated other modes, safety card, boat facilities, easy access, technical engineering on bridge, river depth control, pedestrian access , activity centers, selection of boat types, practical payments, information systems, low costs, easy payments to waiting room facilities.

Life jacket

Life jackets are one of the emergency rescue equipment in a state of danger for the safety aspects of passengers [13]. The life jackets is placed under each passenger seat, under the driver's seat, under the closest seat to the standing passenger and the boat conductor. The available life jackets are 110% of the capacity of the boat [13], which are stored in the storage area on the boat or near the boat conductor.

Boat maintenance

Boat maintenance must be carried out regularly to ensure the safety of the passengers. Boat maintenance includes: daily (cabin) maintenance of the boat, maintenance of boat safety equipment, maintenance of boat equipment and supplies, maintenance of boat engines and pumps, periodic painting and cleaning of the hull, periodic replacement of lubricants and grease [14]. There must also be 1 shipyard for maintenance.

River discharge control

River discharge control is intended to determine the safety of river discharge for boats to pass through, carried out in collaboration with the Meteorology, Climatology and Geophysics Agency and the Ciliwung-Cisadane River Basin Development Agency to monitor river discharge and rainfall intensity at monitoring posts, because during the flood season and high rainfall intensity, rivers are very dangerous when traversed by boats.

For recommendations to anticipate high river discharge conditions, it can be done by building a dam at the upstream of the Cisadane river in Tangerang City area to reduce the high flow of the Cisadane river during rainy / flood conditions. The dam can also be installed with a net / filter to keep the garbage coming from upstream (South Tangerang and Bogor) before entering the river in Tangerang City area, which can reduce the comfort for cisadane river transportation passengers as applied to the Manggarai dam.

Integrated other modes
Each designated shelter point must have integration with other modes so that public transportation in Tangerang City can be connected to each other and make it easier for passengers of public transportation to switch the transportation modes.

Safety instruction card
A safety instruction card must be available in each passenger seat pocket which contains the safety aspects in the boat and how to save yourself in a dangerous situation on the boat.

Boat facilities
The facilities available on the boat are air conditioning, comfortable seats for passengers, running text and loudspeakers to provide information about stopping points, and comply with the minimum service standards for regular economy passenger's cabin in the comfort category according to Minister of Transportation Regulation No. 62 of 2019 [13] includes: the minimum height of the cabin 1.90 m; passenger seats with at least a width of 50 cm and a length of 50 cm; fan / air conditioner; TV / Video / Audio; trash can; 100% clean area; loudspeaker; and equipped with air vents.

Easy to access
The alternative of easy-to-access strategies means that stopping points should be located in locations that are easily accessible to passengers, have close access to the roads and be linked by sidewalks for pedestrians.

Bridge technical engineering
During the rainy season or when the maximum flood water level occurs, several bridges along the fairway cannot be traversed by boats so it is necessary to anticipate flood conditions through bridge engineering technical on several bridges. From the type of boat that has been determined, has a height of 1.6 meters. so that the height of the bridge clearance during the maximum flood water level must have a height of> 1.6 meters.

River depth control
The control of the river depth is intended to prevent silting in the fairway which can cause the boat hull to get stuck. Previously, it had to be determined in advance the fairway that the boat had to go through. So that the depth can be controlled by periodically dredging the fairway and stopping points.

Pedestrian access
In relation to easily accessible alternative strategies, each stop point / shelter must have pedestrian access. Such access must connect the shelter with sidewalk or with integrated stations and bus stops. Canopy pedestrian access is also recommended to protect pedestrians from rain and sun shine

The hub
The hub means that the determination of the shelter point must consider the location of the activity center / the hub. At the designated shelter points, the six shelters are located near the activity center (hub) / movement points of Tangerang citizen.

Selection of boat types
Selection of boat types is not only based on capacity and facilities provided [13], it is also based on dimensions. The height of the boat must be able to pass the area under the bridges that cross along the fairway or have a maximum height under the bridge clearance height. The dimensions of the hull depth (draft) shall not be greater than the depth of the river along the fairway.

Practical
The practical alternative strategy is that the payment system can be carried out with various non-cash payment systems, from card-based electronic money with various types of merchants to application-based electronic money as a form of transportation mode integration development.

information Systems
The facilities and infrastructure in the information system are in the form of boat departure information screens such as those already in several Transjakarta bus stops; running text and loudspeakers; information boards, wayfinding signage and mode integration guide as well as the availability of information center officers at each shelter who can assist passengers in providing information. So that the information conveyed on the boat to service users can be read and heard and informed

Cheap
Ferry transportation fare are set by the Regent / Mayor for ferry transportation within the city [14]. Cheap payments / fares are not only parameterized at a small nominal value, but also in comparison with existing transportation, *angkutan kota* (local transportation).

Easy
Based on the measurement of the timeliness of queuing in ticket sales services [15], non-cash payment is an easy payment solution for passengers and it will minimize queuing time for ticket purchases. This is accompanied by the availability of self ticket vending machines that make it easier for passengers to buy entrance cards / tickets.

The waiting room
The waiting room is a place provided for passengers before boarding the boat. The facilities and infrastructure in the waiting room include: waiting room seats, trash cans, information facilities (information boards & departure information screens), air conditioning or fans to meet the comfort aspect for passengers.

4. CONCLUSION

Based on the results of the analysis, an appropriate strategy was obtained in planning the Cisadane River transportation to reduce urban traffic congestion, which includes: paying attention to safety aspects by preparing life jackets, safety card in each seat pocket, and boat maintenance; pay attention to security aspects based on the type of boat, river discharge control, bridge technical engineering, and river depth control; provide facilities and infrastructure consisting of boat facilities, waiting rooms, information systems and pedestrian facilities; selecting a stop point based on a location close to the center of activity (hub), integrated with other transportation, and easily accessible; prepare easy, cheap and practical payments. The safety criteria with a weight of 0.29 and the sub-criteria for life jackets with a weight of 0.118 have the greatest weight in the order of priority so that it becomes the main strategy in planning Cisadane River transportation in Tangerang City.

5. REFERENCES

[1] Novalia, Cindy, et al.. 2016. *Analysis and Solutions for Traffic Congestion on City Roads (Case Study on Jalan Imam Bonjol - Jalan Sisingamangaraja).* JRSDD, Vol. 4, No. 1.
[2] Prayogo, F. R., et al.. 2016. *Geographical Information System Application for Locating Type A Passenger Terminal in Klaten Regency.* INKOM Journal Library, Faculty of Geography, Gajah Mada University.
[3] Susantono, B.. 2014. *Transportation Revolution.* Jakarta: PT Gramedia Pustaka Utama.
[4] Kartini, Y.H.. 2013. *Study on the Use of River Transportation in Jambi City*. Journal of Geography UGM.
[5] Government of Indonesia. 2017. *Regulation of the Minister of Transportation No. 104 of 2017 concerning the Implementation of Cross Transportation*. Jakarta: Ministry of Transportation.
[6] Government of Indonesia. 2012. *Regulation of the Minister of Transportation No. 52 of 2012 concerning River and Lake Fairways*. Jakarta: Ministry of Transportation.
[7] Abidin, Zainal. 2016. *Revitalization Study of River Transportation as a Mode of Urban Transportation in Banjarmasin City.* Journal of Civil Engineering, University of Muhammadiyah Surabaya, Vol.1, No. 1.
[8] Fahmi, Irham. 2011. *Decision Making Management*. Bandung: CV. Alfabeta
[9] Rangkuti, Freddy. 2014. *SWOT Balanced Scorecard*. Jakarta: PT Gramedia Pustaka Utama.
[10] Cahyaningsih, L.P.. 2019. *Strategy Analysis of Work Accident Reduction at PT. XYZ by Using SWOT and AHP* [Thesis]. Jakarta: Pancasila University.
[11] Eko, et al.. 2014. *Application of the AHP Method to Determine the Quality of Tumbu Sugar.* Central Java: Muria Kudus University.
[12] Haryanto, E. G.. 2019. *Accident Risk Analysis on Toll Roads using the FMEA and AHP methods.* [Thesis]. Jakarta: State Polytechnic of Jakarta.
[13] Government of Indonesia. 2019. *Regulation of the Minister of Transportation No. 62 of 2019 concerning the Minimum Service Standards for Ferry Transportation.* Jakarta: Ministry of Transportation.
[14] Government of Indonesia. 2019. *Regulation of the Minister of Transportation No. 66 of 2019 concerning the Determination Mechanism and Formulation for the Calculation of Ferry Transportation Fares*. Jakarta: Ministry of Transportation.
[15] Government of Indonesia. 2015. *Minister of Transportation Regulation No. 39 of 2015 concerning Service Standards for Ferry Transportation Passengers.* Jakarta: Ministry of Transportation.

LOGIC
Journal of Engineering Design and Technology
Vol. 21 No.1 March 2021; p. 23 - 30

p-ISSN : 1412-114X
e-ISSN : 2580-5649
http://ojs.pnb.ac.id/index.php/LOGIC

NATURAL LIGHTING OF STUDIO APARTMENT WITH EAST-ORIENTED OPENING

Aisyah Anindya Putri[1], Dyah Nurwidyaningrum ✉[2], Tri Wulan Sari ✉[3]

1,2,3) Department of Civil Engineering, Politeknik Negeri Jakarta, Jl. Prof. Dr. G.A Siwabessy, Kampus Baru UI, Depok 16424

Corresponding email [1)] :
aisyahanindyap@gmail.com
dyah.nurwidyaningrum@sipil.pnj.ac.id ✉
tri.wulansari@sipil.pnj.ac.id ✉

Abstract. Less optimized natural lighting would result in apartment residents being dependent on artificial lighting, thus increasing energy consumption. Building opening orientation considerably influences the natural light intensity. This research aimed to analyze the natural lighting pattern on apartment units with east-oriented opening orientation and determine methods to support the existing condition to be optimized. This research applied the descriptive analysis research method assumed from calculation outcome of the software DIALux. Results indicated a proportion of units in The H-Residence Apartment do not meet the requirements specified by SNI 03 6197-2011, predominantly in the kitchen area. The average light intensity in a day in units with east-oriented opening reached its peak at 08.00 – 09.00 a.m. and decreased towards 16.00 p.m. following the sun path. The light intensity in numerous areas exceeded the requirements significantly. Other factors influencing the natural light distribution are layout and interior element. Several ways to optimize the natural light intensity utilization are adding suitable shading device, using dark-colored interior elements, and considering the sun path in designing building openings.

Keywords : Apartment lighting, Opening orientation, Natural lighting

1. INTRODUCTION

The building sector in Indonesia is the largest energy consumer after the industrial and transportation sector, reckoned at 24% in 2004 and still expected to rise to 39% by 2030. The energy consumption generated by the use of artificial lighting contributes about 15%– 25% to building's total energy consumption [1]. In countries with tropical climate, lighting system that depends on natural lighting from the sun could decrease the use of artificial lighting, thus reducing energy consumption. However, excessive incoming light intensity might cause visual or thermal discomfort, therefore causing apartment residents to block incoming natural light with light control devices [2]. Less optimized natural lighting intensity might result in apartment residents being dependent on artificial lighting, accordingly increasing energy consumption per unit so as affecting the expenses paid by the residents [3].

One of the factors influencing the penetration depth of natural light is window or opening orientation [4], [5]. This theory is based on the sun path throughout the day that progresses from east to west, influencing the natural lighting received by building opening depending on its orientation. The optimal opening orientation for buildings in Jakarta that is located in the equator area would be facing south or north to avoid excessive radiation and high temperature [6, 7].

This research aims to analyze natural lighting pattern on apartment units with east-oriented opening orientation and determine methods to support the existing condition to be optimized. Research simulation was run in natural lighting condition, meaning no lamps were switched on, and without assessing the glare factor. Regulation used to examine the average natural lighting intensity calculation result is SNI 03-6197-2011. This

research can be used as a recommendation in lighting system design and reference to advance the natural lighting issue on apartments or high-rise buildings so that it could be further optimized.

2. METHODS

This research was done on studio apartments in both empty and furnished setup in The H Residence Apartment located at Jl. MT Haryono Kav 6-7, Cipinang, Cempedak, East Jakarta. The studio unit area is 37 m^2 with 1.3 m^2 balcony and 2.7 m floor-to-roof height. Referring to **Figure** 1, the rooms inside consist of a bedroom, a kitchen area, and a bathroom.

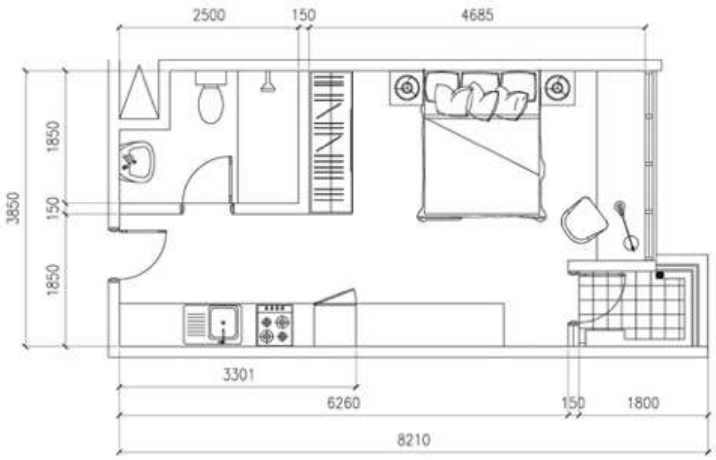

Figure 1. Studio Apartment Plan

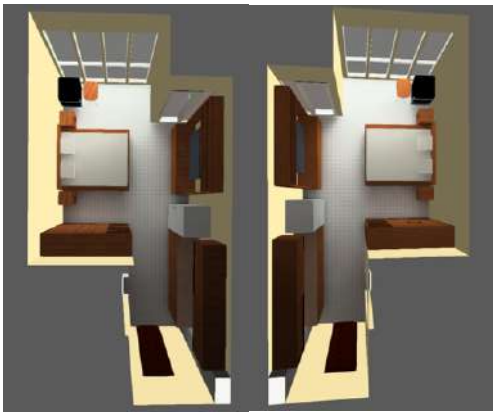

Source : Document of The H Residence Apartment Management

Figure 2. Unit with South-corner Balcony (left) and North-corner Balcony (right)

As shown in **Figure 2**, the unit layout is divided in two types, one of them with balcony at the unit's south corner and the other at the north corner. A wall divides each unit's balcony, causing the south-corner balcony to end up with the wall on the right side, while the north-corner with the wall on the left.

This research began with searching the unit property data consist of the size and materials used for the interior elements. Then, a model was constructed using DIALux evo 9 for units with both empty and furnished setup. Afterwards, a simulation was run in various conditions namely at 8.00 a.m., 12.00 p.m., and 4.00 p.m. on June 21 and December 21 2020. Working plane was set on 0.75 m from the ground [9]. Digital simulation was chosen because of the high accuracy rate and the ability to cover plenty parameters with realistic result [10].

This research applies the descriptive analysis method that shows detailed data through words [11]. Average natural lighting intensity acquired from digital simulation was compared to requirements stated in SNI 03-6197-2011 about Energy Conservation on Lighting System, specifically 250 lux for bedroom and kitchen [12]. Further calculation was done in Microsoft Excel, with the 15th floor representing other floors due to its central position.

Table 1. Interior Elements Description

The H Residence Apartment	DIALux Evo 9
Painted Jotun	Standard Wall - white 90% 1000 (Green Beige)
Homogenous Tile - white	Tile, square, white 76%
Rustic Tile	Default floor element
Painted Ceiling - white	Default ceiling material
Concrete Table - white	Painted white 90%
Laminated Door	Lemon wood dark 9%
Aluminum & Glass Wall	Frame 9006 (white aluminum), default transparent glass
Bed	Pear dark 11% and 7044 (Silk grey)
Cupboard	Pear dark 11%
Kitchen counter	Pear dark 11% and Linoleum 1 38%
TV Set	Pear dark 11%
Night table	Pear dark 11%
Sofa	Painted black 0% and grey 32 %
Table	Pear dark 11% and default material 50%

T**able 1** shows the comparison between material used in existing apartment and digital simulation. Aside from wall, floor, ceiling, and opening, a set of furniture was added with heavy reference to actual studio apartment presented in The H Residence Apartment. All materials used in simulation model were adjusted to match the actual model, using the materials provided by DIALux evo 9 library.

3. RESULTS AND DISCUSSION

3.1 Average Lighting Intensity Summary

Table 2 and 3 show the calculation result summary from DIALux software in which numerous areas do not meet the requirements specified by SNI, specifically the kitchen area. The kitchen area possesses low average intensity due to its location being far from window opening and surrounded by dark-colored interior elements, namely entrance and bathroom door

Table 2. Average Lighting Intensity Summary Compared to SNI – June 21 2020

Time	Apartment Setup	Minimum Intensity Met	Minimum Intensity Not Met
8.00 a.m.	Empty	100.00%	0.00%
	Furnished	50.00%	50.00%
12.00 p.m.	Empty	58.33%	41.67%
	Furnished	50.00%	50.00%
4.00 p.m.	Empty	50.00%	50.00%
	Furnished	50.00%	50.00%

Table 2 indicates that at 8.00 a.m. all units with empty setup meet the requirement, whereas only 50% furnished units do. At 12 p.m., 58.33% empty units and 50% of furnished units meet the requirement. At 4 p.m., both empty and furnished units only meet the requirement by 50%.

Table 3. Average Lighting Intensity Summary Compared to SNI – December 21 2020

Time	Apartment Setup	Minimum Intensity Met	Minimum Intensity Not Met
8.00 a.m.	Empty	100.00%	0.00%
	Furnished	50.00%	50.00%
12.00 p.m.	Empty	58.33%	41.67%
	Furnished	50.00%	50.00%
4.00 p.m.	Empty	50.00%	50.00%
	Furnished	50.00%	50.00%

Table 3 indicates that at 8.00 a.m. all units with empty setup meet the requirement, whereas only 50% furnished units do. At 12 p.m., 58.33% empty units and 50% of furnished units meet the requirement. At 4 p.m., both empty and furnished units only meet the requirement by 50%.

3.2 False-Color Diagram

Based on false color diagram generated in DIALux for unit number 1528 (Room 7, top, south-corner balcony) and number 1530 (Room 5, bottom, north-corner balcony) with both empty and furnished setup, on June 21 and December 21 the highest lighting intensity is located at the main window and the lowest being at the kitchen area.

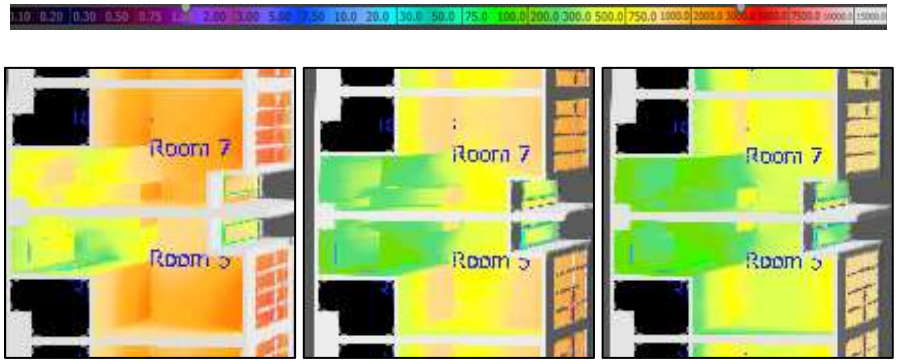

Figure 3. False Color Diagram for Empty Unit – June 21 at 8.00 a.m. (left), 12.00 p.m. (middle), 4.00 p.m. (right)

Figure 3 shows a drastic change of natural lighting intensity with 8.00 a.m. being the time it is highest. The intensity gradually decreased throughout the day. The area with highest lighting intensity, marked by the color orange and red, ranging from 2000 – 7500 lux, is located near the window opening. While, the area with lowest lighting intensity, marked by the color blue and green, ranging from 5 – 300 lux, is located around the kitchen area.

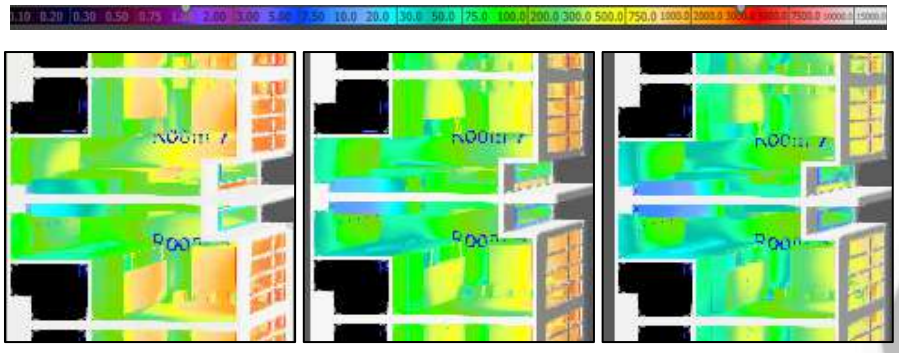

Figure 4. False Color Diagram for Furnished Unit – June 21 at 8.00 a.m. (left), 12.00 p.m. (middle), 4.00 p.m. (right)

Figure 4 shows the same progress, although not as drastic as the empty setup, lighting intensity reaches its peak at 8.00 a.m. The area with highest lighting intensity, marked by the color red and orange, ranging from 2000 – 7500 lux, is located near the window opening. While, the area with lowest lighting intensity, marked by the color purple to green, ranging from 0 – 300 lux, is located around the kitchen area.

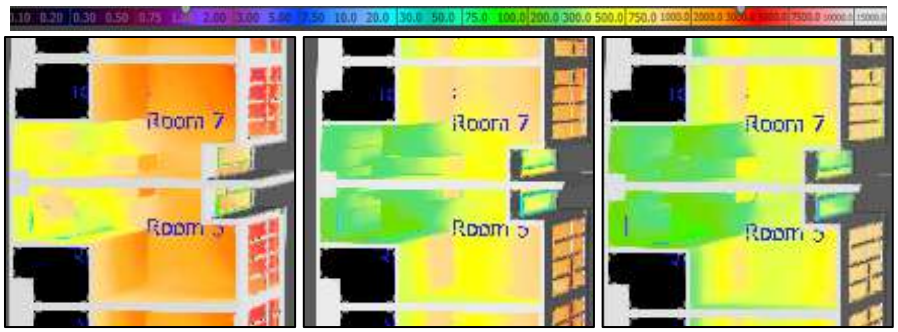

Figure 5. False Color Diagram for Empty Unit – December 21 at 8.00 a.m. (left), 12.00 p.m. (middle), 4.00 p.m. (right)

Figure 5 shows that similar occurrence with Figure 4 happened, with the lighting intensity reaching its peak at 8.00 a.m. and gradually decreases throughout the day. However, intensity produced on December 21 is far higher than on June 21. The area with highest lighting intensity, marked by the color red and orange, ranging from 2000 – 7500 lux, is located near the window opening. While, the area with lowest lighting intensity, marked by the color blue and green, ranging from 5 – 300 lux, is located around the kitchen area.

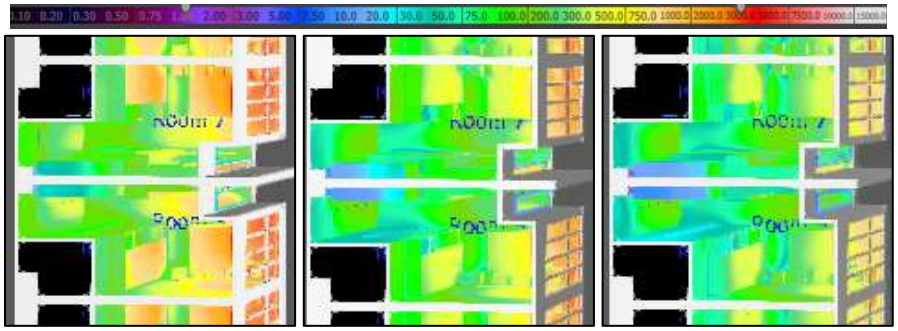

Figure 6. False Color Diagram for Furnished Unit – December 21 at 8.00 a.m. (left), 12.00 p.m. (middle), 4.00 p.m. (right)

Figure 6 shows similar progress with Figure 5, although with far higher lighting intensity. The area with highest lighting intensity, marked by the color red and orange, ranging from 2000 – 7500 lux, is located near the window opening. While, the area with lowest lighting intensity, marked by the color purple to green, ranging from 0 – 300 lux, is located around the kitchen area.

3.2 Lighting Intensity Pattern

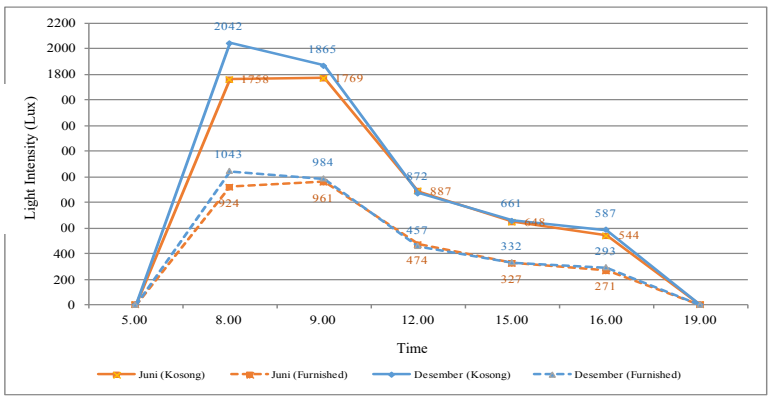

Figure 7. Daily Natural Lighting Intensity – Unit No. 1528

Figure 7 shows that on June 21, the initial lighting intensity was 1758 lux for empty setup and 924 for furnished setup then it increased by 0.63% for empty setup and 4% for furnished setup towards 9.00 a.m., being the time it reached its peak at 1769 lux and 961 lux. A decrease of 49% took place towards 12.00 p.m. where lighting intensity became 887 lux and 474 lux. Towards 4.00 p.m., there was a decrease of 38.67% for empty setup to 544 lux and 42.83% for furnished setup to 271 lux. On December 21, highest lighting intensity was at 8.00 a.m. namely 2042 lux for empty setup and 1043 lux for furnished setup. A decrease of 57% took place towards 12.00 p.m. where lighting intensity became 872 lux and 457 lux. Towards 4.00 p.m., there was a decrease of 32.68% for empty setup to 587 lux and 35.89% for furnished setup to 293 lux.

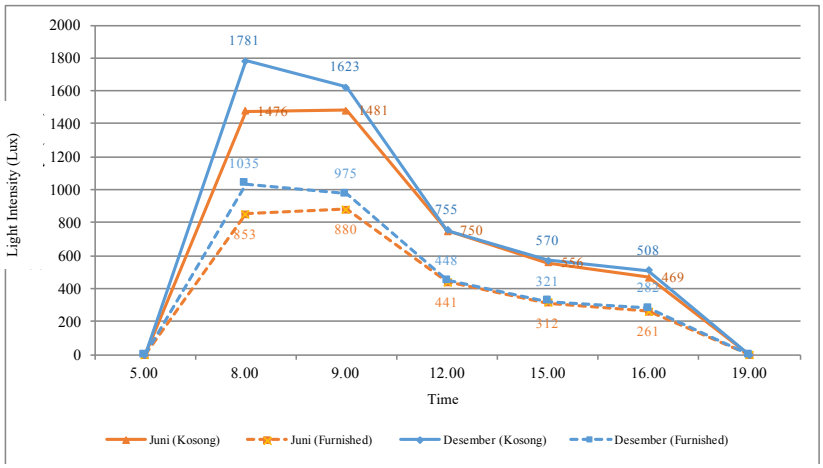

Figure 8. Daily Natural Lighting Intensity – Unit No. 1530

Figure 8 shows that on June 21, the initial lighting intensity is 1476 lux for empty setup and 853 lux for furnished setup then it increases by 0.34% for empty setup 481 lux to 3.17% for furnished setup to 880 lux. A decrease of 49% takes place towards 12.00 p.m. where lighting intensity becomes 750 lux and 441 lux. On December 21, highest lighting intensity is at 8.00 a.m. namely 1781 lux for empty setup and 1035 lux for furnished setup. A decrease of 57% takes place towards 12.00 p.m. where lighting intensity becomes 755 lux and 448 lux. Towards 4.00 p.m., there is a decrease of 32.72% for empty setup to 508 lux and 37.05% for furnished setup to 282 lux.

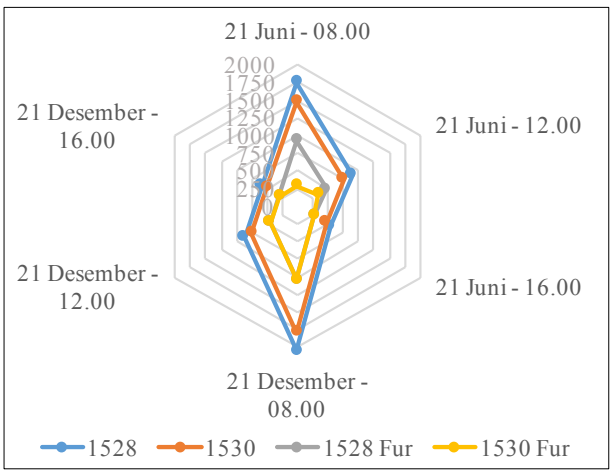

Figure 9. Radar Diagram of Natural Lighting Intensity for East-Oriented Unit

Based on **Figure 9,** both units reached peak lighting intensity between 08.00 – 09.00 a.m. in accordance with the sun path moving from east to west causing the culmination to happen in the morning. The average natural lighting intensity declines in the evening following the sun moving west [13]. Apartments with opening not meeting the requirements might result in unit receiving sufficient lighting intensity for only half a day since there will be a drastic decrease after noon.

Apartment number 1528 with south-corner balcony possesses higher average lighting intensity in comparison with apartment number 1530 with north-corner balcony. This occurrence is caused by a 3° deviation to the south on the building, therefore making apartment number 1528, with a wall dividing each studio located at the right side of the balcony, to receive more light from the sun.

Average lighting intensity from both units far exceeded the minimum requirements stated in SNI. While maximum requirements are not mentioned, requirements of maximum 300 lux for bedroom and 750 lux for kitchen area are mentioned in IESNA [14]. Excessive average lighting intensity might cause visual discomfort such as glare and thermal discomfort or high temperature, causing the residents to block incoming light and using artificial light instead [15]. High average intensity might be caused by the area of window opening, creating visual discomfort [16].

Bigger opening area causes the window-to-wall-ratio (WWR) to exceed reasonable limit. While there is a research that states the energy used for artificial lighting increases as WWR decreases, it is possible for residents to cover openings instead to avoid glare and heat, thus increasing the use of energy for artificial lighting [17]. Other previous research states energy use will decrease as WWR decreases [18].

In both units, average intensity on December is considerably higher compared to June. Because the building coordinate is located at 6°14'S and 106°52'E, lighting intensity will differ between the two solstices. This happens because sun's latitude on June 21 is situated at 23.5°N and on December 21 at 23.5°S.

Figure 9 also indicates that empty unit possesses higher average lighting intensity compared to furnished unit caused by the dark-colored interior elements where the reflection factor is lower. Interior elements with dark colors might cause 50% decrease of lighting intensity [19]. Furthermore, the materials used also influence visual discomfort. Materials such as glass and wood can be used for interior wall, gypsum board can be used for ceiling and ceramic for tiles [20].

4. CONCLUSION

East-oriented opening possesses higher average of natural lighting intensity in the morning and decreasing throughout the day given the sun path moving from east to west. Average intensity received by all units exceeds the requirement stated in SNI 03-6197-2011 and SNI 03-6575-2011. Several ways that can be applied to optimize unit's natural lighting state are adding horizontal shading device and using dark-colored interior elements. Preliminary to designing building opening, a suitable opening orientation in accordance with the sun path must be considered. Further similar research to concern the unit layout aspect and external factors from surrounding environment.

5. REFERENCES

[1] Pemerintah Provinsi DKI Jakarta, *Introduction – Green Building User Guidance*, 2012
[2] C. R. Putri, *Efisiensi Pencahayaan Pada Bangunan Gedung Dengan Bantuan Perangkat Lunak (Studi Analisa Pada Gedung Sarana Jaya 3 Pramuka-Jakarta Timur)*, Jakarta: State University of Jakarta, 2015.
[3] Y. Suriansyah, "Kualitas Pencahayaan Alami pada Enam Rumah Susun di Bandung, Cimahi, Soreang, dan Baleendah" in *Prosiding Seminar Nasional dan Pameran Kebijakan Strategi Pengadaan Perumahan Berkelanjutan di Indonesia 22 – 23 November 2011*, Bandung, Indonesia.
[4] M. Boubekri, *Daylighting Design: Planning Strategies and Best Practice Solutions*, USA: Elsevier Ltd, 2014.
[5] Y. Suriansyah, *Potensi Pencahayaan Alami pada Rumah Susun Sarijadi Bandung*, Bandung: Lembaga Penelitian dan Pengabdian Masyarakat Universitas Parahyangan, 2013.
[6] Pemerintah Provinsi DKI Jakarta, *Panduan Pengguna Bangunan Gedung Hijau Jakarta Vol. 3 Sistem Pencahayaan*, 2012.
[7] I. Basthian, "Pengaruh Desain Bukaan pada Selubung Bangunan Terhadap Efisiensi Energi pada Rumah Susun Sederhana Sewa", rijurnal.lemlit.trisakti.ac.id, [retrieved: August 2, 2020].
[8] Pemerintah Provinsi DKI Jakarta, *Panduan Pengguna Bangunan Gedung Hijau Jakarta Vol.1 Selubung Bangunan*, 2012.
[9] A. Mandala, A. Ritva, and R. Gunawan, *Komparasi Metode Perhitungan Pencahayaan Alami (Perhitungan Manual, Simulasi Maket, dan Simulasi Digital)*, Bandung: Lembaga Penelitian dan Pengabdian Masyarakat Universitas Parahyangan, 2016.
[10] SNI 03-6575-2011, *Tata Cara Perancangan Sistem Pencahayaan Buatan pada Bangunan Gedung*, 2011.

[11] Badan Pengembangan Bahasa dan Perbukuan. *Kamus Besar Bahasa Indonesia Daring*. https://kbbi.kemdikbud.go.id/, [retrieved: 21 Maret 2020]
[12] SNI 03-6197-2011, *Konservasi Energi pada Sistem Pencahayaan*, 2011.
[13] F. S. Fadzil et al, "The Impact of Varied Orientation and Wall Window Ratio (WWR) Distribution in Residential Room", in *International Symposium on Construction in Developing Economies: Commonalities Among Diversities*, 2011.
[14] Illuminating Engineering Society, *IES Lighting Handook 10th Edition*, Cary: Illuminating Engineering Society, 2011.
[15] N. Lechner, *Heating, Cooling, Lighting*, New Jersey: John, Wiley & Sons, 2015
[16] D.L. Sari, A.M. Nugroho, and B.S. Sudarmo, "Pengaruh Window-To-Wall Ratio Terhadap Kenyamanan Visual pada Apartemen Mahasiswa di Surabaya", *Jurnal Mahasiswa Jurusan Arsitektur, vol. 5 no. 1*, 2017.
[17] S. Pathirana, A. Rodrigo, dan R. Halwatura, "Effect of Building Shape, Orientation, Window to Wall Ratios and Zones on Energy Effciency and Thermal Comfort of Naturally Ventilated Houses in Tropical Climate", *International Journal of Energy and Environmental Engineering, vol 10*, 2019.
[18] J. M. Kim et al, "An Effect of the Change of Orientation and Window Area Ratio upon Building Energy Requirement in Apartment Housings", *KIEAE Journal,vol. 13 no. 2*, 2013.
[19] P. Kinasih dan R. Prayogi, *Penilaian* Green Building *dari Aspek Kualitas Udara dan Kenyamanan Ruang pada Apartemen Green Pramuka City*, Depok: State Polytechnic of Jakarta, 2014.
[20] G. Averina and O.T. Putri, "Analisis Pemilihan Material, Pencahayaan, dan Penghawaan pada Apartemen Trillium Surabaya (Kajian Terapan Eko-Interior)" *in Prosiding SEMSINA 31 Oktober 2019*, Malang, Indonesia, National Institute of Technology Malang.

LOGIC
Journal of Engineering Design and Technology
Vol. 21 No.1 March 2021; p. 31 - 39

p-ISSN : 1412-114X
e-ISSN : 2580-5649
http://ojs.pnb.ac.id/index.php/LOGIC

THE COMPARISON BETWEEN THE BOQ OF CONVENTIONAL AND BIM METHOD ON BPJS BUILDING IN CENTRAL JAKARTA

Mutia Hanuun Ufaira Akbar [1], I Ketut Sucita [2], Erlina Yanuarini [3]

1,2,3) Department of Civil Engineering, Politeknik Negeri Jakarta, Jl. Prof. Dr. G.A Siwabessy, Kampus Baru UI, Depok, 16424

Corresponding email [1] :
mutiahanuun@gmail.com
i.ketutsucita@sipil.pnj.ac.id
erlina.yanuarini@sipil.pnj.ac.id

Abstract. In the construction planning process, the calculation of the quantity of each project work was packaged in a Bill of Quantity (BoQ) to complete the project and greatly affected the continuity of the entire construction construction process. With advances in technology in the world of construction, it could simplify planning in built a building and could increased the accuracy of calculations without using assumptions that could increased the volume of work. One of the results of current technological advances was the creation of the Building Information Modeling (BIM) method, a method that was able to simulate all information in a development project into a 3-dimensional model. Currently the use of the BIM method in Indonesia was still limited so that in this research, the aim was to determine the effectiveness of the use of BIM on the accuracy calculation of the volume of the BoQ and to know the percentage comparison. The building project that was used as a comparison was a building with the middle rise building category, namely the Central Jakarta BPJS Building. Based on the research conducted, it was found that the difference between conventional and BIM results on pilecap components was 5%, column 6%, beam 35%, floor slabs 2%, stairs 22%, ceiling 2.26% floor coverings 14% lower than conventional calculations but for the wall component the BIM calculation is 0.78% greater than the conventional calculation. So that the total percentage ratio is 10%, thus this proves that the use of the BIM method in calculating quantity was effective in terms of calculation accuracy.

Keywords : Bill of Quantity; BIM; Construction

1. INTRODUCTION

With the development of the construction industry requires planners and construction service implementers to improve the quality and effectiveness of the construction process. The construction industry requires construction service actors to complete projects in a short time but still with good quality in the most cost efficient manner possible. However, in reality, current construction projects often experience problems, both in collaboration between design modeling and construction analysis [1]. Design modeling which often changes according to field conditions, can increase construction costs and tends to take a long time, and the resources used also become inefficient [2]. Design modeling also affects the volume of preparatory, structural, architectural and mechanical work that is packaged in the BoQ [3]. The conventional method of BoQ, the calculation still uses manual calculations, namely by reference to CAD drawings and Ms. Excel calculations which can be wrong due to human error [4]. This problem can be minimized by utilizing the latest technology, namely BIM at the construction concept stage [5, 6].

The method or sequence of work on a project that is applied is based on related information from all aspects of building work that are managed and then projected into a 3-dimensional model based on technology

[7, 8]. This technology-based concept, namely Building Information Modeling (BIM) [9], where its use can produce buildings with a fast execution process and all the detailed information is contained in one Big Data, it can minimize errors at the construction stage in the Architecture Engineer Construction industry (AEC) of Indonesia [10].

One of the BIM method based software is Autodesk Revit [11,12]. Autodesk Revit can be used for project drawing, project management, project control, and work volume calculation [13,14].

The performance efficiency between conventional methods and the BIM concept in terms of time, human resource and cost requirements for project planning that use applications with the BIM concept can expedite the project planning time twice times faster than the original plan, reduces human resource requirements by 26.66%, and saves employee costs by 52.25% compared to using conventional applications [15].

2. METHODS

The data obtained is processed and analyzed according to the problems that have been identified. Data analysis was performed with the help of several software including; Autodesk Revit, Autodesk CAD, and Microsoft Excel. The research location is the Central Jakarta BPJS Building Project which is on Jl. Central Salemba-Central Jakarta

Research in this study includes several stages. The flow chart in this final project research is presented in Figure 1.

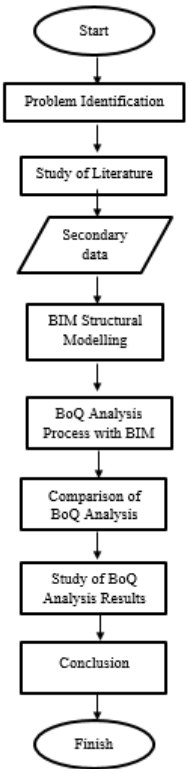

Figure 1. Research Stages Flowchart

3D modeling

This stage uses software in the form of Autodesk Revit with a research period ranging from May 2020 to June 2020.

The 3D modeling steps in Autodesk Revit begin by reading the DED image that has been obtained through the project contractor, then the modeling is divided into structural and architectural modeling which will be explained as follows:

1. Create the main structure starts from the bottom structure, namely the foundation by selecting open families, and selecting the structural foundations template
2. Set the size of the foundation according to the project's drawing based on the DED image by creating a Reference Plane reference line then creating a 3D material with Create Extrusion and changing the default foundation material to concrete
3. After finishing to make the family foundation, then proceed by opening a new project fil for placing the overall building as shown in Figure 2.

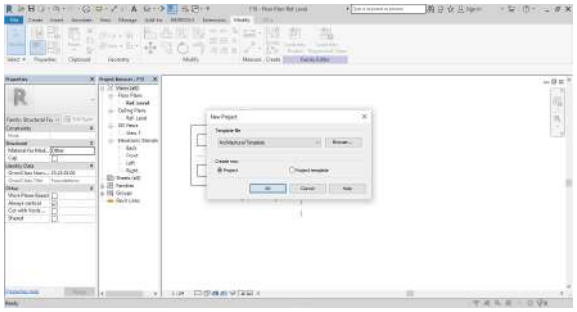

Figure 2. New Project View

4. Adjust the height of the building per floor by creating a level on the Elevations tab as shown in Figure 3.

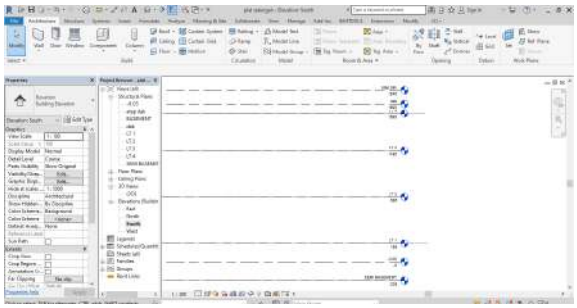

Figure 3. Elevation Tab View

5. Insert AutoCAD drawings as drawing references in Autodesk Revit with the Insert – Link CAD command as shown in Figure 4.

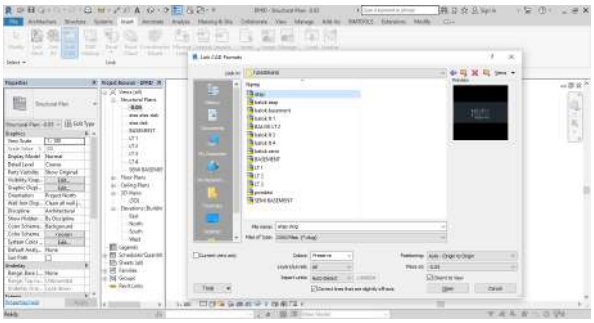

Figure 4. Insert Tab View

6. Building axles created using the grid in the Ribbon Architecture on the Structural Plans tab as shown in Figure 5.

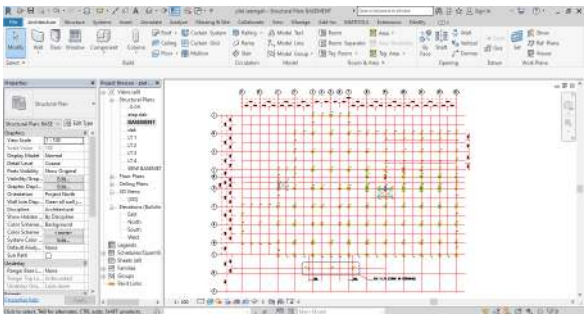

Figure 5. Structural Plans Tab

7. Place the foundation according to the foundation plan into the grid using the Ribbon Structure then selecting Isolated, then there will be a foundation that has been made in the project family as shown in Figure 6.

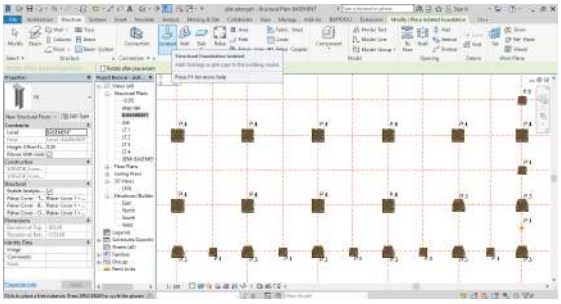

Figure 6. Foundation View in Structural Plan

8. Make the dimensions of the upper structure, namely columns, beams, and floor plates which will be used by entering the existing family and then placing the columns and beams according to the plan as shown in Figure 7.

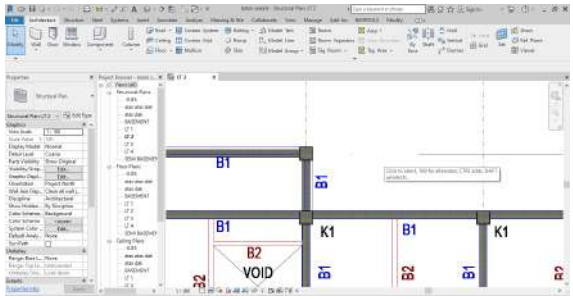

Figure 7. Upper Structure View in Structural Plan

9. Adjust the floor plate placement and empty the voids according to the DED plan by using the Ribbon Structure then selecting Floor as shown in Figure 8.

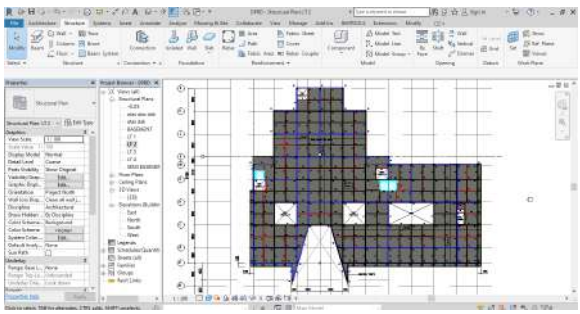

Figure 8. Floor Plate View in Structural Plan

10. Create architectural components starts from the ladder that matches the DED image by changing the initial settings in the Ribbon Architecture then selecting Stair as shown in Figure 9.

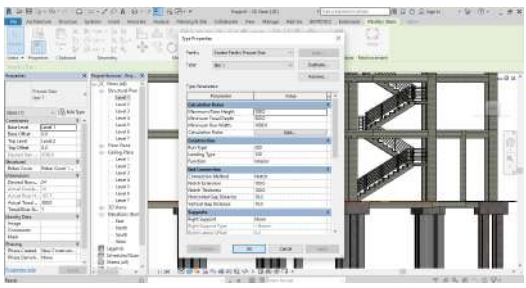

Figure 9. Stair View

11. Create walls, doors, and windows by selecting Wall, Door, and Window in the Ribbon Architecture and changing their Properties to match those used in the project as shown in Figure 10.

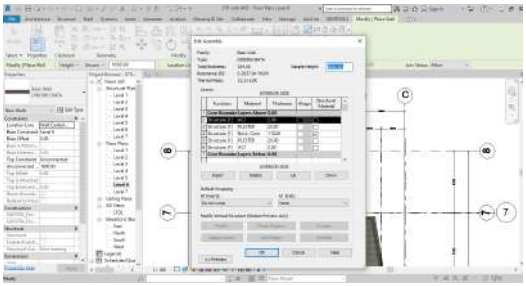

Figure 10. Edit Assembly Tab View

12. Create a ceiling on the Views Floor Plans and select Ceiling in the Ribbon Architecture as shown in Figure 11.

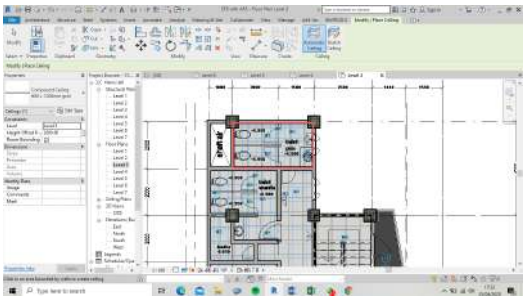

Figure 11. How to Create a Ceiling

13. Make floor coverings according to the type, size and placement as shown in Figure 12.

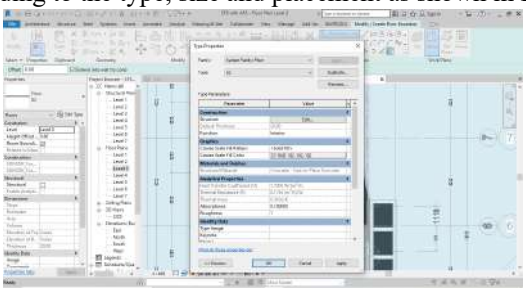

Figure 12. Type Properties to Make Floor Coverings

3. RESULTS AND DISCUSSION

The calculation result of the effectiveness using BIM on the accuracy of the BoQ:

Pile Cap Validation

Figure 13 is the results of the pile cap volume output:

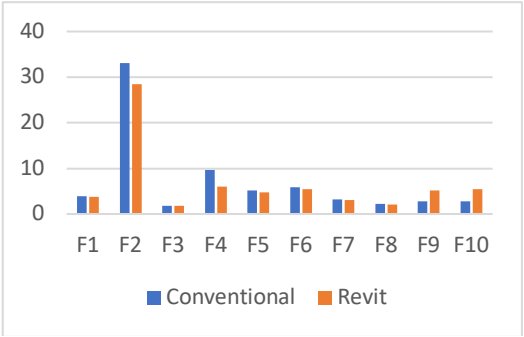

Figure 13. Pile Cap Comparison Graph

The output volume of Revit is 5.93% lower than conventional calculations because Revit calculations are more accurate in calculating irregular pile cap shapes such as the F2 type pile cap.

Column Validation

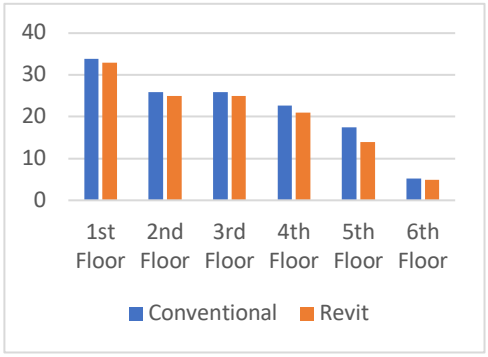

Figure 14. Column Comparison Graph

Figure 14 shows the comparison graph between the calculation of conventional and Revit. Revit result column volume 6.19% slightly smaller than the volume stated in the BoQ because the conventional calculation assumptions and Revit are the same, but a significant difference on the 5th floor occurs because of an error in the estimator in calculating the number of columns.

Beam Validation

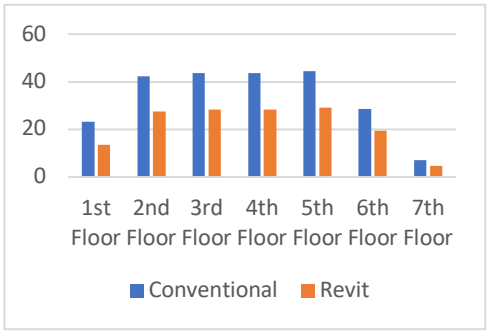

Figure 15. Beam Comparison Graph

The calculation of the beam in Revit uses the net span of the outer side of the column and for the beam sloof uses the net span of the outer side of the pile cap, while the conventional calculation uses the span of the axle to the axle of the beam without reducing the volume of the column side and the side of the pile cap. The differences can be showed in Figure 15. The meeting of the plate and beam also affects the volume of the beam, this causes a significant difference 35.27% between the Revit calculation and manual calculation.

Floor Plate Validation

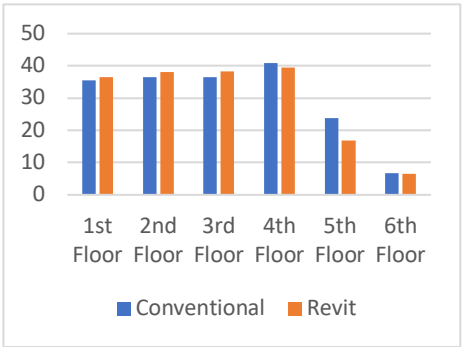

Figure 16. Floor Plate Comparison Chart

Furthermore, for the plate volume from Revit, which is to directly calculate the entire slab area multiplied by the thickness of each floor, without reducing the area of the columns and beams, so that the results do not have a significant difference with conventional calculations as shown in the Figure 16 which is only 2%. If there is a significant change, it can be caused by the incompatibility of the plan drawing with the calculation of the BoQ.

Stairs Validation

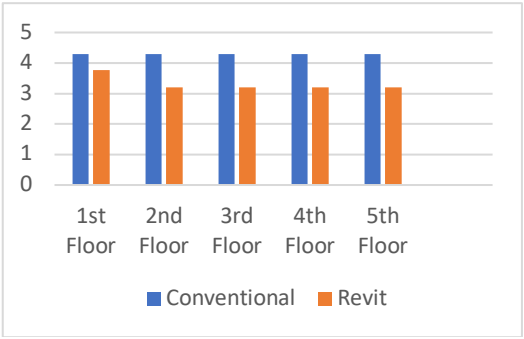

Figure 17. Stairs Comparison Graph

The volume of stairs produced by Revit with conventional calculations differs by almost 20% as shown in Figure 17, this is because Revit calculates the suitability of the height of the stairs and the width of the steps widths with the floor height of the building. So that if its not ideal, Revit will automatically resize it.

Wall Validation

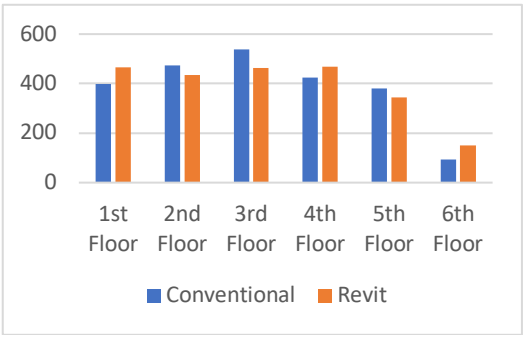

Figure 18. Wall Comparison Graph

The wall calculation by Revit does not have a significant difference with conventional calculations as shows in Figure 18, which is only 0.78% different, however, for the wall drawing must be careful because Revit does not reduce the wall area when drawing on the axle of the column, so the wall drawing must start on the outer side of the column. The calculation can also be more accurate because the wall area can be automatically reduced when entering door and window materials.

Validation of Floor Coverings and Ceiling

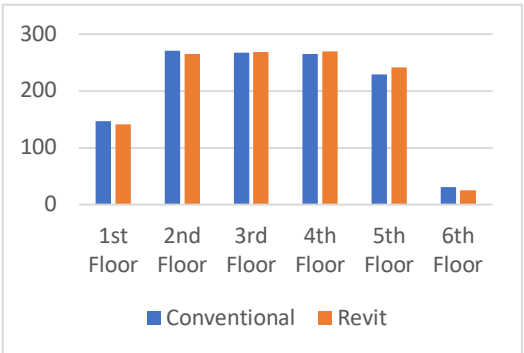

Figure 19. Floor Coverings Comparison Graph

Figure 19 and Figure 20 shows the comparison graph between the calculation of conventional and Revit. The area of floor coverings and ceilings is not automatically reduced when there are walls or columns around them, so the drawing must be done carefully to achieve accurate results.

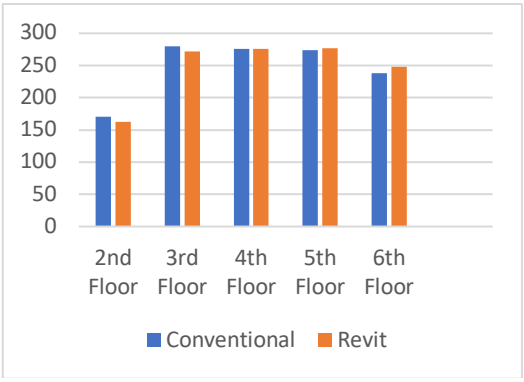

Figure 20. Ceilings Comparison Graph

All comparison data for each component are summed and the average difference is obtained as in the Table 1.

Table 1. Average differences in calculations

Component	Difference in calculation (%)
Pile Cap	5
Column	6
Beam	35
Platform	2
Stairs	22
Ceiling	2.26
Floor Covering	14
Wall	-0.78
Total	85.48
Average	10.68

4. CONCLUSION

The difference between conventional BoQ calculations and Revit calculations is around 10%, therefore this proves that the BIM method can help calculate quantity more quickly and accurately.

5. REFERENCES

[1] Saravanan S, "A Study of Role of Building Information Modeling in Life Cycle Based Integrated Project Delivery Process." International Research Journal of Engineering and Technology (IRJET),Vol.3, pp 1305-1309, 2016.
[2] Autodesk Revit, Wikipedia : https://en.wikipedia.org/wiki/Autodesk_Revit.
[3] CRC Construction Innovation. "Adopting BIM for Facilities Management: Solutions for Managing the Sydney OperaHouse, Cooperative Research Center for Construction Innovation, Brisbane," . 2007
[4] Eastman, C., "BIM Handbook: A Guide to Building Information Modeling for Owners, Managers, Designers, Engineers and Contractors (1st ed.). Hoboken, John Wiley, New Jersey." 2008.
[5] Ardianto, O. P. S., Kristianto, T. A., Budianto, C. A., Rucitra, A. A., & Wardoyo, A. Evaluasi Media Presentasi Perancangan Interior Rumah Air Surabaya Berbasis Virtual Tour sebagai Usaha Penerapan Building Information Modelling pada Perancangan Interior. Jurnal Desain Interior, 4(1), 11-36. Australia. 2019.
[6] Bergin, M. S. A brief history of BIM. Archdaily, 7, 12., http://www.archdaily.com/302490/abrief-history-of-bim/. 2012.
[7] Haron, A. T., "Buildng Information Modelling in Intergrated Practice. Manchester: University of Salford."

2009.
[8] Laksito, Boedhi. “Metode Perencanaan & Perancangan Arsitektur. Jakarta: Griya Kreasi.” 2014.
[9] Khan, Muhammad Shoaib & Khalil, Fatima & Adil, Mohammad & Khan, Adeed. “Role Of Building Information Modeling (BIM) In Building Design Industry. International Journal of Scientific and Engineering Research.” Volume 9.https://www.ijser.org/onlineResearchPaperViewer.aspx?Role-of. 2018.
[10] Laorent, D., Nugraha, P., & Budiman, J. “Analisa Quantity Take-Off dengan Menggunakan Autodesk Revit.” Dimensi Utama Teknik Sipil, 6(1), 1-8, 2019.
[11] Lu, W., Pexng, Y., Shen, Q., & Li, H. “Generic model for measuring benefits of BIM as a learning tool in construction tasks. Journal of Construction Engineering and Management.” 139(2), 195-203. 2012.
[12] Rizaldi, R. I., Farni, I., & Mulyani, R. “Kajian Potensi Bangunan Building Information Modeling (BIM) dalam Merencanakan Gedung di Indonesia.” Abstract of Undergraduate Research, Faculty of Civil and Planning Engineering, Bung Hatta University, 2(2), 2016.
[13] Smith, D., “An Introduction to Building Information Modelling (BIM), Journal of Building Infromation Modelling.” 4-12, 2007.
[14] Utama, W. P. “Standarisasi Pengukuran Kuantitas Pekerjaan Konstruksi di Indonesia : Suatu Gagasan. Fakultas Teknik Sipil dan Perencanaan Universitas Bung Hatta.” 2009.
[15] Berlian, C. A., Adhi, R. P., Hidayat, A., & Nugroho, H. “Perbandingan Efisiensi Waktu, Biaya, dan Sumber Daya Manusia Antara Metode Building Information Modelling (BIM) dan Konvensional (Studi Kasus: Perencanaan Gedung 20 Lantai)”. Jurnal Karya Teknik Sipil. 5(2): 220–229. 2016.

LOGIC
Journal of Engineering Design and Technology
Vol. 21 No.1 March 2021; p. 40 - 51

p-ISSN : 1412-114X
e-ISSN : 2580-5649
http://ojs.pnb.ac.id/index.php/LOGIC

SETTLEMENT OF GEOSYNTHETIC ENCASED STONE COLUMNS LIQUEFACTION CONDITION IN BOX CULVERT

Maftuh Ahnan[1)], Putera Agung Maha Agung [2)]

1,2) Department of Civil Engineering, Politeknik Negeri Jakarta, Jl. Prof. Dr. G.A Siwabessy, Kampus Baru UI, Depok 16424

Corresponding email [1) 2)]:
maftuhahnan82@gmail.com
putera.agungmagung@sipil.pnj.ac.id

Abstract. When the box culvert system is placed on a sandy soil layer with a relatively low bearing capacity and is disposed to potential liquefaction, the soil layer must be repaired to avoid damages to the box culvert structure. The proposed method is Geosynthetic Encased Stone Columns (GESC) to increase the bearing capacity and anticipated the liquefaction potential. however, to meet the criteria for a stable and safe GESC soil improvement in liquefaction conditions, the value of the settlement must meet the requirements for the settlement permit limit. This research was conducted to determine the potential for liquefaction at the study location, to calculate the value of single and group settlements in liquefaction conditions and to analyze the stability of single and group settlements including safe or unsafe in liquefaction conditions. Analysis of liquefaction potential was analyzed based on SPT data using the Valera and Donovan method, and settlement analysis applied the Almeida and Alexiew method. The analysis shows that potential liquefaction due to an earthquake with a magnitude of 9.0 SR will be at a depth of 4 to 8 m. Single and group settlements (144 sets) with an installation distance of 1.2 m with a diameter of 0.4 m and at a depth of 10 m are 246.23 and 214.92 mm, respectively. The entire GESC system is considered to be in an unstable and unsafe condition against potential liquefaction and box culvert loading.

Keywords : Settlement, Geosynthetic Encased Stone Columns, Liquefaction, Box Culvert

1. INTRODUCTION

Box culvert structure is a water drainage that is placed on land with loose or sandy soil layers that have low soil bearing capacity and are susceptible to liquefaction potential [1], [2]. This can be dangerous the box culvert structure. Thus, it is necessary to improve the soil layer. The method proposed in soil improvement, namely Geosynthetic Encased Stone Column (GESC), functions to increase soil bearing capacity, reduce liquefaction that occurs as gravel drainage in air-saturated sand soils, reduce pore water pressure [3]–[6]. Geosynthetic Encased Stone Column can also be used to strengthen road embankment stability and peat soil layer strengthening [7], [8].

However, to meet the criteria for stable and safe soil improvement, the value of the settlement in the Geosynthetic Encased Stone Column (GESC) as a subgrade improvement in the box culvert structure must meet the requirements for a settlement permit limit of 25.4 mm. settlement beyond the permit limit can result in damage to the box culvert structure [9], [10].

Geosynthetic Encased Stone Columns settlement in sandy or loose soil layers was calculated using the Almeida and Alexiew method with using the principles of the Raithel and Kempfert models. where this model assumes a constant column volume subject to uniform lateral deformation over the entire column, and lateral stress from the surrounding soil assuming the ground pressure at rest [7], [11]–[13]. settlement of the geosynthetic encased stone column in sandy soil or loose sand is calculated using the Almeida and Alexiew method shown in Eq. (1) with parameters and E * or modified modulus in Eq. (2) and (3) [14].

$$\left\{\frac{\Delta\sigma_{v,s}}{E_{oed,s}} - \frac{2}{E^*}.\frac{vs}{1-vs}\left[K_{a,c}.\left(\frac{\Delta\sigma_v}{a_E} - \frac{1-a_E}{a_E}.\Delta\sigma_{v,s} + \Delta\sigma_{v,o,c}\right) - K^*_{0,S}.\Delta\sigma_{v,s} - K_{0,s}.\Delta\sigma_{v,o,s} + \frac{J(r_{geo}-r_c)}{r^2_{geo}} - \frac{J.\Delta r_c}{r^2_{geo}}\right]\right\} \quad (1)$$

$$\Delta r_c = \frac{\Delta\sigma_{h,diff}}{E^*}.\left(\frac{1}{a_E} - 1\right).r_c \quad (2)$$

$$E^* = \left(\frac{1}{1-vs} + \frac{1}{1+vs}.\frac{1}{a_E}\right).\frac{(1+v_S)-(1-2v_S)}{(1-vs)}.E_{oed,s} \quad (3)$$

Then in reviewing the dangers and analysis of the potential for liquefaction, the method used by Valera and Donovan aims to find the critical value of SPT or Ncrit as a determination of liquefaction or non-liquefaction conditions with the following Eq. (4) [15]–[17].

$$N_{crit} = \eta[1 + 0{,}125(ds - 3) - 0{,}05(dw - 2) \quad (4)$$

Where N_{crit} is the critical value of N-SPT, d_s is the depth of the sand layer being reviewed, then d_w is the depth of the groundwater level from the ground surface then the value η is a function of the vibration intensity due to tectonic earthquakes. The MMI scale is determined based on the damage to buildings and things felt by humans due to the earthquake.

When liquefaction, the frictional strength of the clay layer only receives 30 percent of the total overburden stress, meaning that the frictional resistance is corrected up to 30 percent [18], [19]. In this study, it is determined that the resistance of friction is corrected by 30-50% of phenomena due to liquefaction that can affect the value settlement of Geosynthetic Encased Stone Columns in single or group settlement.

The purpose of this study was to see the potential for liquefaction in the sewer box review area using the Valera and Donovan method based on standard penetration test (SPT) data. then to calculate the settlement of single and group Geosynthetic Encased Stone Columns in liquefaction conditions based on the results of potential analysis liquefaction method of Valera and Donovan. and for analysis stability the settlement of Geosynthetic Encased Stone Columns in single and group against box culvert loading.

.

2. METHODS

In this study, the box culvert planning located at STA 127 + 100 Trans Sumatra Toll Road Kisaran-Tebing Tinggi section Indrapura-Kisaran with a sandy soil layer that has a relatively low bearing capacity and is in an area with a high potential for earthquakes and the potential for liquefaction shown in Figure 1. In this case, the Geosynthetic Encased Stone Columns was provided as soil improvement at the STA 127 + 100 box culvert location.

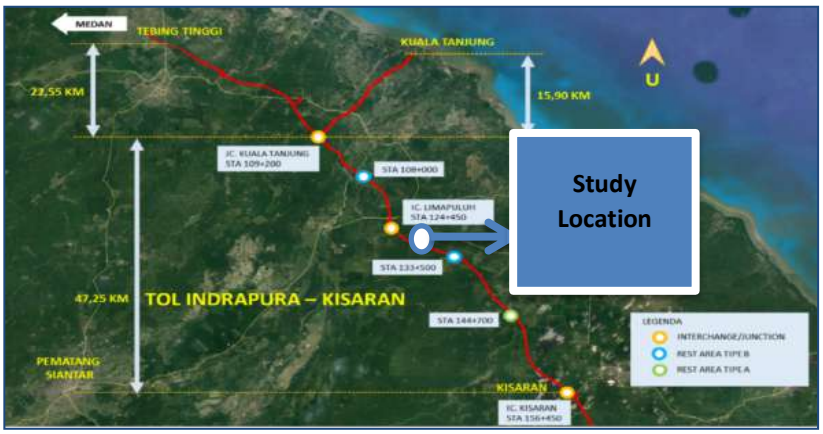

Figure 1. Trans Sumatra Toll Road Kisaran - Tebing Tinggi section Indrapura - Kisaran

2.1 Design Data

The data used in this study are secondary data from the results of field investigations standard penetration test (SPT) point BH-01 STA 127 +100 and laboratory testing by PT. Cipta Indah Citra and PT. PP also USU soil mechanics laboratory are shown in Table 1 and Figure 2. and other data in the form of box culvert dimensions, road cross-sections shown in figure 3.

Table 1. Resume of Laboratory Testing Results

FORM SUMMARY OF TESTS

Project : Rencana Akhir (DED) Jalan Tol Indrapura - Kisaran

Location : Indrapura - Kisaran

Location	Sample no.	Sample Type	Depth	Depth	Water Content	Unit Weight	Dry Density	Specific Gravity	Saturability	Void Ratio
			(m)	(m)	Wn (%)	γn (gr/cm^3)	γn (gr/cm^3)	G_s (gr/cm^3)	Sr (%)	e -
Sta. 122+525	BH-19	UDS	3.50-4.00	4	32,75	1,682	1,267	2,59	81	1,049
Sta. 122+525	BH-19	UDS	5.50-6.00	6	35,79	1,854	1,365	2,69	98,95	0,976
Sta. 122+525	BH-19	DS	13.50-14.00	14	30,62	1,923	1,472	2,71	98,49	0,844
Sta. 122+525	BH-19	DS	19.50-20.00	20	26,83	1,947	1,535	2,69	95,52	0,758

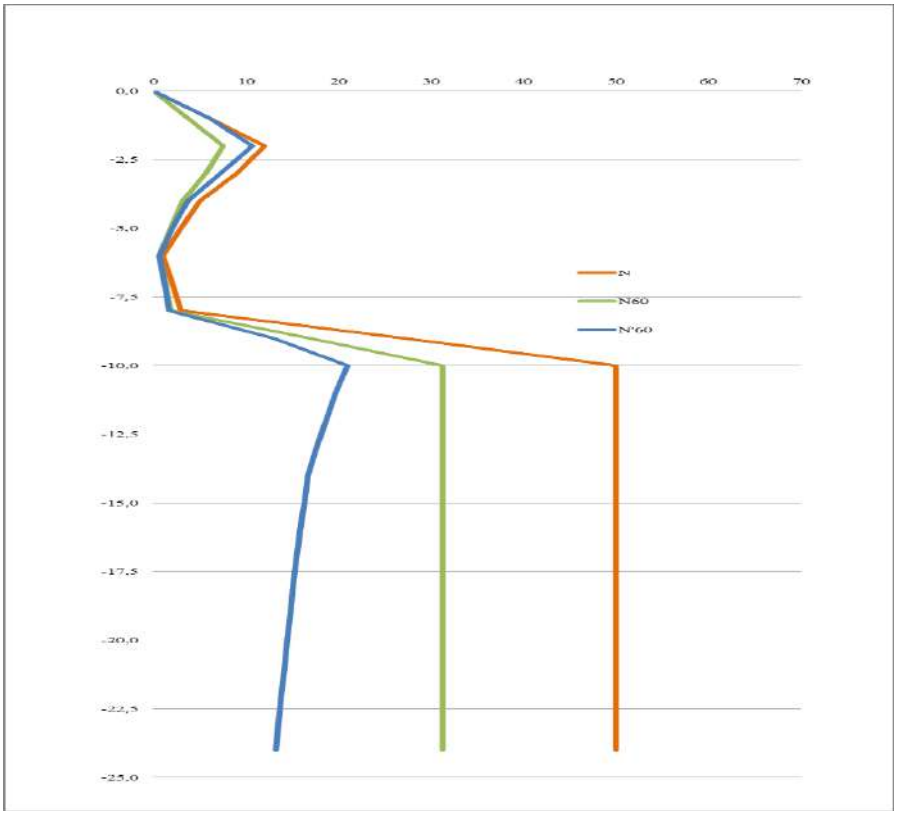

Figure 2. N-SPT BH-01

As an preliminary design planning for the box culvert design, dimensions of 1.5 x 1.5 are used with a length of 86 m according to the cross section of the road STA 127+100 shown in figure 3. Then in the initial design Geosynthetic Encased Stone Columns using a diameter of 0.4 m and 3D distance or 1.2 m with a length of 10 m using Ringtrac 6500 PM geosynthetic tubular protective material with a diameter of 0.4 m shown in figure 4.and then stone material with specifications γs is 2.2 t/m², ϕ is 34˚, C or cohesion is 0 t / m² [7], [20].

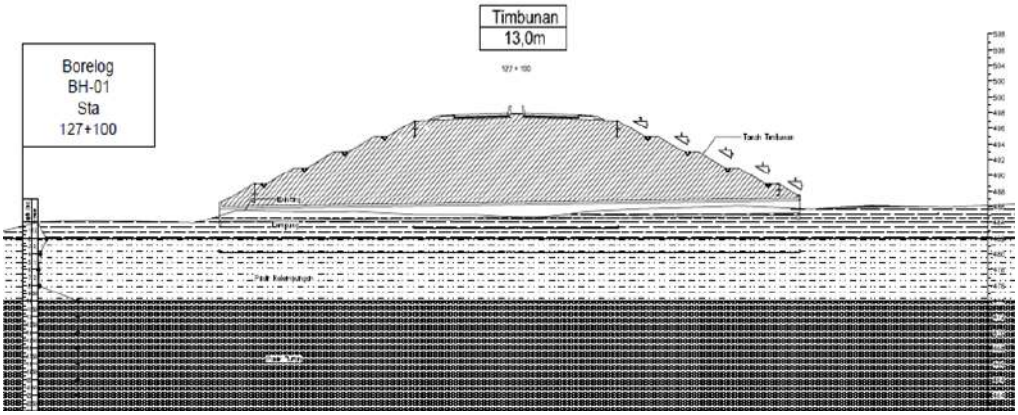

Figure 3. Cross Section STA 127+100 Trans Sumatra Toll Road Kisaran - Tebing Tinggi Section Indrapura – Kisaran

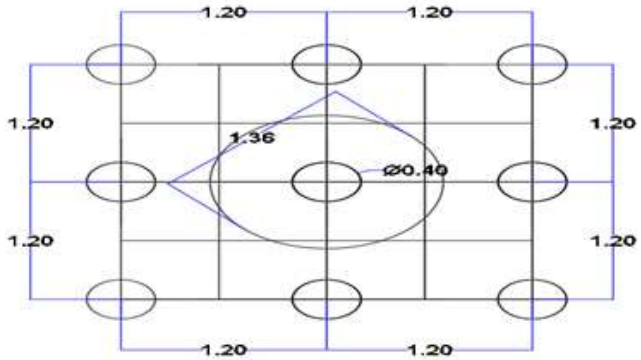

Figure 4. Visualization of The Unit Cell Concept

Research in this study includes several stages, including preliminary design, calculation of loading, soil cohesion analysis and correction of N on N-SPT, etc. there are several stages in this research that must be carried out in data analysis.

1. Calculating the load on the box culvert using references to SNI 1725: 2016 and SNI 1726: 2019 [21], [22]. Calculated based on the dimension data of the box culvert and the cross section of the road.
2. Perform axial, transverse and moment force analysis on the calculation results of the box culvert loading using SAP 2000 software.
3. Calculate soil cohesion along the soil layer depth and make corrections to the N value using standard penetration test (SPT) data
4. Performing critical Ncrit or N calculations along the depth of the soil layer based on standard penetration test data and determining the soil condition for potential liquefaction or non-liquefaction based on the Valera and Donovan liquefaction potential analysis method.
5. Calculating and determining the geosynthetic encased stone column design parameters in liquefied soil conditions, namely the corrected soil cohesion in the soil layer that occurs liquefaction based on the results of the analysis of the potential liquefaction of the Valera and Donovan method and several other parameters such as void ratio, soil weight, active soil pressure coefficient and passive, lateral rest pressure coefficient based on Broker and Ireland also Jaky, Poisson ratio, modulus of soil elasticity based on Webb [23].
6. Planning a geometric pattern of the distance and diameter of the geosynthetic encased stone column based

on the Raithel and Kempfert models.

7. Calculating column and soil stress, vertical stress on the column and, also calculate horizontal stress on the column and the surrounding soil based on the Raithel and Kempfert method.
8. Calculating the geotextile requirement using the Ringtrac 6500 PM to produce the horizontal geotextile stress and the total horizontal soil stress based on the Raithel and Kempfert methods
9. Perform geosynthetic settlement calculations for single and group encased stone columns using the Almeida and Alexiew method [14].
10. Analyze settlement stability of single and group Geosynthetic Encased Stone Columns.
11. Conducting final conclusions on single and group settlement of Geosynthetic Encased Stone Columns under liquefaction conditions based on the analysis of liquefaction potential using the Valera and Donovan method .

3. RESULTS AND DISCUSSION

3.1 Calculation of box culvert loading

Calculation of box culvert loading using SNI 1725: 2016 and 1726: 2019 and loading analysis using SAP 2000 [21], [22]. The following are the results shown in Table 2.

Table 2. Result of Calculation and Analysis of Box Culvert Loading

Data	Nilai	Satuan
Pv	4330,66	ton
Mx	0	ton-cm
My	27979,77	ton-cm
Mx(Gempa)	20597,17	ton-cm
My(Gempa)	39250,31	ton-cm
Mx total	20597,17	ton-cm
My total	67230,08	ton-cm
H	30	cm
Berat Isi	2.4	t/m3
Wpile-cap Grup 144	123,84	ton
Σ(tiang) (n)	144	buah
Ptotal/n	30,93	ton
My . x	4033805	ton-cm . cm
Σx2	518400	cm2
My . x/Σx2	7,781	ton
Mx . y	1235830	ton-cm . cm
Σy2	518400	cm2
Mx . y/Σy2	2,384	ton
Pmaks	41,1	ton

3.2 Soil Cohesion Analysis

Secondary data obtained were processed by data processing in the form of soil cohesion analysis and N correction on the N-SPT data. The results are shown in Table 3.

Table 3. Result of Calculation and Analysis of Soil Cohesion

STANDARD PENETRATION TEST

Project	**: Pondasi Box Culvert**	**Date**	
Test No.	**: BH-01 (STA 127+100)**	**Tested by**	**:**
Site name	**: Jalan Tol Indrapura - Kisaran**	**Weather**	**: Fine**
Location	**: Kabupaten Batubara, Sumatera Utar**	**GWL**	**: -14,0 m**

PERHITUNGAN DATA SPT

Depth	N	Parameter-parameter koreksi peralatan dan lokasi					Cu	Cu	γ_m	σ_v'	σ_r	Perbandingan	Koreksi	N'60	Lapisan tanah
		E_m	C_B	C_S	C_R	N_{60}	(t/m2)	(kPa)	(t/m^3)	(t/m^2)	(t/m^2)	(σ_v'/σ_r)	(C_N)		
(A)	(B)	(C)	(D)	(E)	(F)	(G)	(H)	(H)	(I)	(J)	(K)	(L)	(M)	(N)	(O)
0,00	0	0,5	1,0	1,0	0,75	0,00	0,00	0	1,58	0,00	10	0,00	1,83	0,00	
-1,00	6	0,5	1,0	1,0	0,75	3,75	3,60	35	1,64	1,64	10	0,16	1,61	6,05	Lempung
-2,00	12	0,5	1,0	1,0	0,75	7,50	7,20	71	1,70	3,40	10	0,34	1,43	10,71	
-3,00	9	0,5	1,0	1,0	0,75	5,63	5,40	53	1,670	5,01	10	0,50	1,29	7,28	
-4,00	5	0,5	1,0	1,0	0,75	3,13	3,00	29	1,630	6,52	10	0,65	1,19	3,71	
-5,00	3	0,5	1,0	1,0	0,75	1,88	1,80	18	1,610	8,05	10	0,81	1,10	2,06	
-6,00	1	0,5	1,0	1,0	0,75	0,63	0,60	6	1,590	9,54	10	0,95	1,02	0,64	Pasir Kelempungan
-7,00	2	0,5	1,0	1,0	0,75	1,25	1,20	12	1,600	11,20	10	1,02	0,95	1,19	
-8,00	3	0,5	1,0	1,0	0,75	1,88	1,80	18	1,610	12,88	10	1,07	0,88	1,66	
-9,00	27	0,5	1,0	1,0	0,75	16,88	16,20	159	1,850	16,65	10	1,28	0,77	12,96	
-10,00	50	0,5	1,0	1,0	0,75	31,25	30,00	294	2,080	20,80	10	1,49	0,67	20,96	
-11,00	50	0,5	1,0	1,0	0,75	31,25	30,00	294	2,080	22,88	10	1,53	0,63	19,71	
-12,00	50	0,5	1,0	1,0	0,75	31,25	30,00	294	2,080	24,96	10	1,56	0,60	18,60	
-13,00	50	0,5	1,0	1,0	0,75	31,25	30,00	294	2,080	27,04	10	1,59	0,56	17,61	
-14,00	50	0,5	1,0	1,0	0,75	31,25	30,00	294	2,080	29,12	10	1,62	0,54	16,72	
-15,00	50	0,5	1,0	1,0	0,75	31,25	30,00	294	2,080	30,20	10	2,01	0,52	16,29	
-16,00	50	0,5	1,0	1,0	0,75	31,25	30,00	294	2,080	31,28	10	1,96	0,51	15,88	
-17,00	50	0,5	1,0	1,0	0,75	31,25	30,00	294	2,080	32,36	10	1,90	0,50	15,50	
-18,00	50	0,5	1,0	1,0	0,75	31,25	30,00	294	2,080	33,44	10	1,86	0,48	15,13	Pasir Tufan
-19,00	50	0,5	1,0	1,0	0,75	31,25	30,00	294	2,080	34,52	10	1,82	0,47	14,78	
-20,00	50	0,5	1,0	1,0	0,75	31,25	30,00	294	2,080	35,60	10	1,78	0,46	14,44	
-21,00	50	0,5	1,0	1,0	0,75	31,25	30,00	294	2,080	36,68	10	1,75	0,45	14,12	
-22,00	50	0,5	1,0	1,0	0,75	31,25	30,00	294	2,080	37,76	10	1,72	0,44	13,82	
-23,00	50	0,5	1,0	1,0	0,75	31,25	30,00	294	2,080	38,84	10	1,69	0,43	13,52	
-24,00	50	0,5	1,0	1,0	0,75	31,25	30,00	294	2,080	39,92	10	1,66	0,42	13,24	

3.3 Analysis of the Liquefaction Potential of the Valera and Donovan method

In the analysis of the liquefaction potential of the Valera and Donovan method, the largest earthquake data in the last 100 years was used, namely the Aceh earthquake in 2004, the magnitude of the earthquake was 9.0 SR including the maximum intensity on the MMI level IX scale [24]. The value of η with MMI level IX was obtained values of 16 blows/feet [15]–[17].

then based on SPT data that the depth of the groundwater level is 14 m, then the N_{crit} calculation can be done according to the depth of the soil. From several N_{crit} calculations, it can be compared between N and N_{crit} at a depth of 0-24 m at the test point BH-01 STA 127 +100.

If $N > N_{crit}$, which means that there is no liquefaction in the existing depth with a 9.0 SR earthquake, then if the results are $N < N_{crit}$, which means the soil is in the existing depth of liquefaction with a 9.0 SR earthquake, the results of the analysis and calculation of the potential liquefaction of the Valera and Donovan method can be seen in Table 4.

Table 4. N_{crit} Calculation and Evaluation Results at STA 127 + 100 Valera and Donovan Method

No	STA	MAT	Depth (m)	N (blow/ft)	Ncrit(blow/ft)	Evaluation
1	127+100	14	0	0	0	No Liquefaction
			1	6	2,4	No Liquefaction
			2	12	4,4	No Liquefaction
			3	9	6,4	No Liquefaction
			4	5	8,4	Liquefaction
			5	3	10,4	Liquefaction
			6	1	12,4	Liquefaction
			7	2	14,4	Liquefaction
			8	3	16,4	Liquefaction
			9	27	18,4	No Liquefaction
			10	50	20,4	No Liquefaction
			11	50	22,4	No Liquefaction
			12	50	24,4	No Liquefaction
			13	50	26,4	No Liquefaction
			14	50	28,4	No Liquefaction
			15	50	30,4	No Liquefaction
			16	50	32,4	No Liquefaction
			17	50	34,4	No Liquefaction
			18	50	36,4	No Liquefaction
			19	50	38,4	No Liquefaction
			20	50	40,4	No Liquefaction
			21	50	42,4	No Liquefaction
			22	50	44,4	No Liquefaction
			23	50	46,4	No Liquefaction
			24	50	48,4	No Liquefaction

Table 4 shows the results at a depth of 4-8 m, there will be liquefaction, so that the area is safe at a depth of more than 8 m.

3.4 Settlement Geosynthetic Encased Stone Column

Design Parameters

The GESC design parameters are determined in liquefaction conditions at a depth of 4-8 m based on the analysis of the liquefaction potential of the Valera and Donovan method, namely the value of FS or in this case the corrected cohesion of 30% at a depth of 0 to 8 m. and corrected 50% at a depth of 9 to 24 m is shown in Table 5.

Table 5. Design Parameters Geosynthetic Encased Stone Columns

Depth (m)	e0	Cu (t/m2)	φ (°)	γt (t/m3)	γsat (t/m3)	vs	kos	E (t/m²)	Eoed,s t/m2	kac	kpc
0-2	1.05	1.62	25	1.682		0.4	0.69	2039	432	0.2827	3.537
2-10	0.98	3.40	25	1.854		0.3	0.58	1245	1417	0.2827	3.537
10-14	0.76	15	40	1.947		0.3	0.36	3175	6037	0.2827	3.537
14-24	0.76	15	40		1.966	0.3	0.36	3175	6037	0.2827	3.537

Geometric Plan Geosynthetic Encased Stone Columns

Diameter GESC is 0.4 m with a distance of 1.2 m with a rectangular pattern. then calculate several parameters including calculated area of the column (Ac) see in Eq. (5).

$$Ac = \frac{\pi}{4}.D^2 = 0.13 \quad (5)$$

Diameter unit cell area refer to Eq. (6) and Unit Cell Area (Ae) refer to Eq. (7)

$$De = 1.13.S = 1.13 \times 1.2 = 1.36\,m \quad (6)$$

$$Ae = \frac{\pi}{4}.D^2 = 0.13 \quad (7)$$

Area replacement ratio stone column refer to Eq. (8)

$$\alpha c = \frac{A_c}{A_e} = 0.09 \quad (8)$$

Area replacement ratio of the surrounding soil refer to Eq. (9)

$$\alpha s = 1 - \alpha c = 0.91 \quad (9)$$

Stress Ratio on column refer to Eq. (10).

$$qc = \frac{n}{1+(n-1)\propto c} = \frac{5}{1+(5-1)0.09} = 3.71 \quad (10)$$

Stress Ratio on Soil refer to Eq. (11).

$$qc = \frac{n}{1+(n-1)\propto c} = \frac{1}{1+(5-1)0.91} = 0.21 \quad (11)$$

Calculation of vertical and horizontal stress Column and Soil

Vertical Stress

Calculation of the stress received by the stone column and surrounding soil is calculated by multiplying the stress due to the box culvert load by the stress ratio. For vertical stress on column refer to Eq. (12).

$$\sigma_{vc} = q_o.q_c = 41.1 \times 3.71 = 152.44\ {}^{t}/_{m^2} \quad (12)$$

And vertical stress on soil refer to Eq. (13).

$$\sigma_{vs} = q_o.q_s = 41.1 \times 0.21 = 8.84\ {}^{t}/_{m^2} \quad (13)$$

After that, the calculation of the vertical stress on the soil and stone column per soil layer is shown in Table 6. due to loading on the box culvert structure produces horizontal pressure. And The summary of the horizontal stresses from the column (σhc) and the horizontal stresses from the surrounding soil (σhs) is shown in Table 7 and 8.

Table 6. Summary of The Calculation of Vertical Stress In The Surrounding Soil and Stone Column

Surrounding soil							Stone Column			
Depth Column (m)	h (m)	γt (t/m3)	γsat (t/m3)	Vertical Stress (σ'v,o,s) - t/m² Layer 1	Layer 2	Σσ'v,o,s (t/m²) Per Layer	Depth Column (m)	h (m)	γc (t/m3)	Vertical Stress
0-2	2	1.682		1.68		1.68	0-2	2	2.2	4.4
2-10	8	1.854		13.46	7.42	20.87	2-10	8	2.2	17.6

Table 7. Summary of The Calculation of Horizontal Stress In The Surrounding Soil

Surrounding Soil								
Depth Column (m)	h (m)	Kos	Vertical Stress (σ'v,o,s) - t/m² Layer 1	Layer 2	Σσ'v,o,s (t/m²) Per Layer	σro'=Σσ'v,o,s x Kos (t/m2)	σvs x Kos (t/m2)	σhs (t/m2)
0-2	2	0.69	1.68		1.68	1.16	6.11	7.27
2-10	8	0.58	13.46	7.42	20.87	12.04	5.10	17.14

Table 8. Summary of the calculation of horizontal stress in stone column

Depth Column (m)	h (m)	Kac	Stone Column Vertical Stress (σ'v,o,c) t/m²	(σ'v,o,c) x Kac (t/m²)	(σvc) x Kac (t/m²)	σh,c (t/m²)
0-2	2	0.2827	4.40	1.244	43.09	44.34
2-10	8	0.2827	17.60	4.976		48.07

Horizontal stress calculation after encased is installed

From Table 7 and 8, it can be seen that the soil is not able to withstand the horizontal stress from the column because ($\sigma h_c > \sigma h_s$) it requires a geotextile. calculation of σh_{geo} with the Ringtrac 6500 PM high modular low creep geotextile encased material refer to Eq. (14)-(15).

$$\Delta Fr = J \times \frac{\Delta r}{r_{geo}} = 650 \times \frac{0{,}009}{0{,}4} = 28.29 \ {}^{t}/_{m^2} \quad (14)$$

$$\sigma h_{geo} = \frac{r}{rgeo} = \frac{28{,}29}{0{,}2} = 141.40 \ {}^{t}/_{m^2} \quad (15)$$

After obtaining the horizontal stress that the geotextile is able to withstand, it can be added with the horizontal stress of the soil in an effort to withstand the horizontal stress of the column. A summary of these conditions can be seen in Table 8.

Table 8. Horizontal Stress Comparison After Encased Installed

σh,c column (t/m²)	σh,s soil (t/m²)	Information	σh diff (t/m²)	σh geo (t/m²)	σhs total (t/m²)	condition (t/m²)
44.339	7.275	need encased	37.064	141.40	148.676	safe
48.071	17.141	need encased	30.930	141.40	158.542	safe

Single Settlement of Geosynthetic Encased Stone Columns

In the results of the design parameters, the calculation of vertical and horizontal stresses can be calculated settlement consisting of Layer 1 with a length of 2 m at a depth of 0–2 m and Layer 2 with a length of 8 m at a depth of 3–10 m. with the modulus of constrain, it is determined by an average value of 8D above and 4 D down of 3757.9 t / m². The following is the calculation of a single settlement Geosynthetic Encased Stone Columns using the Almeida and Alexiew method at the length of the Geosynthetic Encased Stone Columns 0-2 m depth refer to Eq. (16)-(21).

$$E^* = \left(\frac{1}{1-vs} + \frac{1}{1+vs}.\frac{1}{a_E}\right).\left(\frac{(1+vs)-(1-2vs)}{(1-vs)}.E_{oed,s} = 3790.2\ {}^{t}/_{m^2}\right. \quad (16)$$

$$\frac{\sigma v,s}{E_{oed,s}} - \frac{2}{E^*}.\frac{vs}{(1-vs)} = 0.0020 \quad (17)$$

$$K_{ac}.\left(\frac{\Delta\sigma_v}{a_E} - \frac{1-a_E}{a_E}.\Delta\sigma_{v,s} + \Delta\sigma_{v,o,s}\right) = 10.06 \quad (18)$$

$$\frac{J.\Delta rc}{r_{geo}^2} = \frac{J.\frac{\Delta\sigma h_{diff}}{E^*}.\left(\frac{1}{a_E}-1\right).rc}{r_{geo}^2} = -9.77 \quad (19)$$

$$K_{0,s}^*.\Delta\sigma_{v,s} - K_{0,s}.\Delta\sigma_{v,o,s} + \frac{J.(r_{geo}-r_c)}{r^2} - \frac{J.\Delta rc}{r^2} = 14.7 \quad (20)$$

$$Sc = (12.(\ 13\text{-}15)).h = \text{-}1.87 \text{ mm} \quad (21)$$

From the calculation results, the results can be formulated in Table 9.

Table 9. Result Single Settlement of The Geosynthetic Encased Stone Columns

Data	Value	Unit
Sc1	-0.0187	M
Sc2	0.2648	M
Sc Total	0.2462	M
	246.23	mm

Group Settlement of Geosynthetic Encased Stone Columns

In calculating settlement in Geosynthetic Encased Stone Columns Group with the formation of 144 Geosynthetic Encased Stone Columns, namely 2 rows of 72 columns, it begins with calculating q group GESC refer to Eq. (22-24).

$$q_{groupGESC} = \frac{Q_g}{(B_g \times L_g)} = \frac{Pmaks \times n}{(B_g \times L_g)} = \frac{41.1 \times 144}{2 \times 86} = 34.41\ {}^{t}/_{m^2} \quad (22)$$

$$\sigma_{v,c} = q_{groupGESC} \times q_c = 34.41 \times 3{,}71 = 127.62\ {}^{t}/_{m^2} \quad (23)$$

$$\sigma_{v,s} = q_{groupGESC} \times q_s = 34.41 \times 0{,}21 = 7.40\ {}^{t}/_{m^2} \quad (24)$$

Calculation of the Settlement of the 144 Geosynthetic Encased Stone Columns group using the Almeida and Alexiew method. The calculation results are then recapitulated in Table 10.

Table 10. Result Group Single Settlement of The Geosynthetic Encased Stone Columns

Data	Value	Unit
Sc1	-0.0114	m
Sc2	0.226	m
Sc Total	0.2149	m
	214.92	mm

Stability Analysis on Single Settlement of Geosynthetic Encased Stone Columns

From the calculation results shown in Table 9 for a single settlement Geosynthetic encased stone columns, it was found that 246.23 mm exceeded the permit requirements of 25.4 mm. thus the single settlement of the

geosynthetic encased stone column is considered unstable and unsafe. excessive settlement can also cause damage to the box culvert structure.

Stability Analysis on Group Settlement of Geosynthetic Encased Stone Columns

From the calculation results shown in Table 10, for the settlement of 144 geosynthetic encased stone column formation, it was found that 214.92 mm exceeded the settlement permit requirement of 25.4 mm. Soil repair with the encased stone column Geosynthetic method was not appropriate for the box culvert structure with an earthquake load of magnitude 9.0 SR

4. CONCLUSION

From the analysis and discussion of the settlement in geosyntetics encased stone column liquefaction condition in box culvert, the following conclusions can be drawn:

1. Based on the results of the analysis of the potential for liquefaction with the Valera and Donovan method, it is found that at a depth of 4 to 8 m, there is a liquefaction with an earthquake of magnitude 9.0 SR.
2. Based on the results of calculations and analysis of the settlement of the Almeida and Alexiew method on a single settlement in the Geosynthetic Encased Stone Columns, it is obtained 246.23 mm. Then on settlement of the 144 Geosynthetic Encased Stone Columns formation group obtained 214.92 mm.
3. In the stability analysis on single and group settlement 144 Geosynthetic Encased Stone Columns exceeds the settlement requirement of 25.4 mm, the single and group settlement does not meet the requirements and is declared unstable and unsafe under liquefaction conditions against box culvert loading.

5. ACKNOWLEDGEMENT

The authors would like to thanks the UP2M of Politeknik Negeri Jakarta for the funding provided by the BTAM program.

6. REFERENCES

[1] P. A. M. Agung and M. B. A. Ahmad, “Potential Liquefaction Of Loose Sand Lenses (Case Study In Surabaya East Coastal Plain , Indonesia),” vol. 6, no. 2, pp. 1–10, 2014.

[2] T. W. Kuningsih, A. Rifa’i, and K. B. Suryolelono, “Analisis Ketahanan Tanah Dasar Fondasi Candi Prambanan Terhadap Ancaman Likuifaksi Berdasar Simplified Procedure,” *Politeknologi*, vol. 16, no. 1, pp. 7–14, 2017.

[3] L. Zhang and M. Zhao, “Deformation analysis of geotextile-encased stone columns,” *Int. J. Geomech.*, vol. 15, no. 3, pp. 1–10, 2015, doi: 10.1061/(ASCE)GM.1943-5622.0000389.

[4] C. Yoo, “Performance of geosynthetic-encased stone columns in embankment construction: Numerical investigation,” *J. Geotech. Geoenvironmental Eng.*, vol. 136, no. 8, pp. 1148–1160, 2010, doi: 10.1061/(ASCE)GT.1943-5606.0000316.

[5] E. Guler, D. Alexiew, A. Abbaspour, and M. Koc, “Seismic performance of geosynthetic-encased stone columns,” *Transp. Res. Rec.*, vol. 2462, pp. 77–88, 2014, doi: 10.3141/2462-10.

[6] Y. Zhou, G. Kong, Q. Yang, and H. Li, “Deformation analysis of geosynthetic-encased stone column using cavity expansion models with emphasis on boundary condition,” *Geotext. Geomembranes*, vol. 47, no. 6, pp. 831–842, 2019, doi: 10.1016/j.geotexmem.2019.103498.

[7] I. D. G. W. WIDIARTHA, “Installation of Strengthening Peat Soil Layer in,” *Sipil, Jur. Tek.*, 2015.

[8] A. D. Wicaksono, N. E. Mochtar, and P. T. Kumalasari, “Perencanaan Perbaikan Tanah Dasar dan Perkuatan Stabilitas Timbunan Jalan Tol Pasuruan-Grati STA 30+100 s.d STA 31+500,” *J. Tek. ITS*, vol. 6, no. 2, pp. 72–76, 2017, doi: 10.12962/j23373539.v6i2.26381.

[9] S. Rahmatika, “ANALISIS DAYA DUKUNG DAN PENURUNAN PONDASI OIL STORAGE TANK PADA PROYEK PEMBANGUNAN TERMINAL TRANSIT BAUBAU DI SULAWESI,” *J. IPB*, 2016.

[10] R. Yuliawan, Eko; Tanjung, “ANALISIS DAYA DUKUNG DAN PENURUNAN PONDASI TIANG BERDASARKAN PENGUJIAN SPT DAN CYCLIC LOAD TEST,” *J. Konstr.*, vol. 9, 2018.

[11] C. Yoo and S. Bin Kim, “Performance of a two-tier geosynthetic reinforced segmental retaining wall under a surcharge load: Full-scale load test and 3D finite element analysis,” *Geotext. Geomembranes*, vol. 26, no. 6, pp. 460–472, 2008, doi: 10.1016/j.geotexmem.2008.05.008.

[12] B. Kempfert, Hans-Georg ; Raithel, Marc ; Indraratna, *Soil Improvement and Foundation Systems with Encased Columns and Reinforced Bearing Layers*. Oxford: Butterworth-Heinemann, 2015.

[13] M. Raithel and H. G. Kempfert, “Calculation models for dam foundations with geotextile coated sand columns,” *ISRM Int. Symp. 2000, IS 2000*, 2018.

[14] D. Marcio de Souza Soares de; Filho, Mario Viccente Riccio; Babaei, Iman Hosseinpour; Alexiew, “Geosynthetic Encased Columns for Soft Soil Improvement,” in *Geosynthetic Encased Columns for Soft Soil Improvement*, London: Taylor & Francis Group, 2019, p. 14.

[15] H. Hasmar, *Dinamika Tanah dan Rekayasa Kegempaan*. Yogyakarta: UII Press, 2013.
[16] Srikit, "Analisis potensi likuifaksi berdasarkan distribusi ukuran butir dan data n-spt," *UIII J.*, 2019.
[17] F. Selviana, "Analisis dan Tinjauan Potensi Likuifaksi pada Lapisan Pasir di Bawah Jembatan Weri-Saharei Kabupaten Fakfak , Papua Barat(Menggunakan Metode Kishida, Whitman, dan Valera and Donovan)," *J. Civ. Eng. Student*, vol. 1, no. 1, pp. 25–31, 2019.
[18] I. M. Idriss and R. W. Boulanger, "Center for Geotechnical Modeling Cpt and Spt Based Liquefaction Triggering Procedures Cpt and Spt Based Liquefaction Triggering Procedures," *Cent. Geotech. Model.*, no. April, p. 134, 2014.
[19] R. W. Boulanger, I. M. Idriss, and R. W. Boulanger, "CPT and SPT Based Liquefaction Triggering Procedures," *Cent. Geotech. Model.*, no. 10–02, p. 134, 2010, [Online]. Available: https://faculty.engineering.ucdavis.edu/boulanger/wp-content/uploads/sites/71/2014/09/Boulanger_Idriss_CPT_and_SPT_Liq_triggering_CGM-14-01_20141.pdf%0Ahttp://nees.ucdavis.edu/publications/Boulanger_Idriss_CPT_and_SPT_Liq_triggering_CGM-14-01_2014.pdf.
[20] HUESKER Synthetic GmbH, *Reliable Ground Improvement Particularly for Soils with very low Bearing Capacity*. Gescher: HUESKER Synthetic GmbH, 2020.
[21] SNI 1726-2019, "Tata Cara Perencanaan Ketahanan Gempa Untuk Struktur Bangunan Gedung dan Non Gedung," *Bandung Badan Stand. Indones.*, no. 8, p. 254, 2019.
[22] SNI 1725-2016, "Standar pembebanan untuk jembatan," *Badan Stand. Indones.*, 2016.
[23] J. Ameratunga, N. Sivakugan, and B. M. Das, *Correlations of Soil and Rock Properties in Geotechnical Engineering*. 2016.
[24] Badan Meteorologi Klimatologi dan Geofisika, *Katalog Gempa Bumi Signifikan dan Merusak Tahun 1821 - 2018*. Jakarta: Badan Meteorologi Klimatologi dan Geofisika, 2019.

LOGIC
Journal of Engineering Design and Technology
Vol. 21 No.1 March 2021; p. 52 - 63

p-ISSN : 1412-114X
e-ISSN : 2580-5649
http://ojs.pnb.ac.id/index.php/LOGIC

PLANNING FOR MAINTENANCE AND REPAIR OF CONTINUOUS SHIP UNLOADER USING THE IRRO METHOD

Syamsul Hadi [1)], Alfarizi Al Azis [2)], Vinan Viyus [3)], Etik Puspitasari [4)], Ahmad Hanif Firdaus [5)], Andri Setiawan [6)]

[1],2,3,4,5,6) Mechanical Engineering Department, State Polytechnic of Malang, Jl. Soekarno-Hatta 9, Malang 65141, Indonesia

Correponding email [1)] :
syamsul.hadi@polinema.ac.id
syampol2003@yahoo.com

Abstract. The problem faced is damage, especially to the screw conveyor from the Continuous Ship Unloader (CSU) as a dry bulk material transfer equipment (phosphate rock) which is taken from the ship's hold which is flowed by a screw conveyor followed by the belt conveyor to the material warehouse to be processed into a type of fertilizer. The purpose of planning is to obtain a schedule and estimated cost of maintenance and repair of CSU for the period 2022 to 2025, and to obtain the ratio of maintenance-repair costs to the profit of the machine. Planning methods uses the IRRO (Inspection, Replace, Repair, and Overhoul) method include data collection of machine maintenance history and component breakdowns, checking CSU specifications, making a list of component life predictions and component prices, predicting costs and duration of component dissasembly, screw conveyor repair, maintenance and repair scheduling, and maintenance and repair cost estimates. The real results of planning in the form of a maintenance and repair schedule for the period of 2022 to 2025; maintenance and repair costs respectively for the years 2022 to 2025 are IDR 136,873,000; IDR 335,986,000; IDR 160,687,000; and IDR 464,733,000; and the ratio between maintenance costs to profit for the years 2022 to 2025 is 0.51, 1.22, 0.57, and 1.63 which means the machine is still fit for use without the need for refurbishment because it is still prospective.

Keywords : Continuous ship unloader, screw conveyor, dry bulk material, phosphate rock, belt conveyor, IRRO.

1. INTRODUCTION

Industrial development in Indonesia, especially the chemical industry has increased from year to year. Progress in the industrial sector has a very important role in national development in all fields in order to improve people's welfare. Especially in industries that have a role to support the provision of national fertilizers to achieve food self-sufficiency program and support the economy, especially the agricultural sector. The expansion of the agricultural sector in the early 1970-1980s was inseparable from the role of the fertilizer industry which enabled farmers to optimize the results of the green revolution to increase their production. Along with the increasing area of agricultural land and plantations in Indonesia, the need for fertilizer is increasing from year to year. One of the fertilizer industries in Gresik, east Java, Indonesia is the port of Terminal for Own Activities for loading and unloading activities, one of the equipment used in the loading and unloading process is the CSU (Continuous Ship Unloader). Raw materials that are transported/unloaded are phosphate rock, ZA steel grade, ZA-caprolactam, MOP-red, MOP-white, MOP-pink, sulfur and SP 36. The way CSU works is that the material in the hold of the ship is sucked in through the feeder inlet then followed by a vertical screw conveyor through the horizontal screw conveyor then the material falls through the hopper and the material dust is sucked in by the dust collector at the end of the hopper, so that the material falls on the belt conveyor to be forwarded to the warehouse. Due to the important role of CSU at Terminal for Own Activities, an effective maintenance and repair plan must be made to avoid damage that causes breakdown.

Maintenance is an attempt to eliminate the causes of the breakdown, if possible before the congestion occurs. These efforts can take the form of cleaning, lubrication, periodic inspections, servicing, and tune-ups so that their performance remains within the expected performance range. Repair is the treatment of the effects of a congestion event. So the difference between maintenance and repair lies in the effort before the congestion/damage occurs and treatment of the effects after the congestion incident [1]

Screw conveyors are generally right-hand with screw designs that are selected according to the material being moved, trough screw or continuous screw is selected to move dry granules or powder. Screw normally made of steel sheet which is welded to the shaft [2].

In operational, maintenance and repair activities must comply with the principles of occupational health and safety (OHS). Safe and healthy at work is the condition of workers that must be realized in the workplace, of course with all efforts based on science and thought to protect workers in accordance with human rights and applicable laws and standards [3].

Total Productive Maintenance/TPM is a treatment related to all elements of the company with the aim of achieving zero product defects, zero breakdown and zero accident. TPM as a maintenance method that maximizes efficiency, solidifies preventive maintenance systems, maximizes productivity, reduces downtime, and motivates all company production lines to avoid sudden repairs and minimize unscheduled maintenance [4]-[5].

Preventive Maintenance (PM) policy is a proactive technique that has been used since the inception of maintenance systems research [6]. The efficiency of PM when applied to leased objects is considered the determinant of revenue for the next rental period [7].

The total average cost per unit time which includes production costs, warranty, and system maintenance is applied to the useful life of the equipment [8].

The case study model of multi-objective genetic algorithm can increase availability, reduce maintenance costs, increase plant profits, can be applied in a continuous operating system for chemical plants with modifications to its operating characteristics [9].

An increase in the predictive maintenance level can lead to a lower quality control cost [10].

The balance between preventive maintenance and corrective maintenance to minimize costs varies between organization and assets, but there is a rule of thumb for balancing preventive maintenance and corrective maintenance with an 80/20 ratio [11].

Preventive maintenance and predictive maintenance are based on a history of maintenance which gives an indication of the degree of damage periodically with possible shifting of component life due to the possible variation in the operating conditions of an equipment. Corrective maintenance is possible if an equipment condition requires adjustment without changing its basic principles in order to keep it functioning. Maintenance and repair costs can increase sharply if good planning is not done, because early symptoms of deterioration are not immediately stopped or reduced through scheduled treatment planning. With scheduled maintenance, unexpected losses can be minimized.

2. METHODS

Planning methods uses the IRRO (Inspection, Replace, Repair, and Overhoul) method include collecting data on CSU operational history and component failure, reviewing CSU specifications, formulating damage problems, making a list of components to be handled, predicting component life, predicting spare parts prices, predicting repair costs, predicting duration and maintenance costs for components assembly, maintenance and repair scheduling, estimated total annual costs for the period of 2022 to 2025.

Figure 1. Continuous Ship Unloader/CSU

The CSU as the object of maintenance and repair planning is shown in Figure 1 which is marked by an oval line, the material in the hold of the ship in the right side is sucked in through the feeder inlet then followed by a vertical screw conveyor through the horizontal screw conveyor (yellow color) then the material falls through the hopper and the material dust is sucked in by the dust collector at the end of the hopper, so that the material falls on the belt conveyor to be forwarded to the warehouse in the left side.

The CSU specification is shown in Table 1 [12].

Table 1. The CSU Specification [12]

No.	Unit		Description
1	Inlet Feeder		
	Transmission	:	Enclosed oil lubricated gear
	Motor Type	:	Electrical
	Control System	:	Stepless control or automatic mode
	Motor Location	:	On top of vertical conveyor
	Other	:	Overload protection
2	Vertical Arm Conveyor		
	Type	:	VST-640
	Length	:	22 m
	Transmission	:	Enclosed oil lubricated gear
	Motor Type	:	AC-motor
	Control System	:	Direct Start
	Other	:	Speed guard
3	Horizontal Arm Conveyor		
	Type	:	HST-1000
	Length	:	28,75 m
	Transmission	:	Enclosed oil lubricated gear
	Motor Type	:	AC-motor
	Control System	:	Direct Start
4	Hydraulic System		
	Location	:	Main unit on the horizontal arm
	Working Preassure	:	250 bar (max)
	Motor Type	:	AC-motor
	Control System	:	Direct Start
	Insulation	:	No
5	Electrical System		
	Supply Voltage Power	:	6 kV
	Frequency	:	50 Hz
	Voltage On The Ship Unloader		
	Motor Voltage	:	380 V/50 Hz
	Operating Voltage	:	230 V/50 Hz
	Transformer	:	2500 kVA
	Type	:	Dry insulated
	Location	:	In the electrical container
	Power		
	Installed	:	1629 kW
	Largest Motor	:	400 kW

The sections of the CSU are shown in Figure 2 [12].

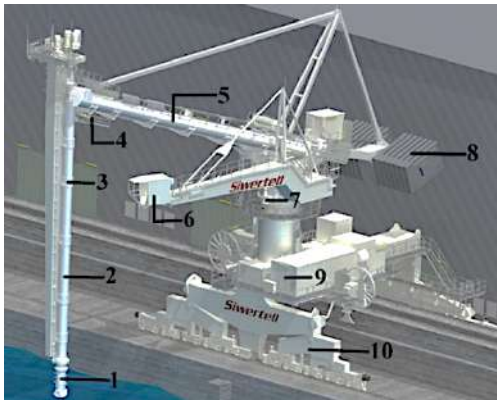

1	Inlet feeder	6	Operator cabin
2	Vertical arm conveyor	7	Upper turret
3	Intermediate bearing and shaft	8	Counter weight
4	Auxiliary hoist	9	Electrical system
5	Horizontal arm conveyor	10	Travelling beam

Figure 2. Parts of the CSU [12]

3. RESULTS AND DISCUSSION

CSU maintenance is carried out to obtain stable performance by conducting inspection, replace, repair, and overhaul.

Inspection activities to check the cleanliness, good or bad condition of existing components, check whether the existing lubricant/oil/grease is sufficient, insufficient, contaminated or dirty. CSU inspections are carried out every 3-4 months for components and for lubricants, inspections are carried out once a month. Weekly inspections, before and after full retrieval of one hold is carried out by the CSU operator, but by visual inspection and from inside the cabin by checking from the monitor or from the control room. The good synergy between the operator and the maintenance mechanic makes equipment maintenance better.

One such inspection with an example of greasing the end bearing is shown in Figure 3 [12].

Figure 3. Greasing of the end bearing [12]

An example of an inspection of intermediate shaft and screw conveyor is shown in Figure 4 [12].

Figure 4. Inspection of intermediate shaft and screw conveyor [12]

Checking the conveyor screw by hearing or from the sound of the motor that increases the load whether the material coming out is unstable or not suitable, if so, then the horizontal arm conveyor casing is opened to check the clearance between the flight screw and the inside of the vertical arm conveyor casing, in case of overclearance due to friction from the material, then the screw conveyor is immediately replaced with a spare screw conveyor, after that contact the Fabrication Department and report the conveyor screw to be repaired or reconditioned.

Replacement of spare parts according to the predicted component life is shown in Table 1 [12]. The price and lifetime predictions of the CSU components are shown in Table 1 [12]. Indonesian currency unit is Rp which is stated in IDR.

Spare parts are replacement components that are prepared based on the limited life time prediction of components due to the limited nature of the material, the shorter the component's life time, the more spare parts

that must be prepared. The price of spare parts can be predicted based on the purchase note of the same spare parts in the previous period by adding the price related to inflation to the previous purchase period, for example an increase in price of about 4% per year, if inflation is expected (decrease in the value of money due to the influence of the amount of money in circulation is more than required [1] Calculation of the price of spare parts using formula (1).

N = (Initial Price x 4%) + Initial Price (1)

where:

N : Price prediction for the next period
Initial Price: The price of the current/initial period
4% : Inflation per year (as an example)

Predictions of spare parts prices can be obtained from sources including: 1) Purchase notes for spare parts, 2) Information from shops selling or supplying spare parts, 3) Price information from the internet online, 4) Workshop where to order spare parts, and 5) Maintenance planners can make predictions based on the function of components relative to other components [1].

Table 1. Price and Life Time Predictions of CSU Components [12]

No.	CODE	UNIT/PART	PRICE (X1,000 IDR)	LIFE TIME		PRICE PREDICTED/YEAR (X1,000 IDR)				PCS
				HOUR	WEEK	2022	2023	2024	2025	
1	BCSU1-1-IF	Inlet Feeder								
	BCSU1-1-IF-FS	Flange Shaft	70	10,000	178	70	71	71	71	8
	BCSU1-1-IF-HB	Hanger Bearing	90	6,000	107	90	91	91	92	16
	BCSU1-1-IF-UJC	U-Joint Shaft	1,80	6,000	107	1,81	1,82	1,83	1,84	2
	BCSU1-1-IF-P	Pinion	85	6,000	107	85	86	86	87	1
	BCSU1-1-IF-SB	Slewing Bearing	45,00	12,000	214	45,45	45,67	45,90	46,13	1
	BCSU1-1-IF-GB	Gearbox-IF	600,00	15,000	268	606,01	609,04	612,09	615,15	1
2	BCSU1-2-VC	Vertical Arm Conveyor								
	BCSU1-2-VC-SC	Screw Conveyor	75,00	15,000	268	75,75	76,13	76,51	76,89	5
	BCSU1-2-VC-EB	End Bearing	3,50	6,000	107	3,53	3,55	3,57	3,58	2
	BCSU1-2-VC-IBS	Intermediate Bearing and Shaft	78,70	15,000	268	79,48	79,88	80,28	80,68	4
	BCSU1-2-VC-GB	Gearbox-VC	600,00	15,000	268	606,01	609,04	612,09	615,15	1
3	BCSU1-3-HC	Horizontal Arm Conveyor								
	BCSU1-3-HC-SC	Screw Conveyor	75,00	15,000	268	75,75	76,13	76,51	76,89	6
	BCSU1-3-HC-EB	End Bearing	3,50	6,000	107	3,53	3,55	3,57	3,58	2
	BCSU1-3-HC-IBS	Intermediate Bearing and Shaft	78,70	15,000	268	79,48	79,88	80,28	80,68	5
	BCSU1-3-HC-GB	Gearbox-HC	600,00	15,000	268	606,01	609,04	612,09	615,15	1
4	BCSU1-4-DC	Dust Collector								
	BCSU1-4-DC-FB	Fan/Blower	4,50	12,000	214	4,54	4,56	4,59	4,61	1
	BCSU1-4-DC-FB	Filter Bag	12	6,000	107	12	12	12	12	9
5	BCSU1-5-HS	Hydraulic System								

No.	CODE	UNIT/PART	PRICE (X1,000 IDR)	LIFE TIME		PRICE PREDICTED/YEAR (X1,000 IDR)				PCS
				HOUR	WEEK	2022	2023	2024	2025	
	BCSU1-5-HS-HP	Hydraulic Pump								
	BCSU1-5-HS-HP-HP	Pump Hose	3,00	5,000	89	3,03	3,04	3,06	3,07	1
	BCSU1-5-HS-HP-CV	Control Valve	35,00	12,000	214	35,35	35,52	35,70	35,88	1
	BCSU1-5-HS-HP-HF	Hydraulic Filter	1,20	5,000	89	1,21	1,21	1,22	1,23	1
	BCSU1-5-HS-HP-GP	Gear Pump	15,00	12,000	214	15,15	15,22	15,30	15,37	1
	BCSU1-5-HS-HP-HOC	Hydraulic oil cooler	10,00	12,000	214	10,10	10,15	10,20	10,25	1
	BCSU1-5-HS-HP-S	Seal	1,80	5,000	89	1,81	1,82	1,83	1,84	1
6	BCSU1-6-HCI	Hydraulic Cylinder Pendulum								
	BCSU1-6-HCP-S	Seal	2,10	5,000	89	2,12	2,13	2,14	2,15	2
	BCSU1-6-HCP-OR	O ring	1,20	5,000	89	1,21	1,21	1,22	1,23	2
	BCSU1-6-HCP-RP	Piston Rod	15,10	13,000	232	15,25	15,32	15,40	15,48	2
7	BCSU1-7-HCI	Hydraulic Cylinder Luffing								
	BCSU1-7-HCL-S	Seal	2,10	5,000	89	2,12	2,13	2,14	2,15	2
	BCSU1-7-HCL-OR	O ring	1,20	5,000	89	1,21	1,21	1,22	1,23	2
	BCSU1-7-HCL-RP	Rod piston	15,10	13,000	232	15,25	15,32	15,40	15,48	2
8	BCSU1-8-HS	Hydraulic Slewing								
	BCSU1-8-HS-SB	Slewing Bearing	150,00	13,000	232	151,50	152,26	153,02	153,78	1
	BCSU1-8-HS-PSG	Pinion Spur Gear	1,80	6,000	107	1,81	1,82	1,83	1,84	1
	BCSU1-8-HS-HM	Hydraulic Motor	75,00	15,000	268	75,75	76,13	76,51	76,89	1
9	BCSU1-9-AH	Auxiliary Hoist								
	BCSU1-9-AH-WR	Wire Rope	36,00	9,000	160	36,36	36,54	36,72	36,90	90m
	BCSU1-9-AH-H	Hook	13,00	10,000	178	13,13	13,19	13,26	13,32	1
	BCSU1-9-AH-GB	Gearbox-Auxiliary Hoist	600,00	15,000	268	606,01	609,04	612,09	615,15	1
10	BCSU1-9-AH	End Carriage								
	BCSU1-9-AH-IW	Idler Wheel	7,80	15,000	268	7,87	7,91	7,95	7,99	40
	BCSU1-9-AH-GB	Gearbox-EC	200,00	15,000	268	202,00	203,01	204,03	205,05	8
11	BCSU1-9-O	Oil								
	BCSU1-9-O-H46	Hydraulic Oil	5,50	2,000	36	5,55	5,58	5,61	5,63	209l
	BCSU1-9-O-G32	Gearbox Oil	4,90	2,000	36	4,94	4,97	4,99	5,02	209l
	BCSU1-9-O-GFC	Grease	8,20	500	9	8,28	8,32	8,36	8,40	209l

The costs and duration of disassembly and assembly of CSU are shown in Table 2 [12].

Table 2. Cost and Duration of disassembly and assembly of CSU [12]

No.	PART	TECH. LEVEL	DURATION (HR/PART)	COST/HR (X1,000 IDR)			
				2021	2023	2024	2025
1	Inlet Feeder						
	Flange Shaft	SHS	0.5	19	21	22	23
	Hanger Bearing	SHS	0.5	19	21	22	23
	U-Joint Shaft	SHS	0.5	19	21	22	23
	Pinion	SHS	2	19	21	22	23
	Slewing Bearing	3-Year Dipl.	8	21	23	24	25
	Gearbox-IF	SHS	4	19	21	22	23
2	Vertical Arm Conveyor						
	Screw Conveyor	3-Year Dipl.	4	21	23	24	25
	End Bearing	SHSl	2	19	21	22	23
	Intermediate Bearing and Shaft	3-Year Dipl.	3	19	21	22	23
	Gearbox-VC	SHS	4	19	21	22	23
3	Horizontal Arm Conveyor						
	Screw Conveyor	3-Year Dipl.	4	21	23	24	25
	End Bearing	SHS	2	19	21	22	23
	Intermediate Bearing and Shaft	3-Year Dipl.	3	21	23	24	25
	Gearbox-HC	SHS	4	19	21	22	23
4	Dust Collector						
	Fan Blower	SHS	1	19	21	22	23
	Filter Bag	SHS	0.25	19	21	22	23
5	Hydraulic System						
	Hydraulic Pump						
	Hose pump	SHS	1	19	21	22	23
	Control Valve	SHS	1	19	21	22	23
	Hydraulic Filter	SHS	1	19	21	22	23
	Gear Pump	SHS	2	19	21	22	23
	Hydraulic oil cooler	SHS	2	19	21	22	23
	Seal	SHS	1	19	21	22	23
6	Hydraulic Cylinder Pendulum						
	Seal	SHS	2	19	21	22	23
	O ring	SHS	4	19	21	22	23
	Rod piston	SHS	4	19	21	22	23
7	Hydraulic Cylinder Luffing						
	Seal	SHS	2	19	21	22	23
	O ring	SHS	4	19	21	22	23
	Rod piston	SHS	4	19	21	22	23
8	Hydraulic Slewing						
	Slewing Bearing	3-Year Dipl.	168	21	23	24	25
	Pinion Spur Gear	SHS	4	19	21	22	23
	Hydraulic Motor	SHS	4	19	21	22	23
9	Auxiliary Hoist						
	Wire Rope	SHS	4	19	21	22	23
	Hook	SHS	2	19	21	22	23
	Gearbox-Auxiliary Hoist	SHS	3	19	21	22	23
10	End Carriage						
	Idler Wheel	SHS	3	19	21	22	23
	Gearbox-EC	SHS	3	19	21	22	23
11	Oil						
	Hydraulic Oil	SHS	2	19	21	22	23
	Gearbox Oil	SHS	2	19	21	22	23
	Grease	SHS	2	19	21	22	23

Note: SHS: Senior High School

CSU repairs, especially in the reconditioning of screw conveyors, are carried out every 6000 hours or 107 weeks provided that they operate in one day with 1 shift for 8 working hours [12]. The repair work is carried out by the Fabrication Department who has a special duty or a specialist in screw conveyor repair.

The damage that occurs due to erosion of the flight surface due to friction causes the conveyor screw to wear out. The friction that occurs is the friction between the screw conveyor and the material and the casing, because if the material between the flight/blade of screw conveyor and the casing is left alone, the effect will be even greater. The effect of screw conveyor damage is less optimal/efficient in the transportation process. If the friction that occurs is greater, it can cause motor power to be wasted to overcome the friction and a lot of residual material settles on the casing due to not being moved. If this is continued, it can cause more fatal energy wasted because the efficiency of transportation of materials decreases.

Figure 5. Examples of worn screw conveyor blades [12]

The prediction of material prices for CSU repair activities is shown in Table 3 [12].

Table 3. Predictions of material prices for CSU repair activities [12]

No.	PART NAME	PRICE (X1,000 IDR)	PRICE PREDICTION/YEAR (X1,000 IDR)				PCS
			2022	2023	2024	2025	
1	Plate Duplex	250	253	254	255	256	34
2	Electrode E2209	1,500	1,515	1,523	1,530	1,538	4
3	Electrode E8838	1,700	1,717	1,726	1,734	1,743	7
4	Cleanser SKC-S	90	91	91	92	92	2
5	Liquid Penetrant Red SKL	90	91	91	92	92	2
6	Developer SKD-S2	95	96	96	97	97	2

The process of repairing screw conveyors includes the following stages:

1) The cutting of a duplex plate of 16 mm thick with a width of 25 mm using plasma cutting is shown in Figure 6 [12].

Figure 6. Cutting duplex plates with Plasma Cutting [12]

2) Installation of cylinder shock at both ends of the screw conveyor shaft which serves as a support for the bearings/rollers is shown in Figure 7 [12].

Figure 7. Installation of cylinder shock at both ends of the screw conveyor shaft as a support for the bearing/roller [12]

3) Reduction of the flight screw conveyor to ϕ 585 mm with a lathe is shown in Figure 8 [12].

Figure 8. Reducing the diameter of the flight screw conveyor to ϕ 585 mm with a lathe [12]

4) Coating flight screw conveyor with coating material from duplex plate with a thickness of 16 mm and a width of 25 mm using welding with an electrode E22209 which follows the Welding Procedure Standard. The welding is carried out along the flight screw conveyor on 2 sides which a process called layding/lining is shown in Figure 9 [12].

Figure 9. Coating flight screw conveyor with coating material from duplex plate [12]

5) After cleaning from the crust, the duplex plate is then overlaid or coated on both sides of the duplex plate using the E8838 electrode to exceed ϕ635 mm. The electrode used is similar to the E2209 electrode, but has a higher hardness value, so that the flight screw conveyor surface becomes harder [12].
6) The finishing process of a flight screw conveyor with a turning using a 6000 mm lathe, the diameter of the flight screw conveyor turned into 635 mm is shown in Figure 10 [12].

Figure 10. The finishing process of a flight screw conveyor with a turning using a 6000 mm lathe [12]

7) The screw conveyor is carried out by a balancing process with a balancing machine to balance its rotation when used and to minimize vibration.
8) Visual check, dye penetrant test, and dimensional check to ensure the quality of repairs, if the screw conveyor does not meet the requirements, it is repaired and if it meets the requirements, then the screw conveyor shown in Figure 11 [12] is ready to be installed into the CSU.

Figure 11. Screw conveyor after repaired [12]

Overhaul at CSU is carried out every 15,000 hours or 268 weeks provided that it has been operating for one day with 1 shift for 8 hours [12]. Some large and expensive components such as gearbox, motor, and slewing bearings replacement can take up to 2 weeks to take apart with additional overtime. Since CSU maintenance and repair planning has a period limit of 4 years or 11,648 hours or 208 weeks while the overhaul schedule is 15,000 hours or 270 weeks, the overhaul activity does not go into details and cost estimates.

The CSU has a loading/unloading capacity of up to 1000 tons per hour which makes CSU the backbone of loading/unloading activities, however, with the high utility of CSU, the number of damage also increases, even CSU often experiences a breakdown [13].

CSU 1 experienced a breakdown of 52 times from November 2015 to January 2016, so it is necessary to analyze the damage data for the formulation of its maintenance policy by using two alternative policy models, namely repair maintenance policy and preventive maintenance policy. From the calculation results, it is found that the maintenance policy is better for preventive maintenance which has an average machine runtime/period and a smaller repair cost compared to the maintenance repair policy, which is carried out every 7 weeks at a cost of IDR 4,291,241.00 [14].

Using the CSU greatly affects the productivity of loading and unloading activities, because the tonnage yield achieved when unloading using the CSU tool is greater than using other tools, and the unloading is completed faster [15].

An important element in the electric steam power plant (*PLTU*) is the Ship Unloader (SU) as the main loading and unloading facility for coal fuel from the barge to the stockpile. SU is only treated after damage occurs which is analyzed for treatment planning using the Markov Chain method. The Markov Chain results show that the cost of preventive maintenance at moderate status is decreasing by 84.40% from IDR 1,505,211.50 to IDR 234,820.77 for SU 1 and the cost of preventive maintenance in mildly damaged status decreased by 86.22% from IDR 1,019,642. 35 to IDR 137,893.05 for SU 2 [16].

An example of the results of making a CSU Maintenance and Repair Schedule in the 2023 period is shown in Table 4 [12].

Table 4. Example of CSU Maintenance and Repair Schedule in the 2023 Period [12]

No.	COMPONENTS AND MAIN PARTS	WEEK OF THE YEAR OF 2023																											
		JAN			FEB		MAR		APR	MAY			JUNE				JUL		AUG			SEP			OCT		DEC		
		1	3	4	8	9	10	13	14	18	19	21	22	23	24	25	29	30	31	33	34	35	36	38	39	40	49	50	52
1	Inlet Feeder																												
	Flange Shaft				I								I										I					I	
	Hanger Bearing		Rc		I								I										I					I	
	U-Joint Shaft		Rc		I								I										I					I	
	Pinion		Rc		I								I										I					I	
	Slewing Bearing				I								I										I					I	
	Gearbox-IF				I								I										I					I	
2	Vertical Conveyor																												
	Screw Conveyor		Rr		I								I										I					I	
	End Bearing		Rc		I								I										I					I	
	Intermediate Bearing and Shaft		Rr		I								I										I					I	
	Gearbox-VC				I								I										I					I	
3	Horizontal Conveyor																												
	Screw Conveyor		Rr		I								I										I					I	
	End Bearing		Rc		I								I										I					I	
	Intermediate Bearing and Shaft		Rr		I								I										I					I	
	Gearbox-HC				I								I										I					I	
4	Dust Collector																												
	Fan				I								I										I					I	
	Filter Bag		Rc		I								I										I					I	
5	Hydraulic System																												
	Hydraulic Pump																												
	Hose pump				I								I										I					I	
	Control Valve				I								I										I					I	
	Hydraulic Filter				I								I										I					I	
	Gear Pump				I								I										I					I	
	Hydraulic oil cooler				I								I										I					I	
	Seal				I								I										I					I	
6	Hydraulic Cylinder Pendulum																												
	Seal			I									I													I			
	O ring			I									I													I			
	Rod piston			I									I													I			
7	Hydraulic Cylinder Luffing																												
	Seal			I									I													I			
	O ring			I									I													I			
	Rod piston			I									I													I			
8	Hydraulic Slewing																												
	Slewing Bearing			I									I													I			
	Pinion Spur Gear		Rc	I									I													I			
	Hydraulic Motor			I									I													I			
9	Auxiliary Hoist																												
	Wire Rope		Rc		I								I										I					I	
	Hook				I								I										I					I	
	Gearbox-Auxiliary Hoist				I								I										I					I	
10	End Carriage																												
	Idler Wheel			I									I													I			
	Gearbox-EC			I									I													I			
11	Oil																												
	Hydraulic Oil		I	Rc		I			I		I				I		I				I				I	Rc		I	
	Gearbox Oil		I	Rc		I			I		I				I		I				I				I	Rc		I	
	Grease			Rc				Rc					Rc						Rc							Rc	Rc		

Remarks: I: inspection, Rc: Replace, Rr: repair, O: Overhoul

In Table 4, due to the limited journal space, columns that do not have activity content are deleted to only display the column containing the activity contents.

From the CSU maintenance and repair schedule planning for the period 2022 to 2025 only shows an example for 2023 period where there are screw conveyor repair activities.

The ratio between maintenance cost and profit is shown in Table 5 [12].

Table 5. The ratio between maintenance costs and profits [12]

Year	Maintenance Cost (IDR)	Annual Profit (Idr)	Maintenance/Profit Ratio (%)
2022	136,873	26,829,682	0.51
2023	335,986	27,336,275	1.22
2024	160,687	27,883,000	0.57
2025	464,733	28,440,660	1.63

4. CONCLUSION

The results of planning in the form of a maintenance and repair schedule for the period of 2022 to 2025; maintenance and repair costs for the years 2022 to 2025 are IDR 136,873,000; IDR 335,986,000; IDR 160,687,000; and IDR 464,733,000; and the ratio between maintenance costs to profit for the years 2022 to 2025 is 0.51; 1.22; 0.57; and 1.63 respectively which means the machine is still fit for use without the need for refurbishment because it is still prospective.

5. ACKNOWLEDGEMENT

The authors gratefully Head of the Fabrication Department and Port Management Department (Lolapel) of PT. Petro Kimia Gresik for the support of information and data related to maintenance and repair planning for the Continuous Ship Unloader (CSU).

6. REFERENCES

[1] S. Hadi, *Maintenance and Repair for Industrial Machinery*, Yogyakarta: Andi Publisher, 2019.
[2] A.M. Zainuri, *Material Handling Equipment*, Yogyakarta: Andi Publisher, 2008.
[3] H. Rarindo, *Basic Principles of Work Safety*, Malang: Polinema Press, 2019.
[4] F. Kurniawan, *Industrial Maintenance Management, Engineering and Applications: Implementation of Total Productive Maintenance, Preventive Maintenance and Reliability Centered Maintenance*, Yogyakarta: Graha Ilmu, 2013.
[5] J. X. Wang, *Lean Manufacturing Bussiness Bottom-Line Based*, USA: CRC Press, Taylor and Francis Group, 2011,
[6] E. I. Basri, I. H. Abdul Razak, H. Ab-Samat, S. Kamaruddin, "Preventive maintenance (PM) planning: a review," *J. of Quality in Maint. Eng.*, vol. 23, no. 2, pp. 114-143, 2017.
[7] A. B. Mabrouk, A. Chelbi, M. Radhoui, "Optimal imperfect preventive maintenance policy for equipment leased during successive periods," *Int. J. of Prod. Research*, vol. 54, no. 17, pp. 5095-5110, 2016.
[8] M. N. Darghouth, D. Ait-Kadi, A. Chelbi, "Joint reliability based design and periodic preventive maintenance policy for systems sold with warranty," *J. of Qua. in Maint. Eng.*, vol. 22, no. 1, pp. 2-17, 2016.
[9] D. D. Adhikary, G. K. Bose, D. K. Jana, D.Bose, S. Mitra, "Availability and cost-centered preventive maintenance scheduling of continuous operating series systems using multi-objective genetic algorithm: A case study," *Qua. Eng.*, vol. 28, no. 3, pp. 352-357, 2015.
[10] M. Nourelfath, N. Nahas, M. Ben-Daya, "Integrated preventive maintenance and production decisions for imperfect processes," *Reliab. Eng. & Sys. Safety*, vol. 148, pp. 21-31, 2016.
[11] C. Stenström, P. Norrbin, A.Parida, U.Kumar, "Preventive and corrective maintenance-cost comparison and cost-benefit analysis." *Struc. and Infrastr. Eng.*, vol. 12, no. 5, pp. 603-617, 2015.
[12] A. A. Azis, "Planning for Maintenance and Repair of Siwertell Continuous Ship Unloader Capacity 1,000 Tons/Hour for the Period 2021 until 2025", *Final Project RME650, DIII Mech. Eng. Study Program,* Mech. Eng. Dept, State Polytechnics of Malang, 2020.
[13] I.R. Pramudya, "Maintenance System Planning Using Reliability Centered Maintenance (RCM) Method on Screw Conveyor Continous Ship Unloader-Case Study CSU 02 Dermaga Utama P.T. XY," *Undergraduate Thesis*, Sepuluh Nopember Institute of Technology, Surabaya, 2020.
[14] T. I. Khota and R. Purwaningsih, "Policy Analysis of Continous Ship Unloader 1 Machine Maintenance P.T. Petrokimia Gresik," *Proceeding of National Seminar IENACO-2017*, Industrial Engineering Study Program, Faculty of Engineering, Diponegoro University, Semarang.
[15] M. E. Pratama, E. Pujo A. A., I. Novianto, "Effect Utilization of Continuous Ship Unloaders Against Productivity of Loading and Unloading Dry Bulk (Phospate Rock) at Petrokimia Gresik Special Port," *J. of Shipping and Port App.*, vol. 7, no. 2, pp. 92-104, 2017.
[16] D. P. K. Ariel, "Ship Unloader Maintenance Planning with the Markov Chain Method to Prevent Work Accidents and Reduce Maintenance Costs at PLTU," *Final Project,* State Marine Polytechnic of Surabaya, 2019.

LOGIC
Journal of Engineering Design and Technology
Vol. 21 No.1 March 2021; p. 64 - 69

p-ISSN : 1412-114X
e-ISSN : 2580-5649
http://ojs.pnb.ac.id/index.php/LOGIC

EFFECT OF HEAT RADIATION ON WORKLOAD AND GAMELAN CRAFTS PRODUCTIVITY

I Ketut Gde Juli Suarbawa [1], M. Yusuf [2]

1,2) Mechanical Engineering Department, Politeknik Negeri Bali, Indonesia

Correponding email [1]: julisuarbawa@pnb.ac.id

Abstract. The production process of making gamelan in Tihingan Village still uses the traditional way, namely using prapen with an open flame both for the melting process and in the formation process. This causes the workload of craftsmen to be quite heavy due to exposure to radiant heat and dust. The results of microclimate measurement of the work environment obtained an average dry temperature of 33.2ºC, an average wet temperature of 24ºC. The average globe temperature was 33ºC, WBGT 26.3ºC and the mean humidity (RH) was 59.0%. The average light intensity at work reaches 319.2 lux. The average temperature of the furnace at low heat is 340ºC and during the combustion process it reaches 860 ºC. The results of measurements of air quality in the workplace include levels of NO2 17.00 µg /m3 (increased by 112.50%), SO2 5.33 µg/m^3 (increased by 45.23%), CO 407.16 µg/m^3 (increased by 217, 99%), oxidants (Ox) 61.00 µg/m^3 (increased by 1.67%) and dust 48.50 µg/m^3 (increased by 125.58%). The mean pulse of the nguwad workers reached 125.81±1.35 beats/minutes (heavy workload). This causes the productivity of craftsmen to be low due to the increase in musculoskeletal disorders and craftsmen fatigue. To overcome this condition, the workings of the craftsmen need to be improved immediately through the application of appropriate technology in the form of furnace repair so that the flames and dust produced can be removed from the workplace, then exposure to heat air and combustion dust will no longer expose the craftsmen.

Keywords: heat temperature radiation, workload, productivity

1. INTRODUCTION

Gamelan is one of the traditional music that is very well known and almost owned by every traditional village in Bali. Gamelan has a very important meaning and role for the Balinese people as a means of traditional and religious ceremonies. Gamelan can also be used as a means of entertainment such as the gong kebyar festival, bleganjur competition which can also help the tourism industry in Bali. Apart from Bali, gamelan is also well known on the islands of Java, Madura and Lombok. One of the places that is famous as a gamelan craftsman village in Bali is Tihingan Village, which is located in Banjarangkan Subdistrict, Klungkung Regency, which is 3 km to the west of Semarapura City. In this village the population is mostly (almost 90%) gamelan craftsmen who produce various types of gamelan such as: gamelan gong kebyar, gamelan semar pegulingan, gender wayang, kelentang/angklung and others.

From all stages of the process of making gamelan instruments, the process of melting and nguwad is a work process with the heaviest workload felt by the craftsman. The open flame of the perapen causes the radiant heat temperature and the hot dust from the combustion to directly expose the craftsmen. Likewise, the way and work posture that is not natural causes more rapid increase in complaints of skeletal muscles and craftsman fatigue.

Exposure to hot temperatures will affect the conditions of workers, especially on work productivity [1], [2]. If exposure to hot temperatures is allowed and no repairs are made, it will result in poor health conditions for workers and a decrease in work productivity [3], [4].

Based on the description above, it is deemed necessary to conduct research to determine the effects of exposure to hot temperatures and a work attitude that is not yet ergonomic in affecting the workload and

productivity of craftsmen. Improvement of working conditions and environment through improvement of workplace perapen, work organization, and work environment through ergonomic intervention with the concept of applying appropriate technology and the SHIP (Systemic, Holistic, Interdisciplinary and Participatory) approach [5] is very necessary to be able to reduce workload, musculoskeletal complaints. and fatigue which in turn will increase work productivity and crafters' income. In addition, the quality of nguwad products has also increased, which is marked by a decrease in the number of defective products.

2. METHODS

This research is a one-short case study with a pre and post test group design which is conducted observational to crafters in the nguwad process. The workload of the crafter is measured from the pulse of work. The microclimates in the workplace measured are wet temperature, dry temperature, humidity, noise intensity, and light intensity and air quality. Subjective complaints were predicted from a 30 item fatigue questionnaire with four Likert scales, and skeletal muscle complaints were predicted using a Nordic Body Map questionnaire. Statistical analysis was carried out descriptively and inferential to workload, skeletal muscle complaints, and fatigue. The pre and post difference test was carried out with the t-test at a significance level of = 5%.

3. RESULTS AND DISCUSSION

3.1 Work Time

The nguwad work process usually starts at 07.00 a.m. in the morning and breaks at 11.00 a.m. - 12 p.m. then the next work starts again at 12.00 to 15.00. This nguwad job requires a large amount of energy to forge the raw materials to form the desired mortar. The working tools used are generally still classified as traditional working tools which are a legacy of the work tools of their predecessors consisting of large hammers for forging workers. The prying tool is for man who the grill and the clamp tool in the form of long pliers for man who the clamp. The hammer used weighed 4.5 - 5.5 kg and the prying tool used by the man who the grill weighed about 2.1 kg and the long pliers used by the man who the clamp weighed 0.5 kg. The use of traditional equipment requires patience and accuracy and requires considerable energy and a lot of calorie intake to be able to compensate for the amount of calories and energy that is expended while doing the job [6], [7].

3.2 Crafter Characteristics

The characteristics of gamelan craftsmen in the gamelan ngiwad process in Tihingan Village, which include age, weight, height, body mass index (BMI) and work experience, are presented in the Table 1.

Table 1. Subject Characteristics Data

Variable	Mean	SD	Range
Age (years)	26.64	5.81	19.50 - 35.50
Weight (kg)	58.32	3.91	56.05 - 64.32
Height (cm)	163.20	3.01	159.05 - 169.01
Body Mass Index (kg/cm^2)	22.31	1.31	19.61 - 23.10
Work Eksperience (years)	2.24	0.03	1.50 – 2.51

Note: SD = standard deviation

Table 1 shows that the conditions of the research subjects were normal, healthy, in productive conditions for work, and had sufficient work experience as gamelan craftsmen. Normal worker's body condition can lead to good work productivity as well [2], [8].

3.3 Environmental Conditions

Environmental conditions greatly affect the comfort and health of gamelan craftsmen in the nguwad process which results from the influence of physical and psychological conditions as well as exposure to hot temperatures from perapen and non-ergonomic work postures. If environmental conditions are not good, it will cause health problems, dissatisfaction, decreased motivation and low work productivity. In this study, environmental conditions were measured from morning to noon. Environmental conditions include dry air temperature, wet air temperature, air humidity, wind speed, globe temperature, WBGT (wet bulb globe temperature), and dust in the air.

Table 2. Working Environment Conditions

Variable	Before Work		After Work		p
	Mean	SD	Mean	SD	
Dry Temperature (°C)	30.05	1.08	35.20	0.47	0.000
Wet Temperature (°C)	26.05	0.72	24.03	0.98	0.000
Globe Temperature (°C)	29.06	0.74	33.09	0.52	0.000
WBGT (°C)	27.05	0.54	26.76	0.59	0.031
Relative humidity (%)	70.01	0.74	59.09	0.71	0.000
Wind velocity (m/dt)	0.613	0.016	0.651	0.047	0.068
Light intensity (lux)	316.78	6.34	319.88	4.62	0.166
Sound intensity (dB)	67.10	1.74	85.64	1.04	0.000

Note: SD = standard deviation

Table 3. Air Quality Conditions

variable	Before Work		After Work		p
	Mean	SD	Mean	SD	
NO_2 (µg/m^3)	8.00	0.32	17.00	1.56	0.000
SO_2(µg/m^3)	3.67	0.07	5.33	0.13	0.014
CO (µg/m^3)	128.04	2.34	407.16	5.84	0.002
Ox(µg/m^3)	60.00	2.87	61.00	3.07	0.027
Total dust (µg/m^3)	21.5	1.79	48.50	2.24	0.000

Note: SD = standard deviation

Table 2 and Table 3 show that the working conditions of the gamelan craftsmen are hot. The working room temperature is 35°C, the humidity is low, and the noise is high enough (85.64 dB). The noise threshold is 85 dB [9], while a comfortable working room temperature is 24 - 30°C [10]. The results of measurements of air quality in the workplace include levels of NO2 17.00 µg /m3 (increased by 112.50%), SO2 5.33 µg/m^3 (increased by 45.23%), CO 407.16 µg/m^3 (increased by 217, 99%), oxidants (Ox) 61.00 µg/m^3 (increased by 1.67%) and dust 48.50 µg/m^3 (increased by 125.58%). The dust from the gamelan production process is high enough so that it can affect the health of workers if allowed to continue. Dust will be a problem for the health of workers so it is necessary to provide an immediate solution [11],[12]. Therefore it is necessary to have an ergonomic intervention as a solution to this problem.

3.4 Workload

Workload is calculated objectively by measuring the working pulse frequency (DNK) with the ten pulse method which is calculated based on the increase in the work pulse, namely the difference between resting pulse and working pulse rate. The resting pulse of the craftsman (pulse before work) is as follows.

Table 3. Resting pulse and work rate of craftsmen

craftsman	Resting Pulse (bpm)			Work Rate (bpm)			p
	Mean	Min	Max	Mean	Min	Max	
Perapen craftsman	73.30 ± 1.44	72.07	74.68	115 ± 3.78	112.28	119.68	0.000
Flops craftsman	73.73 ± 1.54	71.89	75.83	113.96 ± 4.96	110.39	118.21	0.000
Nguwad craftsman	74.18 ± 5.26	70.64	79.48	125.81 ± 1.35	124.28	127.81	0.000

Information: Min = minimum value, Max = maximum value, p = significance

The mean pulse rate of the fishermen reached 115 ± 3.78 beats per minute, the clamp workers reached 113.96 4.96 beats per minute and the nguwad workers reached 125.81 1.35 beats per minute. Due to high environmental temperatures, body temperature will increase [3], [13]. Subjective disorders generally felt by all respondents were feeling thirsty, hot skin, and sweating a lot. Meanwhile, what workers have little complaint about is the cramps in

the arm and leg muscles. The increase in body temperature did not exceed the normal body temperature limit of 37°C. Increased body temperature only occurs in workers who have a heavy workload.

An increase in body temperature can cause the hypothalamus to stimulate the sweat glands so that the body produces sweat. In sweat contains various kinds of salt, especially sodium chloride salt. The release of sodium chloride salt with sweat will reduce its levels in the body, thus inhibiting the transportation of glucose as an energy source. This causes a decrease in muscle contraction so that the body experiences fatigue [14]. Therefore, to avoid the occurrence of health problems due to exposure to high heat, the length of work in a hot place must be adjusted to the level of work and the heat stress faced by the workforce. The conditions of a comfortable work environment allow daily work to be done as well as possible and here there is almost the same temperature between the body's metabolism and the surrounding environment [3], [14].

3.5 Musculoskeletal Disorders

Musculoskeletal disorders data obtained subjectively from filling out a Nordic Body Map questionnaire using a Likert scale. The crafter will cross the available numbers from 0-27 according to their perceived complaints. Before testing the effect of using the stirrer, the data obtained is tested by the normality test. Based on the normality test with Shapiro-Wilk, the following results were obtained.

Table 4. Musculoskeletal Disorders

	Before work		After Work		p
	Mean	SD	Mean	SD	
Musculoskeletal disorders	27.42	4.54	56.03	3.93	0.000

Note: SD = standard deviation, p = significance value.

Table 4 shows that the data from musculoskeletal disorders after work are normally distributed. The analysis of significance using the independent samples t-test shows that the value of p = 0.000. This means that the mean score of musculoskeletal complaints after using the mixer is significantly different (p <0.05) or indicates that there is an effect of improving working conditions and environment on reducing musculoskeletal complaints.

The activities of gamelan craftsmen in the work process of nguwad involve more static muscles, resulting in excessive loading on the muscles with a long and repetitive duration of loading so that blood circulation to the muscles decreases, oxygen supply decreases, metabolic processes are inhibited and there is accumulation of lactic acid, causing pain/pain in the skeletal muscles [3], [13], [15].

3.6 General Fatigue

Crafters' fatigue after work is recorded by filling in 30 items of rating scale before and after work. The results of the normality test for the mean fatigue score are presented in Table 5.

Table 5. General Fatigue Craftsman

	Mean	SD	Mean	SD	p
General Fatigue	31.05	4.67	51.49	3.66	0.000

Note: SD = standard deviation, p = significance value

Table 5 shows that the p value of fatigue before work and after work is p <0.05, this indicates an increase in craftsmen fatigue after work. This is caused by repetitive work with exposure to heat and dust and the presence of an ergonomic work posture. Fatigue that occurs in nguwad work processes is caused by repetitive work processes over a long period of time with static work activities. Fatigue caused by static work activities is considered to have a greater influence than dynamic work activities.

Manual and repetitive work in hot environmental conditions is one of the factors that has the potential to increase physical workload and the occurrence of work accidents so that it can cause occupational diseases (musculoskeletal complaints and fatigue) [7], [16], [17]. The temperature conditions of the hot work environment are often referred to as heat stress on workers. This heat pressure is a combination of air temperature and humidity, air flow velocity, radiation temperature with heat generated by the body's metabolism [14], [18].

3.7 Work productivity

Work productivity is measured from the ratio between the output and input per unit time. The work productivity of nguwad is measured from a physiological aspect. Work productivity from a physiological aspect, as the input is the average work pulse (bpm) of the crafter in the nguwad process. Time is measured from the length of the

nguwad process (minutes) and the output is the circumference of the resulting mole (cm). The productivity of nguwad craftsmen is presented in Table 6.

Table 6. Work Productivity

	Nguwad-1	*Nguwad*-2	*Nguwad*-3	*Nguwad*-4
Work time (minutes)	57,75	58,96	59,74	60,12
Work Productivity	1,04	1,02	0,99	1,01

The mean pulse of the nguwad workers reached 125.81±1.35 beats/minutes (including heavy workload) as Table 3. This causes the productivity of craftsmen to be low due to the increase in musculoskeletal disorders and craftsmen fatigue. Heavy workload will cause work productivity to decrease and cause health problems for workers [3], [19], [20]. To overcome this condition, the working conditions of the craftsmen need to be improved ergonomically and the application of appropriate technology in the form of furnace improvements and work layouts so that the flames and dust produced can be removed from the workplace, then exposure to heat air and combustion dust will no longer expose the craftsmen.

4. CONCLUSION

From the results and discussion, it can be concluded that in the process of working on the gamelan:

a. There was a significant increase in the microclimate components of the working environment, workload of craftsmen, musculoskeletal disorders and general fatigue.
b. exposure to hot temperatures causes the work productivity of craftsmen to be not optimal or low.
c. The working conditions of the craftsmen need to be improved ergonomically and the application of appropriate technology in the form of furnace improvements and work layouts.

5. REFERENCES

[1] T. Budiyanto and M. Yusuf, "Improvement of Wok Molding Station Increases Work Comfort and Productivity of the Workers," *Int. J. Psychosoc. Rehabil.*, vol. 24, no. 4, pp. 8883–8892, 2020.
[2] M. Edem, E. Akpan, and N. Pepple, "Impact of Workplace Environment on Health Workers," *Occup. Med. Heal. Aff.*, vol. 05, no. 02, 2017.
[3] K. H. E. Kroemer and E. Grandjean, *Fitting The Task To The Human, Fifth Editione A Textbook Of Occupational Ergonomics*. London: CRC Press, 2009.
[4] A. P. Sarode and M. Shirsath, "The Factors Affecting Employee Work Environment & It's Relation with Employee Productivity," *J. Sci. Res.*, vol. 3, no. 11, pp. 2735–2737, 2014.
[5] A. Manuaba, "Total approach is a must for small and medium enterprises to attain sustainable working conditions and environment, with special reference to Bali, Indonesia," *Ind. Health*, vol. 44, no. 1, pp. 22–26, 2006.
[6] I. G. Santosa and M. Yusuf, "The Application of a Dryer Solar Energy Hybrid to Decrease Workload and Increase Dodol Production in Bali," *Int. Res. J. Eng. IT Sci. Res.*, vol. 3, no. 6, Nov. 2017.
[7] C. Caruso, E. D. Hitchcock R. Russo. J. Schimt, J., and Anonymous, *Overtime and Extended Work Shifts: Recent findings on illness, injuries and health behaviours.*, vol. 143. Columbia: U.S. Department of Health and Human Services, 2004.
[8] Deouskar N, "The Impact Of Ergonomics On The Productivity Of People," *Int. J. Mark. Financ. Manag.*, vol. 5, no. 6, pp. 59–63, 2017.
[9] BSN, *Threshold value for working condition under heat, noise, vibration hand-arm, and ultraviolet sun light exposure, SNI 16-7063-2004*. Jakarta: Badan Standarisasi Nasional, 2004.
[10] A. Manuaba, "Research and application of ergonomics in developing countries, with special reference to Indonesia," *Indones. J. Ergon.*, vol. 1, no. 1, pp. 24–30, 2000.
[11] A. Wibolo and I. N. L. Antara, "DESIGNING PLASTIC CUPES RING CUTTING MACHINE TO INCREASE PRODUCTIVITY," *Log. J. Ranc. Bangun dan Teknol. Vol 18 No 2 Juli 2018*, 2018.
[12] W. Susihono and I. P. Gede Adiatmika, "Assessment of inhaled dust by workers and suspended dust for pollution control change and ergonomic intervention in metal casting industry: A cross-sectional study," *Heliyon*, vol. 6, no. 5, p. e04067, 2020.
[13] R. S. Bridger, *Introduction to Ergonomics, 3rd Edition*. London: Taylor & Francis, 2008.
[14] S. Pheasant and C. M. Haslegrave, *Bodyspace: Anthropometry, Ergonomics and the Design of Work, Third Edition*, 3rd ed. Boca Raton: CRC Press., 2016.
[15] D. P. Sutjana, "Application of Ergonomics at the Bali Sanur Bungalows Hotel," *Indones. J. Biomed. Sci.*, vol. 2, no. 1, pp. 1–11, 2008.
[16] M. Yusuf, N. Adiputra, I. Dewa, P. Sutjana, and K. Tirtayasa, "The Improvement of Work Posture Using

RULA (Rapid Upper Limb Assessment) Analysis to Decrease Subjective Disorders of Strawberry Farmers in Bali," *Int. Res. J. Eng. IT Sci. Res.*, vol. 2605, no. 9, pp. 4290–2016, 2016.

[17] S. R. Kamat, N. E. N. Md Zula, N. S. Rayme, S. Shamsuddin, and K. Husain, "The ergonomics body posture on repetitive and heavy lifting activities of workers in aerospace manufacturing warehouse," *IOP Conf. Ser. Mater. Sci. Eng.*, vol. 210, no. 1, 2017.

[18] N. D. Irwanti, M. Yusuf, N. Y. Anggreni, and L. S. Widiastuty, "Workload Analysis of Front Office Staff at Water Mark Hotel And SPA Jimbaran-Bali," *Int. J. Multidiscip. Educ. Res.*, vol. 7, no. 8(1), p. 63, 2018.

[19] I. K. G. J. Suarbawa, M. Arsawan, M. Yusuf, and I. M. Anom Santiana, "Improvement of environment and work posture through ergonomic approach to increase productivity of balinese kepeng coin workers in Kamasan village Klungkung Bali," in *Journal of Physics: Conference Series*, 2018, vol. 953, no. 1.

[20] A. Manuaba, "Accelerating OHS-Ergonomics Program By Integrating 'Built-In" Within The Industry's Economic Development Scheme Is A Must-With Special Attention To Small And Medium Enteprises (SMEs)," in *Proceedings the 21st Annual Conference of The Asia Pasific Occupational Safety & Health Organization*, 2005.

LOGIC
Journal of Engineering Design and Technology
Vol. 21 No.1 March 2021; p. 70 - 73

p-ISSN : 1412-114X
e-ISSN : 2580-5649
http://ojs.pnb.ac.id/index.php/LOGIC

WORKING PRODUCTIVITY ANALYSIS ON THE PROCESS OF DRYING FISH USING SOLAR DRYERS

I Gede Santosa [1], I Gede Bawa Susana[2]

1) Mechanical Engineering Department, Politeknik Negeri Bali, Bukit jimbaran, Badung Bali
2) Department of Mechanical Engineering, Faculty of Engineering, Universitas Mataram, Mataram-Nusa Tenggara Barat

Correponding email [2] : gedebawa@unram.ac.id

Abstract. The process of drying fish using solar energy is strongly influenced by weather conditions. Sunlight is needed by household scale workers because it is cheap. On the other hand, sun drying creates additional workload for workers. Workers are exposed to hot sun during drying. Continuous heat exposure results in an increased work pulse. This affects the level of worker productivity. To anticipate this, a solar dryer is used by utilizing a solar collector as an absorber of sunlight and a drying chamber for the drying process of fish. The use of solar dryers has been shown to increase drying temperatures and reduce workers' sun exposure. This decreases the workload of workers, so that it has an impact on increasing productivity. Worker productivity increased by 133.94%.

Keywords : solar energy, productivity, solar collector.

1. INTRODUCTION

Indonesia as a tropical country, rural population uses the sun as a source of food preservation. The drying process is carried out for post-harvest handling so that food quality is maintained properly. Sun drying is drying directly in the sun. This affects the need for a large drying area, the product is less hygienic because it is susceptible to animal disturbance and dust, the temperature and drying time are less than optimal. The alternative is to optimize the sun as a source of drying energy through a dryer with a solar collector.

The solar dryer makes use of a flat plate collector for sun absorption so that the ambient air heats up faster. In general, drying can be done through sun drying, namely the product to be dried directly in the sun and drying with a solar dryer, namely the product to be dried is placed in a drying chamber [1]. Sun drying takes a long time and the temperature is not optimal. Sun drying to dry anchovies, which is done when the weather is sunny, takes two days with a drying temperature of ±33.43ºC [2]. Research on the drying process to handle post-harvest both in plantations and fisheries has been widely carried out. The use of computational fluid dynamic (CFD) software to evaluate the drying of the pepper with a solar collector and chimney design obtained a drying room temperature between 335.4 - 352 K [3]. The use of a drying room for the drying process has an impact on increasing worker comfort. The drying process of fish using a drying chamber which is designed based on ergonomic principles can reduce the musculoskeletal complaints of workers by 26.70% [4]. To increase the drying temperature using solar energy sources is done by using a solar collector application. The plates on the collector will absorb sunlight so that the environmental air heating is more optimal. This hot air is flowed into the drying chamber and used to dry food. The use of solar collectors can increase the temperature of the drying chamber. The temperature in the drying chamber is the most important parameter affecting the drying rate directly [5]. The absorption of solar energy is optimized using a flat plate collector by adding an absorber in the form of granite [6].

Dryers with solar collectors called solar dryers are used for the drying process of anchovy on a household scale. Drying is done to preserve the anchovies. Anchovies undergo a fast process of decay due to the high water and nutrient content, so it is easy for bacteria to grow and due to chemical changes in dead fish. To avoid the decay process, preservation is carried out to reduce the water content in the fish. This is so that bacteria do not reproduce. Fish in general have a content varies between 50% -80% [7]. Dried anchovy contains about 33.4% protein and 3% fat only [8]. The drying process with the solar dryer system provides better display quality and nutritional content, and the color of the fish looks cleaner. This has an impact on the productivity level of workers as processors of dried anchovy.

The use of solar dryers in drying fish can reduce the workload of workers. Reduced workload will increase productivity levels. The level of worker productivity is influenced by the workload [9]. Workload arises as a result of physical and mental activity, which is indicated by a change in pulse frequency. The higher the body activity is directly proportional to the higher the pulse frequency [10]. To increase the productivity of workers doing anchovies drying business, use solar dryers. A dryer with a solar collector will convert sunlight to thermal.

2. METHODS

This study used anchovies as a sample. The test is done by comparing the drying process between solar dryers and drying them in the sun. The solar dryer consists of a flat plate type solar collector, a drying chamber with additional shelves inside. The energy source uses the sun. Collector surface area of 1,045 m^2 with absorbent using 1.2 mm aluminum plate painted black with 5 mm clear glass covering material, 1 layer. The area of each shelf in the drying chamber is 0.7505 m^2. The shelf material in the drying chamber is bamboo. Productivity is calculated based on Equation 1.

$$P = \frac{O}{I\,x\,t} \quad (1)$$

P = work productivity (kg / hr.ppm or kg / min.ppm); O = output in the form of dry anchovy weight (kg); I = input in the form of workload calculated based on work pulse (ppm); and t = length of time worked (hours).

The productivity level is calculated for each worker during the drying process using a solar dryer and drying in the sun as shown in Figure 1.

(a) (b)

Figure 1. Drying anchovies a) solar dryer, b) drying in the sun

3. RESULTS AND DISCUSSION

The drying process using solar dryers can increase worker productivity when compared to drying in the sun. This can be seen from the shorter drying times and decreasing workloads. The solar dryer requires an average fish drying time of 6.21 hours. Meanwhile, drying in the sun requires an average drying time of 12.71 hours. Drying time in sunny weather conditions for both treatments. The average sun drying temperature is 35.47°C and the average drying chamber temperature in the use of a solar collector is 47.13°C. The drying process for both treatments was carried out from 09.00 to 15.00. The temperature of the drying chamber with a load of 20 kg of fish of 47.13°C meets the applicable temperature requirements for drying fish. This is in accordance with [7] that the drying temperature for fish is 40-50°C, if the temperature exceeds 50°C it affects the outside of the dry product but the inside is still wet. The drying temperature ratio is as shown in Figure 2.

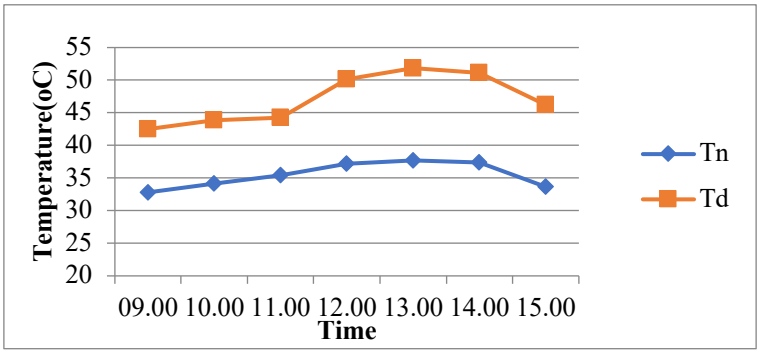

Figure 2. Drying temperature using a solar dryer (Td) and sun drying (Tn)

The drying process using a solar dryer is able to reduce the workload which is calculated based on the pulse of workers from 104.84 pulses per minute (ppm) to 91.22 ppm. This is as a result of the shorter working time on the use of solar dryers. Based on the working time and workload, the work productivity of the fish artisan is obtained as shown in Figure 3.

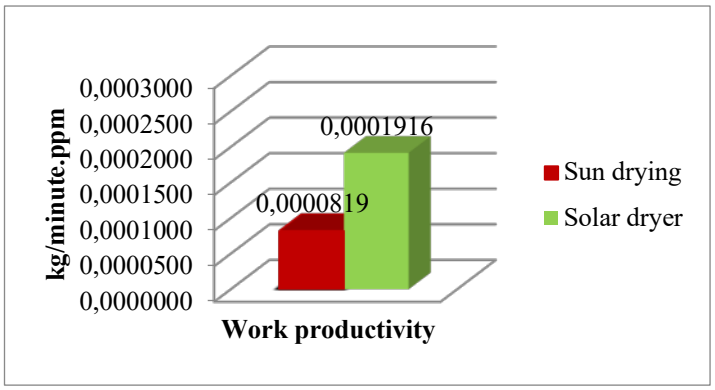

Figure 3. Physiological work productivity of fish artisan

Worker productivity has increased by 133.94%, from 0.0000819 kg/minute.ppm to 0.0001916 kg/minute.ppm. Productivity is affected by the workload which is calculated based on the work pulse. The comparison of the work pulse of the fish artisan between sun drying and using a solar dryer is shown in Figure 4.

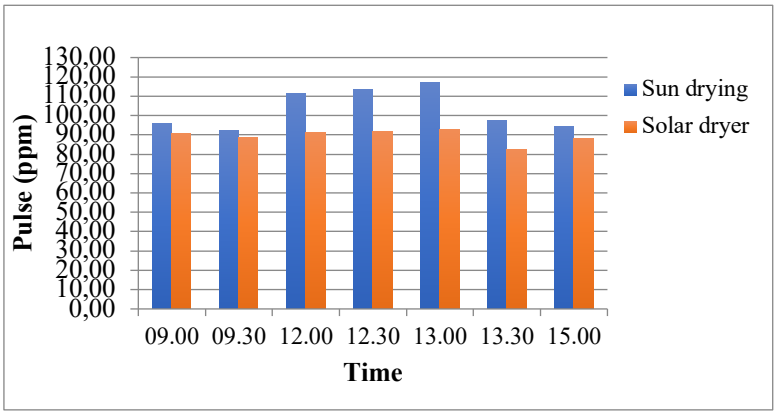

Figure 4. Pulse distribution of workers when drying fish

When drying workers in the sun, they have a higher pulse when compared to using solar dryers. Solar dryers for the fish drying process provide a more efficient way of working for workers. More efficient work is proven to increase worker productivity and has implications for improving worker welfare. Exposure to the sun's heat will affect the emotional level of workers as indicated by an increase in the workers' pulse. This condition will affect worker productivity. This is in line with [11] who tested the effect of emotions on work productivity. It was explained that productivity refers to the efficiency of workers producing products to achieve goals in the business. In addition, increasing productivity is an important consideration for overall well-being.

4. CONCLUSION

Productivity is an important consideration for the welfare of workers. In this study, the measurement of productivity based on the workload of workers is to use the work pulse. The workload has decreased after using the solar dryer for drying fish. This has implications for increasing worker productivity. Productivity increased by 133.94%. Productivity measured based on workload indicates that workers doing work is more comfortable and efficient.

5. REFERENCES

[1] E.S. Heruwati, "Pengolahan ikan secara tradisional, prospek dan peluang pengembangan, pusat riset pengolahan produk dan sosial ekonomi kelautan dan perikanan", *Jurnal Litbang Pertanian*, vol. 21, no. 3, pp. 92-99, 2002.

[2] I G.B. Susana and I G. Santosa, "Peningkatan produktivitas perajin ikan teri dengan konversi energi biomassa", *Jurnal Logic*, vol. 15, no. 1, pp. 47-50, 2015.
[3] A.R.H Rigit and P.T.K. Low, "Heat and mass transfer in a solar dryer with biomass backup burner", *International Journal of Mechanical and Mechatronics Engineering*, vol. 4, no. 2, pp. 133-136, 2010.
[4] I G.B. Susana, "Rancangan ruang pengering berbasis ergonomi menurunkan keluhan muskuloskeletal perajin ikan", *Dinamika Teknik Mesin*, vol. 6, no. 1, pp. 15-21, 2016.
[5] D. Mehmet and K.A. Ebru, " Determination of thermal and drying performances of the solar air dryer with solar tracking system: Apple drying test", *Case Studies in Thermal Engineering*, vol. 21, pp. 1-15, 2020.
[6] M. Wirawan, Mirmanto, I G.B. Susana and R. Sutanto, "Pengaruh susunan pipa laluan terhadap pemanfaatan kalor pada kolektor surya pelat datar absorber granite", *Dinamika Teknik Mesin*, vol. 5, no. 1, pp. 50-55, 2015.
[7] K. Abdullah, "*Fish drying using solar energy, lectures and workshop exercises on drying of agricultural and marine products*, *Regional Workshops on Drying Technology*, pp. 159-191, 2003.
[8] T. Margono, D. Suryati, and S. Hartinah, 2000, *Buku panduan teknologi pangan*. Pusat informasi wanita dalam pembangunan PDII-LIPI bekerjasama dengan Swiss Development Cooperation.
[9] Tarwaka, S.H.A. Bakri and L. Sudiajeng, *Ergonomi untuk Keselamatan, Kesehatan Kerja dan Produktivitas*. Surakarta: UNIBA Press, 2004.
[10] N. Adiputra, "Denyut nadi dan kegunaannya dalam ergonomi", *Jurnal Ergonomi Indonesia,* vol. 3, no. 1, pp. 22-26, 2002.
[11] Y. Kadoya, M.S.R. Khan, S. Watanapongvanich and P. Binnagan, " Emotional status and productivity: evidence from the special economic zone in Laos", *Sustainability*, vol. 12, pp. 1-15, 2020.

LOGIC
Journal of Engineering Design and Technology
Vol. 21 No.1 March 2021; p. 74 - 79

p-ISSN : 1412-114X
e-ISSN : 2580-5649
http://ojs.pnb.ac.id/index.php/LOGIC

COMPARISON OF INVERTER TYPES FOR HOME APPLIANCE USING PUSH-PULL AMPLIFIER

(Experimental Inverter Types at Engineering Laboratory)

Mokh. Hairul Bahri [1], Dudi Irawan[2]

1) Mechanical Engineering Department, Universitas Muhammadiyah Jember, Jl. Karimata 49, Jember, Indonesia
2) Electrical Engineering Department, Universitas Muhammadiyah Jember, Jl. Karimata 49, Jember, Indonesia.

Correponding email [1] : mhairulbahri@unmuhjember.ac.id

Abstract. This paper deals with a comparison of inverter types and develops a system to provide pure sine wave ac voltage. The ac voltage is utilized to drive the compressor ac split. The assembled inverter problem is a square waveform, power losses, torque, efficiency, and a lag behind in terms of performance reliability. The push-pull amplifiers technic is proposed to produce sine wave output from dc input. The output result shows that an experimental pure sin wave obtains a frequency of 50.05 Hz, V max 13.49 Volt, V min -14.49 volt, and duty cycle 50.1%. the assembled inverter has a frequency is 37.87 Hz, V max 11.88 Volt, V min 13.09 volt, and a duty cycle is 50 %. A modified 3-phase inverter attains frequency 50.05 Hz, V max 15.71 Volt, V min -16.11 Volt, and the duty cycle is 50.5 %. The frequency, v max, v min, and duty cycle are bigger than an assembled inverter, then the modified 3-phase inverter has small harmonic distortion. The comparison of inverter types gives information for home appliances.

Keywords: three phase inverter, push-pull amplifier, transformer.

1. INTRODUCTION

The inverter is a popular known as power electronic device that is used for the conversion of dc to ac at various voltage and frequency by switching and control circuits. An output voltage can be supplied by a dc source such as batteries, capacitors, and solar panels [1]. A voltage source inverter is utilized to vary the supply voltage and frequency. The voltage source inverter is independently controlled by ac output voltage waveforms. Three-phase inverter is high-power applications which are widely used in motor drive, air conditioning, and compressor split with switching a capacitor [2]. Power electronics have contributed to developing new powerful applications, these advances have increased the harmonic contamination present line current which ends up distorting the voltage waveforms [3]. For high-efficiency, dc-ac conversion and peak power tracking must have low harmonic distortion and high power [4]. A capacitor has capacitance with a range of 500-5000 μF to keep voltage constant (V_{dc}), but the large capacitance in input current (I_{in}) is severely distorted and power input is low. Furthermore, the use of capacitors has a weakness in reliability [5]. The type of load home appliance is non-linear load. An inverter shall affect a lot of non-linear loads such as water pumps, air conditioning, fans, and refrigerator [6]. The power inverter problem is a square waveform, and a lag behind in terms of performance reliability. The impact of the output inverter is power losses, torque, and efficiency. Moreover, the output sine wave inverter does not achieve to apply home appliance [7].

This paper deals with a comparison of any inverter and develops a system to provide pure sine wave ac voltage. The ac voltage is utilized to drive the compressor ac split. The first measurement of the voltage source is done, the second inverter is assembled to produce a pure sine wave, and the third inverter is modified to obtain a pure sine waveform of an inverter. The proposed system uses the push-pull amplifiers technic to produce sine wave output from dc input. The push-pull amplifiers technic is the process to obtain low harmonic distortion and high frequency. Every half of the wave amplifier conducts a one-half cycle of RF signal for operating cycle 180◦, then the efficiency attains as high as 78.5%. Consequently, the transistor of the circuit push-pull gets ON more than half a cycle class-B, but less than full cycle like class-A. the device does not change suddenly cut-off to mode linear.

2. METHODS

The push-pull amplifier is used to couple amplifier only ac signal. The amplifier has the infinite gain for differential input signal, and it converts a weak signal for home applications. The device of an amplifier can be designed by varying performance parameters to attain the desired result. Adaptive bias is one of a method to solve slew rate, to increase power transistor, and to produce power consumption [8]. The electronic device requires low voltage and power that it can be attained by operating device of a transistor. a supply voltage from dc source and efficiency power which can be achieved by using a push-pull output in the circuit [9]-[10]. A combination of transistor n-channel and p-channel in series or parallel are used to obtain common-mode input range and to increase low frequency. The open-loop gain in offset voltage is produced by connecting the gain boost amplifier [11].

The amplifier of push-pull has a 1KHz input frequency, low load resistance in the range of few Ohms. The high efficiency and high load resistance in the range of KΩ have been developed using a valve based on the circuit [12]. The circuit of the push-pull amplifier is designed by Proteus 8.0 such as initially high load resistance, compressor split, air conditioning, and home appliance which is fundamental level using an active device to approach ac waveforms output. The design of the component is described in figure 1.

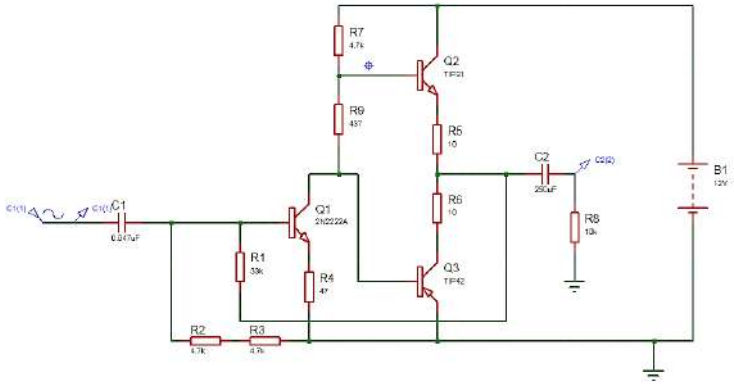

Figure 1. Proposed Push-Pull Amplifier.

The proposed push-pull amplifier in figure 1 is configured by processing dc voltage 12 Volt from a battery source. The Resistance R7 and R9 are placed to series transistor n-channel Q1 2N2222A which input as sinusoidal from the source. Then, the transistor n-channel Q2 TIP31 is series to resistor R5 and R6 that can be switching transistor p-channel Q3 TIP42. The capacitor is parallel between R5 and R6 to obtain desired sine waveform output and a resistor R8 is inverter load. The battery supplies amplifier that the output is depressed by the transformer to 220 Volt. The 12 Volt battery source is connected to an amplifier to produce a sinusoidal waveform with a frequency of 50 Hz to 1 kHz after switching by a transistor. In the output stage push-pull, the supply current is used efficiently. The push-pull is in principle represented by the voltage source, which expresses all its important properties. To set the quiescent current, the sum of the gate-source voltages of the output stage can be controlled in such a way that it is equal to the sum of a reference PNP gate-source voltage and an NPN gate-source voltage, which is obtained by giving the value. Table 1 explains the detailed circuit of components for the push-pull amplifier.

Table 1. Detail Circuits of Component

Variable	Value	Unit
Capacitor (C1)	0.047	uF
Capacitor (C2)	250	uF
Transistor NPN (Q1 2N2222A)	-	H
Transistor NPN (Q2 TIP31)	-	H
Transistor PNP (Q2 TIP42)	-	H
Resistor (R1)	33k	Ω
Resistor (R2)	4.7k	Ω
Resistor (R3)	4.7k	Ω
Resistor (R4)	47	Ω
Resistor (R5)	10	Ω
Resistor (R6)	10	Ω
Resistor (R7)	4.7k	Ω
Resistor (R8)	10k	Ω
Resistor (R9)	437	Ω

3. RESULTS AND DISCUSSION

3.1 Experimental of AC Sine Waveform

Figure 2 describes the experimental AC sine waveform that is conducted by a transformer CT 2A. The experiment is utilized to attain a sine waveform from the AC source, and then a comparison of any inverter applies for compressor split.

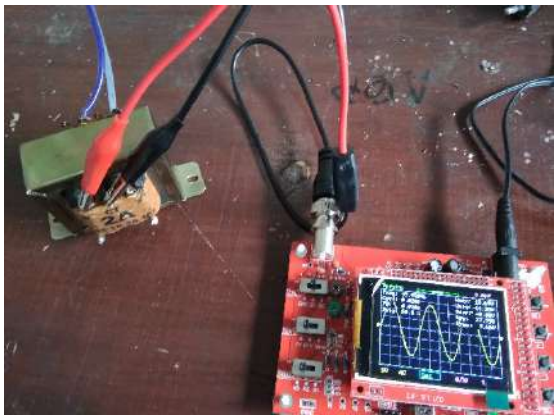

Figure 2. Experimental Sine Waveform of Transformer CT

Figure 3 is an experimental transformer to obtain a sinusoidal waveform. The transformer is supplied by an AC source. This experiment proves a sinusoidal waveform without any load. According to data, every square value is 5 Volt, the frequency is 50 Hz, cycles is 0.019 second, the maximum voltage is 13.49 volt, and the minimum voltage is -14.38 volt.

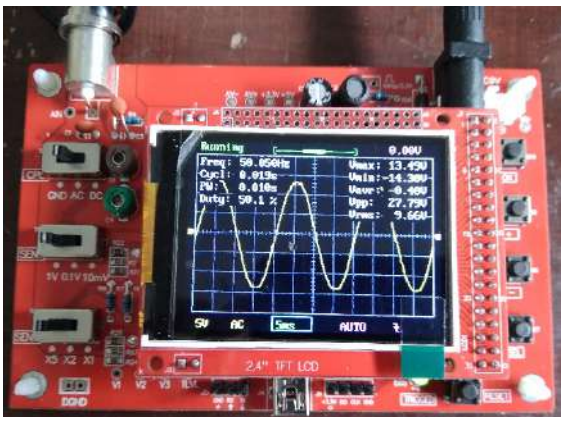

Figure 3. Sinusoidal Waveform of Transformer CT

3.2. Assembled 3-phase Inverter

Figure 4 is assembled 3-phase inverter. The inverter is assembled by a component such as one capacitor 4700 uF, one capacitor 220 uF, one capacitor 10 uF, one capacitor 1 uF, one positive voltage regulator L7808, four IRF 250 N transistors MOSFET, two-transistor NPN C1815, seven diodes IN4007, one resistor 220 ohm, three resistors 10 ohms, one resistor 100 ohm, one IC SG3542N DIP 16 Pin, three resistors 1M ohm, two resistors 10M ohm, one resistor 4M ohm, one transformer CT 10 A, and one transformer 500 mA.

Figure 4. Assembled 3-phase Inverter

Figure 5 is an experimental of an assembled 3-phase inverter. The inverter output does not achieve a sinusoidal waveform. The problem is caused by a voltage drop and high harmonic distortion. Therefore, an inverter does not apply for any home appliance which requires high voltage. Based on the experimental result, the frequency of the assembled 3-phase inverter is 37.87 Hz, the cycle is 0.02 second, maximum voltage 11.88 Volt, the minimum voltage is -13.09 Volt.

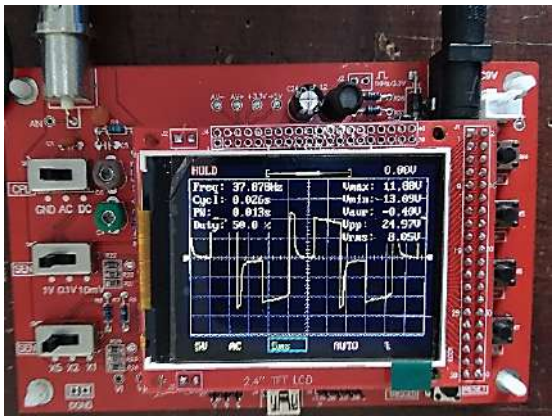

Figure 5. Experimental of Assembled 3-phase Inverter

3.3. Proposed Method of 3-phase Inverter

The proposed method of a 3-phase inverter utilizes a push-pull amplifier. A new concept of the push-pull amplifier is designed by Proteus 8.0 which component assemblies such as battery 12 Volt, resistor, and capacitor. The push-pull amplifier is supplied by dc power to obtain a 12 Volt ac signal source at 1KHz frequency through simulation software. The response of frequency estimates an approach desired sinusoidal waveform. The simulation result is described in figure 6.

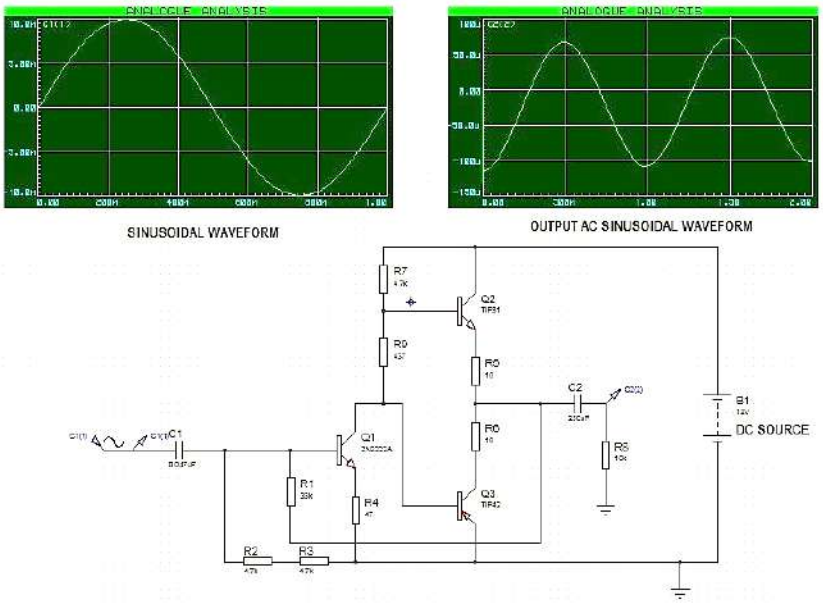

Figure 6. Simulation of Push-Pull Amplifier

Figure 6 the simulation result shows that the proposed method of push-pull amplifier gives sinusoidal waveform with a load resistance RL. An increasing load resistance from 1kΩ to 10kΩ has variation output ac waveform. The capacitor sinusoidal waveform C1 has a maximum voltage of 220 volts, a frequency 1kHz. The capacitor output C2 has AC sinusoidal waveform and a frequency 1kHz. An input signal waveform is caused by the transistor Q1 to operate normally in the active region. Hence, it can decrease crossover distortion. A small collector current flows when the signal input is zero. The transistor Q2 will be ON more than half waveform cycle, but much less than a full cycle is giving a conduction angle between 180◦ to 360◦. The amount of resistor voltage at the terminal of transistor Q3 can be increased several times by adding a series resistor. The output transistor Q1, Q2, and Q3 each half waveform (positive and negative) will be 0.7 Volt. The result two resistors are turn OFF at the same time. A simple way to decrease harmonic distortion is by adding a small voltage to the circuit to refract two-transistor Q2 and Q3.

3.2. Modified Inverter

A modified 3-phase inverter has been designed based on a component that can provide the desired output. The inverter output is an approach of a sinusoidal waveform. The waveform utilizes to drive a compressor split which needs a pure sine wave. The problem-assembled inverter has a square waveform, and a lag behind in terms of performance reliability. The impact of the output inverter is power losses, torque, and efficiency. Moreover, the output sine wave inverter does not achieve to apply home appliance [7]. To solve this problem, the modified inverter is experimented with by using a push-pull amplifier to obtain a sinusoidal waveform. The experiment is conducted at the laboratory. Figure 7 shows the modified 3-phase inverter.

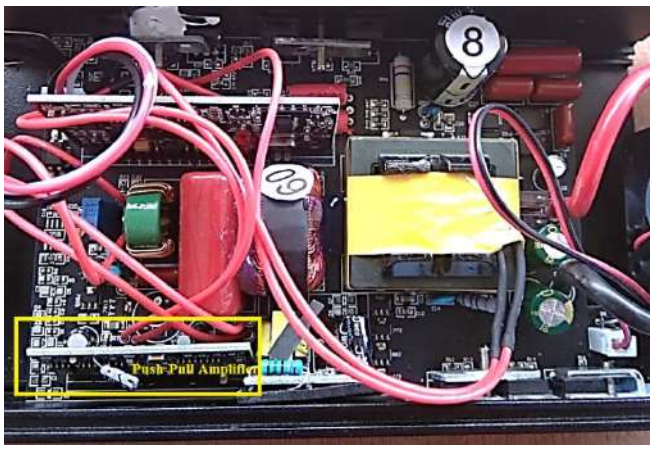

Figure 7. Modified 3-phase Inverter

Figure 8 shows the output 3-phase modified inverter which has a sin waveform of 220 volts. The frequency 50.05 Hz, a cycle becomes 0.019 seconds, a maximum voltage is 15.71 volt, the minimum voltage is -16.11 volt, and root mean square voltage (V_{rms}) is 10.79 volt. The cycle of a square wave is 5 Volt at the time 2 microseconds. The output 3-phase modified inverter can be affected by a push-pull amplifier that is placed a series resistor R7 and R9. The transistor Q2 N-channel is placed by a parallel between R7 and R9 that can decrease harmonic distortion. Then, the transistor Q3 p-channel is connected to a series resistor R5 and R6 to maintain overcurrent from the load.

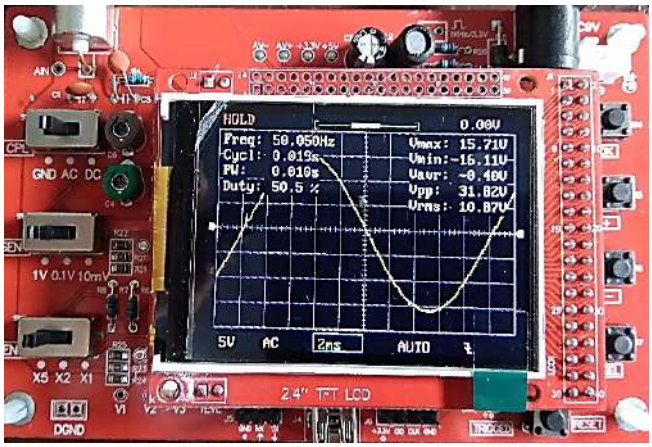

Figure 8. Output 3-phase Modified Inverter.

Table 1. Comparison of Inverter

Inverter	Frequency	V max	V min	Duty Cycle
Pure AC sine wave	50.05 Hz	13.49 V	-14.49 V	50.1 %
Assembled Inverter	37.87 Hz	11.88 V	-13.09 V	50 %
Modified Inverter	50.05 Hz	15.71 V	-16.11 V	50.5 %

Table 1 is a comparison of the output 3-phase inverter. The experimental pure sine wave of transformer

CT 2A obtains a frequency of 50.05 Hz, V max 13.49 Volt, V min -14.49 volt, and duty cycle 50.1%. the assembled inverter has a frequency is 37.87 Hz, V max 11.88 Volt, V min 13.09 volt, and a duty cycle is 50 %. A modified 3-phase inverter attains frequency 50.05 Hz, V max 15.71 Volt, V min -16.11 Volt, and the duty cycle is 50.5 %. The modified 3-phase inverter shows that a sinusoidal waveform output is suitable for a home appliance like compressor split or air conditioning. Therefore, the frequency, v max, v min, and duty cycle are bigger than an assembled inverter, then the modified 3-phase inverter has harmonic distortion is small. The home appliance application requires fewer power losses, and torque to avoid a damaged component.

4. CONCLUSION

The comparison of any inverter is conducted by designing assembled inverter and modified 3-phase inverter. This comparison of any inverter and develops a system to provide pure sine wave ac voltage. The push-pull amplifiers technic proposed to produce sine wave output from dc input. The output result shows that an experiment of pure sin wave obtains a frequency of 50.05 Hz, V max 13.49 Volt, V min -14.49 volt, and duty cycle 50.1%. the assembled inverter has a frequency is 37.87 Hz, V max 11.88 Volt, V min 13.09 volt, and a duty cycle is 50 %. A modified 3-phase inverter attains frequency 50.05 Hz, V max 15.71 Volt, V min -16.11 Volt, and the duty cycle is 50.5 %. Therefore, the frequency, v max, v min, and duty cycle are bigger than an assembled inverter, then the modified 3-phase inverter has small harmonic distortion. The comparison of any 3-phase inverter gives information for home appliances.

5. ACKNOWLEDGMENT

We would like to say thank you very much to:

1. Rector Of Universitas Muhammadiyah Jember and all his staff.
2. Dean of Technical Faculty Of Universitas Muhammadiyah Jember.
3. Head of LPPM Universitas Muhammadiyah Jember for financial supporting in research budget year of 2021.

6. REFERENCES

[1] B. Bhattacharjee, “Analytical Study of Novel Design Inverter,” *Proc. 3rd Int. Conf. Commun. Electron. Syst. ICCES 2018*, no. Icces, pp. 286–290, 2018.

[2] M. Islam, N. Raju, and A. Ahmed, “Sinusoidal PWM Signal Generation Technique for Three-Phase Voltage Source Inverter with Analog Circuit & Simulation of PWM Inverter for Standalone Load & Micro,” *Int. J. Renew. Energy Res.*, vol. 3, no. 3, pp. 647–658, 2013.

[3] M. López G., L. Morán T., J. Espinoza C., and J. Dixon R., “Performance Analysis of a Hybrid Asymmetric Multilevel Inverter for High Voltage Active Power Filter Applications,” *IECON Proc. (Industrial Electron. Conf.*, vol. 2, pp. 1050–1055, 2003.

[4] A. Roshan, R. Burgos, A. C. Baisden, F. Wang, and D. Boroyevich, “A D-Q frame controller for a full-bridge single phase inverter used in small distributed power generation systems,” *Conf. Proc. - IEEE Appl. Power Electron. Conf. Expo. - APEC*, pp. 641–647, 2007.

[5] H. S. Jung, S. J. Chee, S. K. Sul, Y. J. Park, H. S. Park, and W. K. Kim, “Control of three-phase inverter for AC motor drive with small DC-Link capacitor fed by single-phase AC source,” *IEEE Trans. Ind. Appl.*, vol. 50, no. 2, pp. 1074–1081, 2014.

[6] R. Fierdaus, I. Soeprapto, I. H. Purnomo, T. Elektro, T. Elektro, and U. Brawijaya, “Pengaruh bentuk gelombang sinus termodifikasi (,” pp. 0–5.

[7] R. Haider, R. Alam, N. B. Yousuf, and K. M. Salim, “Design and construction of single phase pure sine wave inverter for photovoltaic application,” *2012 Int. Conf. Informatics, Electron. Vision, ICIEV 2012*, pp. 190–194, 2012.

[8] M. Santosh Kumar, D. Asha Devi, and P. Snist, “Design of Power Efficient and High Slew Rate Class AB OPAMP,” no. November, pp. 6159–6162, 2015.

[9] P. Anbarasan, K. Hariharan, and R. Parameshwaran, “Design of gain enhanced and power-efficient op-amp for ADC/DAC and medical applications,” *Indian J. Sci. Technol.*, vol. 9, no. 29, 2016.

[10] K. Langen and J. H. Huijsing, “Compact Low Voltage Power Efficient Opamp Cells for VLSI,” *Jssc*, vol. 33, no. 10, pp. 1–15, 1998.

[11] B. Lee, “Low Voltage / Low Power Rail-To-Rail Cmos Operational Amplifier for Portable ECG,” no. August 2013.

[12] S. Shukla, B. Pandey, and S. Srivastava, “New circuit models of Complementary-Symmetry Class-AB and Class-B Push-Pull Amplifiers,” *2012 10th IEEE Int. Conf. Semicond. Electron. ICSE 2012 - Proc.*, pp. 538–542, 2012.

LOGIC
Jurnal Rancang Bangun dan Teknologi
(Journal of Engineering Design and Technology)
Address : Gedung P3M, lt.1 Politeknik Negeri Bali, Bukit Jimbaran
PO BOX 1064 Kuta Selatan, Badung, Bali - Indonesia
Telp. (+62)361 701981 Fax. (+62)361 701128
Email: logic@pnb.ac.id